CHEMICAL EQUILIBRIUM AND KINETIC STUDY OF THE ESTERIFICATION OF ACRYLIC ACID WITH BUTANOL CATALYSED BY SULFONATED EXPANDED POLYSTYRENE

MUHAMMAD RIDZUAN BIN KAMARUZAMAN

MASTER OF ENGINEERING (CHEMICAL)

UNIVERSITI MALAYSIA PAHANG

CHEMICAL EQUILIBRIUM AND KINETIC STUDY OF THE ESTERIFICATION OF ACRYLIC ACID WITH BUTANOL CATALYSED BY SULFONATED EXPANDED POLYSTYRENE

MUHAMMAD RIDZUAN BIN KAMARUZAMAN

Thesis submitted in fulfilment of the requirements
for the award of the degree of
Master of Engineering (Chemical)

Faculty of Chemical and Natural Resources Engineering
UNIVERSITI MALAYSIA PAHANG

SEPTEMBER 2014

STATEMENT OF AWARD FOR DEGREE

Master of Engineering (by Research)

Thesis submitted in fulfilment of the requirements for the award of the degree of Master of Engineering in Chemical Engineering.

SUPERVISOR'S DECLARATION

I hereby declare that I have checked this thesis and in my opinion, this thesis is adequate in terms of scope and quality for the award of the degree of Master of Engineering in Chemical Engineering.

Signature
Name of Supervisor : Dr. Chin Sim Yee
Position : Associate Professor
Date :

STUDENT’S DECLARATION

I hereby declare that the work in this thesis is my own except for quotations and summaries which have been duly acknowledged. The thesis has not been accepted for any degree and is not concurrently submitted for award of other degree.

Signature :
Name : Muhammad Ridzuan bin Kamaruzaman
ID Number : MKC11019
Date :

DEDICATION

Dedicated to my parents, family and friends.

A special feeling of gratitude to all for words of encouragement, support and for being there for me throughout the entire master program.

ACKNOWLEDGEMENT

Foremost, I would like to express my sincere gratitude to Allah S.W.T, for giving this tremendous opportunity for me to complete this research. May the peace and blessings be upon Prophet Muhammad S.A.W.

I would like to express my deepest gratitude to my supervisor, Assoc. Prof. Dr. Chin Sim Yee for continuous support, motivation, knowledge, and patience. I would also like to thanks to technical staff from the Laboratory of Faculty of Chemical and Natural Resources Engineering who gave guidance for lab work especially in analysing samples using GC-FID.

Special thanks for all my friends who gave supports and insightful suggestion throughout the entire year. Thanks also for the fun we had which make the life as master student was easier although facing many obstacles.

I would like to thank for my father, Kamaruzaman Ab Manaf who give long lasting love and support. I acknowledge the sincerity of my family who encouraged me to carry on my higher studies.

I express my deepest gratitude to UMP and Ministry of High Education (MOHE), Malaysia for the financial support throughout this research work via Graduate Research Scheme (GRS 120315) and MyMaster sponsorship.

ABSTRACT

The wastewater containing low concentration (4-10 wt %) of acrylic acid (AA) was treated by incineration since it is very toxic to the organism if it is discharged to the environment. This valuable compound can be recovered using one of the promising methods, the esterification of the diluted AA with alcohol. The sulfonated expanded polystyrene (SEP) from waste expanded polystyrene is a good catalyst to catalyse the esterification of AA with butanol (BuOH). The production of this catalyst can have high impact in environment since the waste polystyrene is huge environmental issues. The SEP was synthesised via the sulfonation of waste expanded polystyrene using sulphuric acid (H_2SO_4) at 378 K. The slurry obtained after 2 hour of sulfonation was transferred into water and washed with sodium hydroxide, acid hydrochloric and excess water before dried at 343 K. The SEP has a rough surface with minute cracks, can withstand up to 403 K and density of 1.2790 g/cm^3. The swelling effect in SEP helps the reactant access the active sites. The activity and kinetic study for this esterification reaction was carried out in batch system. The effect of various parameters that affecting conversion and yield such as stirring speed, initial molar ratio of AA to BuOH, catalyst loading, temperature and initial water content were studied. The reaction was more sensitive to temperature as compared to other parameters. The best conversion and yield obtained at molar ratio AA to BuOH of 1:3, catalyst loading of 10 wt% and temperature of 353 K were 92% and 75% respectively. The yield of butyl acrylate decrease with the increase of initial water content in the reaction mixture because water shifts the reaction equilibrium to reactants, blocked the reactants from accessing active sites and increase polymerisation on the SEP surface. Nevertheless, the SEP can be regenerated easily using sulphuric acid. The experimental kinetic data was correlated to the several kinetic models which were pseudo-homogeneous (PH), Eley-Rideal (ER) and Langmuir Hinshelwood Hougen Watson (LHHW) model. The activation energy is 73.6 kJ/mol. The best fitted model for the main esterification reaction was shown by the non-ideal ER I model. Taking the polymerisation into account, the experimental data are more comparable with the predicted data.

ABSTRAK

Air sisa yang mengandungi kepekatan asid akrilik (AA) yang rendah iaitu dalam lingkungan 4 hingga 10 berat% dirawat dengan pembakar kerana bertoksik kepada organisma jika dilepaskan ke alam sekitar. AA dalam air sisa ini, boleh diperoleh semula melalui proses pengesteran dengan alkohol. Polisterina tersulfonasi (SEP) yang dihasilkan daripada polisterina terpakai adalah pemangkin yang bagus untuk pengesteran AA dengan butanol (BuOH). Penghasilan pemangkin ini boleh memberi impak yang besar kerana polisterina terpakai adalah salah satu penyumbang terbesar kepada masalah alam sekitar. SEP ini dihasilkan melalui proses sulfonasi antara polisterina terpakai dengan asid sulfurik pada suhu 378 K. Selepas 2 jam proses sulfonasi, buburan dipindahkan kedalam air dan dibasuh dengan larutan natrium hidroksida, asid hidroklorik dan air sebelum dikeringkan pada suhu 343 K. SEP yang dihasilkan berketumpatan 1.2790 g/cm^3. Ia mempunyai rekahan dan permukaan yang kasar dan mampu bertahan sehingga suhu 403 K. Kesan pembengkakan dalam SEP membantu bahan tindak balas bergerak ke tapak aktif dengan lebih mudah. Kajian terhadap aktiviti dan tindak balas kinetik terhadap pengesteran dilakukan dalam reaktor kelompok. Pelbagai parameter yang mempengaruhi kadar tindak balas antaranya kadar kacauan, nisbah awal mol antara AA dan BuOH, muatan pemangkin, suhu dan kandungan awal air dalam bahan tindak balas telah dikaji. Tindak balas pengesteran adalah lebih sensitif terhadap suhu berbanding parameter yang lain. Kadar terbaik penukaran AA dan penghasilan butil akrilik (BA) pada nisbah mol 1:3 antara AA dan BuOH, muatan pemangkin sebanyak 10 berat%, dan suhu 353 K adalah 92% dan 75%. Penghasilan butil akrilik berkurang dengan kandungan awal air dalam campuran bahan tindak balas kerana air telah menganjakkan keseimbangan tindak balas ke bahan tindak balas, menghalang bahan tindak balas daripada mencapai tapak aktif, dan meningkatkan kadar pempolimeran diatas permukaan SEP. SEP juga mudah di jana semula dengan asid sulfurik. Data kinetik eksperimen telah di kaitkan dengan beberapa kinetik model iaitu model pseudo-homogeneous (PH), model Eley-Rideal (ER) dan model Langmuir Hinshelwood Hougen Watson (LHHW). Tenaga pengaktifan yang dikira adalah 73.6 kJ/mol. Model yang terbaik untuk tindak balas pengesteran adalah model bukan ideal, ER I. Dengan mengambil kira pempolimeran, data eksperimen adalah lebih serasi dengan data jangkaan.

.

TABLE OF CONTENTS

CHAPTER 1 INTRODUCTION

CHAPTER 2 LITERATURE REVIEW

CHAPTER 3 RESEARCH METHODOLOGY

CHAPTER 4 RESULTS AND DISCUSSION

CHAPTER 5 CONCLUSIONS AND RECOMMENDATIONS

APPENDICES

LIST OF TABLES

LIST OF FIGURES

LIST OF SYMBOLS

A	Acid
α_i	Activity coefficient of component *i*
E_f	Activity energy of reaction
K	Adsorption constant
B	Alcohol
K_x	Apparent equilibrium constant
Φ	Association parameter
Rc	Catalyst radius
R^2	Coefficient of determination
C_i	Concentration of component *i*
ρ	Density
D_{AB}	Diffusivity
D_{eff}	Effective diffusivity
K_{eq}	Equilibrium constant
X_e	Equilibrium conversion
E	Ester
k_f	Forward rate constant
γ_i	Gamma of component *i*
R	Gas constant
b_i	*i*th adjustable parameter
K	Kelvin

C_{li}	Limiting concentration
K_c	Mass transfer coefficient
M	Molarity
M	Molar ratio
x_i	Mole fraction of component *i*
m	Number of adjusted parameters
d_p	Particle diameter
%	Percent
K_{fo}	Pre-exponential factor
n	Reaction order
r_i	Reaction rate of component *i*
P/P_o	Relative pressure
rpm	Revolution per minute
N_{sc}	Schmitt Number
σ	Standard deviation
ΔH_r^0	Standard enthalpy of reaction
T	Temperature
K_a	Thermodynamic equilibrium constant
V	Volume
ε	Void fraction
μ	Viscosity
W	Water
wt	Weight

LIST OF ABBREVIATIONS

AA	Acrylic acid
BuOH	Butanol
BA	Butyl acrylate
COD	Chemical oxygen demands
CSZ	Conventional sulphated zirconia
ER	Eley-Rideal
EPS	Expanded polystyrene
FID	Flame ionization detector
FT-IR	Fourier Transform spectroscopy
GC	Gas chromatography
HPA	Heteropolyacids
HPLC	High performance liquid chromatography
HRT	Hydraulic retention time
IEC	Ion exchange capacity
LHHW	Langmuir Hinshelwood Hougen Watson
MCMC	Markov chain Monte Carlo
C_M	Mears criterion
MSZ	Mesoporous sulphated zirconia
NA	Not available
OFAT	One factor at a time
PBLR	Packed bed loop reactor

PH	Pseudo-homogeneous
RDC	Reactive distillation column
SEM	Scanning electron microscopy
SMBR	Simulated moving bed reactor
SDP	Sodium dihydrogen phosphate
SEP	Sulfonated expanded polystyrene
TMA	Tetravalent metal acid
TGA	Thermogravimetric analysis
TPA	Tungstophosphoric acid
UNIFAC	Universal functional activity coefficient
UASB	Upflow anaerobic sludge blanket
WCO	Waste cooking oil
C_{WP}	Weisz-Prater criterion
ZCO	Zirconium chloride octahydrate

CHAPTER 1

INTRODUCTION

1.0 INTRODUCTION

Acrylic acid (AA) is commercially important in chemical industry and it is widely used for the production of acrylic esters which are applied in surface coating, textiles, adhesives, paper treatment, polishes, leather, fibre, detergents and super-absorbent material (Xiaobo *et al*., 2006, and Altiokka and Ödeş, 2009). AA is very toxic to aquatic organism and its' release to the effluents should be minimised (Bajt *et al.*, 1997 and Staples *et al.*, 2000).

Wastewater containing AA (1.8-20 g/l) exhibits high chemical oxygen demand (COD) content which renders direct biological treatment of this water takes extremely long time and requires reactor with high capacity (Stewart *et al*., 1995 and Chen *et al.*, 2008). This wastewater is burned in most of the AA production plant using incinerator which is rather expensive and not environmental friendly (Allison *et al.*, 2011). Several methods such as adsorption and wet oxidation were used to remove AA in the diluted system. Even though both of these methods could remove AA for >98%, its applications are only limited to the wastewater containing AA of 50 to 500 mg/l for adsorption and 1000 to 4000 mg/l for wet oxidation (Silva *et al*., 2003 and Kumar *et al.*, 2010). Distillation and extraction are the conventional methods used to recover AA. These methods consumed substantial energy and suffer with phase separation limitation. Esterification can recover diluted acid by converting the acid to the valuable ester (Arpornwichanop *et al*., 2008). The same idea exploited by Saha *et al*. (2000) and Bianchi *et al*. (2003) for the recovery of diluted acetic acid. The equilibrium condition of the esterification reaction can be shifted towards products by continuously removing the products from the reactant mixture. The combine reaction and separation in a single column has saved energy, increased conversion and avoided catalyst poisoning particularly in the aqueous system (Tuchlenski *et al.*, 2001; Omota *et al.*, 2003 and Schimtt *et al.*, 2004).

1.1 PROBLEM STATEMENT

Esterification of AA with alcohol (butanol, ethylhexanol and propylene glycol) produces acrylates by direct acids catalysed esterification at elevated temperature. This process is a reversible process (Chen *et al.*, 1999; Altiokka and Ödeş 2009; Ostrowski *et al.*, 2011 and Komoń *et al.*, 2013). Homogeneous catalyst is used in the conventional method to accelerate the esterification reaction which consuming days to achieve equilibrium. Strong liquid mineral acids such as sulphuric acid, hydrochloric acid, hydrogen iodide and *p*-toluenesulfonic acid have been used for industrial esterification reaction. In spite of the strong activity of these homogeneous catalysts, it imposed several drawbacks such as corrosion problems, difficult to be separated from the reaction mixture and necessity to be neutralized after reaction (Lilja *et al.*, 2002; Jermy and Pandurangan, 2005; Liu *et al.*, 2006; Peters *et al.*, 2006, and Akbay and Altiokka, 2011). Heterogeneous catalyst has been developed to overcome the aforementioned shortcomings. In addition, heterogeneous catalyst also can suppress the side reactions (Rattanaphra *et al.*, 2011, and Akyalçin and Altiokka, 2012).

Ion exchange material is widely used as heterogeneous catalyst for the esterification reaction because of its special characteristics such as insoluble, good selectivity and specificity (Blagov *et al.*, 2005 and Park *et al.*, 2009). The sulfonated expanded polystyrene (SEP) is an ion exchange catalyst which contains high ion exchange capacity and high accessibility to acid sites (Grossi *et al.*, 2010). The catalyst also is inexpensive because can be synthesised from the waste polystyrene (Bekri-Abbes *et al.*, 2008).

In view of the environmental and economic impacts of the wastewater containing AA, practicability of the recovery of AA from wastewater through esterification should be investigated. A suitable water tolerance heterogeneous catalyst should be identified prior to aqueous esterification and process study.

1.2 OBJECTIVES

In the present work, esterification of pure and diluted acrylic acid with butanol was studied with the objectives of:

1. To synthesise, screening and characterise the suitable heterogeneous catalysts.
2. To study the effect of different important operating parameters.
3. To develop the kinetic model for the reaction.

1.3 SCOPES OF STUDIES

1. The catalysts include SEP, Amberlyst-15, sulphated zirconia, molybdenum zirconia, zirconium phosphate, sulfonated carbon, and zeolite ZSM 5 were tested.
2. The SEP was characterized using scanning electron microscopy (SEM) thermal gravimetric analysis (TGA), Fourier transform spectroscopy (FT-IR) and gas pycnometer.
3. The effect of important operating parameters such as stirring speed, reactant molar ratio, temperature, catalyst loading, reusability and initial water content were investigated.
4. The kinetic study was carried out and fit to different types of model such as Eley-Rideal (ER) model, Langmuir Hinshelwood (LHHW) model and pseudo-homogeneous (PH) model.

1.4 SIGNIFICANCE OF STUDY

Study on the esterification of wastewater containing AA with butanol would contribute to the development of a feasible AA recovery method from the wastewater. Wastewater could be treated while producing value added esters. This method is expected to overcome the economic and environmental problems faced by the existing method such as incineration. Moreover, additional income could be generated through the value added product. The present study also would contribute to the discovery of a water tolerance heterogeneous catalyst for esterification of acrylic acid with water.

1.5 ORGANISATION OF THE THESIS

The subsequent sections of the thesis comprise of chapter 2 (literature review), chapter 3 (methodology), chapter 4 (results and discussion) and chapter 5 (conclusions and recommendations).

Chapter 2 includes the review about the existing treatment methods for the wastewater containing carboxylic acid particularly acrylic acid. The literature also focuses on the potential of AA recovery via the esterification reaction followed by the comparison on the performance of difference types of catalyst. The relevant kinetic models are included.

Chapter 3 describes the materials, apparatus and equipment used to synthesise and characterise the catalyst. The procedures for the catalyst synthesis, catalyst characterisation, catalyst activity testing and the reaction product sample analysis are also delineated in detail.

The results obtained in the present research are discussed accordingly to the following sequence in results and discussion chapter: (1) Catalyst screening, (2) Catalyst characterisation, (3) Studies about the effect of important operating parameters, (4) Equilibrium studies using the best catalyst in the esterification of AA with butanol and (5) Kinetic studies.

In the conclusions and recommendations, conclusions are drawn based on the research findings. Recommendations are suggested to improve the future research work in related area.

CHAPTER 2

LITERATURE REVIEW

2.0 INTRODUCTION

This chapter reviews on the methods used to treat wastewater containing AA and the potential methods to recover AA from the wastewater. There are also reviews on the type of catalysts used for the esterification reaction, particularly on the AA esterification. The corresponding kinetic models were reported for the heterogeneously catalysed AA esterification reaction.

2.1 ACRYLIC ACID

Acrylic acid (AA) has several synonyms names which are propionic acid, acroleic acid, ethylene carboxylic acid and vinyl formic acid. AA is a clear colourless liquid, fuming, and corrosive with acrid odour. AA tends to spontaneous polymerise which can be explosive in confined space. The best storage is above melting point to avoid crystallisation. Table 2.1 summaries the physical properties of AA.

Table 2.1: Physical properties of AA

Property	Acrylic acid
Molecular weight	72.06
Density (g/ml) at 298 K	1.045
Melting point (K)	286
Boiling point (K) at 101 Kpa	414
Vapour pressure (kPa) at 298 K	0.57
Heat of polymerization (kJ/mol)	76.99
Refrective index	1.4185
Critical temperature	615K
Critical pressure (bar)	56.6
Critical volume (cm^3/mol)	208
Accentric factor	0.538
Solubility in water and alcohol	miscible

Source: Kricheldorf, 1991; Ostaniewicz-Cydzik *et al.*, 2014

The demand of AA and its derivatives is increasing as they are the basic building blocks for chemical industry especially for polymeric products. The acrylates are intermediate products of high commercial value due to its properties such as excellent clarity, elasticity, colour retention toughness, easy adhesion, chemical inertness and UV stability. The current production of AA in the petrochemical industry involves two-step gas phase oxidation of propylene. The worldwide productivity of AA in 2003 was more than 3 million tons per year. The production increased to 4.7 million tons in 2006. The global demand was estimated to increase 4.8% per year from year 2010 until 2015.

Half of the production is for acrylates, where approximately 60% is for production of butyl acrylate, BA. The acrylates are used in fiberfill bonding, textile bonding or laminating, flocking, back coating, pigment printing binders, leather finishing, adhesives, super-absorbent materials, detergents and varnishes (Saha and Sharma, 1995; Xiaobo *et al*., 2006; Altiokka and Ödeş, 2009; Ortrowski *et al*., 2011 and Niesbach *et al*., 2013). AA are readily absorbed and rapidly metabolized and excreted primarily as carbon dioxide. Inhalation or exposure from polishes, paints, coating, rug backing, adhesives, plastics, textiles, and paper finish acrylic acids is irritating to the eyes, skin, and respiratory system (Idriss, 2002).

2.2 TREATMENT METHODS OF WASTEWATER CONTAINING CARBOXYLIC ACID

In an acrylic manufacturing unit, the typical wastewater contained 10-20 g/l of acrylic acid, whereas the wastewater from the related petrochemical manufacturing unit contained relatively low concentration of AA (1.8 g/l) (Schonberg *et al.*, 1997 and Kumar *et al.*, 2010). Although the AA is in low concentration, is very toxic to living things especially aquatic organism. AA is severely irritates skin, eyes, respiratory system and gastro-intestinal tract of the human being (Idriss, 2002; Silva *et al.*, 2003 and Kumar *et al.*, 2009). The low concentration of AA in wastewater complicates its recovery and treatment processes. The common industry practice used to destruct the wastewater containing AA is by burning it in a chemical incinerator equipped with after burner and scrubber (Vincolli, 1996).

2.2.1 Biological Treatment

Recovery of organic chemicals is desirable from the view point of green chemistry but it is difficult since the AA concentrations are very low in the wastewater. Activated sludge is used to remove the organic compound from the wastewater. These organic compounds are carbon source for the microbe metabolism which would be converted to carbon dioxide (CO_2) and excess activated sludge. The excess sludge is incinerated to generate CO_2 (Igarashi *et al.*, 2012). Activated sludge relies in the self-assembly of an active microbial which can form flocculants aggregates and separated from effluent by gravity settling. The bacteria are dominant to remove oxygen-demand pollutants and bacterial compositions are not affecting the system (Ibarbalz *et al.*, 2013).

Anaerobic digestion, another method under biological treatments degrades and stabilises the organic materials under anaerobic condition by microorganism which producing carbon dioxide and methane. This process uses low energy, due to its ability to recover energy. It does not produced substantial amount of sludge. The wastewater containing AA can be treated with *Arfhrobacter sp*. strain NO-18 because of its capability to grow with solely acrylic acid as a carbon source. However, the system has low operational stability (Schonberg *et al.*, 1997 and Chen *et al.*, 2008). Stewart *et al.*

(1995) studied on the treatment of wastewater containing acrylic acid with the concentration of 100 to 1500 mg/l using glucose-acetate enrichment culture with volatile suspended solid ranging from 2275 to 2625 mg/l. The acrylic acid can be degraded to less than 1 mg/l (>99%) in 40 days.

Demirer and Speece (1998) studied on the anaerobic treatment of diluted acrylic acid in a single stage upflow anaerobic sludge blanket (UASB) reactor using *Methanosarcina* culture. The influent with the AA concentration of 3000 mg/l bio-transformed into intermediate product (acetic acid and propionic acid) at 95% efficiency after 103 days at a loading rate of 2.7 g/l/day and a hydraulic retention time (HRT) of 26 hours. The COD removal was 45%. The COD removal increased to 97% when double stage UASBs was used.

Synthetic wastewater (85 g/l of COD) containing 0.66% of AA and other components were treated in an anaerobic membrane reactor with the loading at 1 L/day and HRT of 25 days. The COD reduced to 0.6% of COD influent. This reactor showed excellent removal of AA (~100% efficiency) and the volatile organic matter in the wastewater was degraded and converted into methane (Bhattacharyya *et al.*, 2013). The conventional biological treatment method (activated sludge) required extremely long residence time to retain the growth of the organism and large vessel for high reactor capacity. The process efficiency of the biological system was limited by biomass concentration and hydraulic retention time. The biomass concentration was very low due to the diluted wastewater (Chen *et al.*, 2008). The limitation of AA concentration was 100 mg/l for anaerobic treatment that used methanogenic cultures because higher concentration will inhibit the cultures and reduced the performance (Demirer and Speece, 1998 and Huang *et al.*, 2014).

2.2.2 Adsorption

Adsorption is an interracial phenomenon controlled by the nature of the absorbent, absorbate and the solution chemistry. This process is simple operation that operating at operates at ambient temperature and pressure. In the water and wastewater treatment, adsorption using activated carbon is a commonly used treatment method due to high surface, high degree of surface activity, large pore volume and excellent efficiency for organic compound (Duan *et al.*, 2002; Oneto *et al.*, 2004; Chai and Ji, 2012; Cabrera-Lafaurie *et al.*, 2014 and Khan *et al.*, 2014). Kumar *et al*. (2009) studied on the potential of powdered activated carbon for the adsorption of AA in aqueous solution (50-500 mg/l). The maximum adsorption was 36.23 mg/g with optimum dosage of 20 g/l for the initial concentration of 100 mg/l. The removal of AA was >84% within 5 minutes contact time and the residual of approximately 1.6% of the initial concentration. The equilibrium data and kinetic data followed Freundlich isotherm and pseudo-second order model respectively. The adsorption of AA was influenced by the decrease of temperature. Mao and Fung (1997) also studied on adsorption of aqueous AA (0.1 M) using alumina as adsorbent. The studies found that the adsorption of AA on alumina depended on the pH and obeyed Langmuir isotherm which showing the dependence of the adsorption on active surface area and surface chemistry of the adsorbents. At optimum pH (4.5), the maximum adsorption was 727 µmol/g and the equilibrium at 48 hours (100% of plateau value). The adsorption treatment method is only economic and feasible for the wastewater containing minute amount (<500 ppm) of AA (Xu *et al.,* 2013).

2.2.3 Wet Oxidation

Wet oxidation is also known as subcritical hydrothermal oxidation for wastewater effluent which is too dilutes for incineration and too concentrated or toxic for biological treatment (Oneto *et al.*, 2004). Catalyst is the key factor in wet oxidation since AA is thermally stable (553 K) and poorly oxidised below 523 K.

The pressurised reactor was injected 1000 ppm of AA with 6 g/l of catalyst loading, oxygen partial pressure of 15 bar and 350 rpm. Different metal oxide used as catalyst with cerium oxide as support at a molar ratio of 70:30. The highest efficiency of oxidation process was 97.7% using manganese/cerium followed by argentums/cerium (85%) and cobalt/cerium (65.1%) (Silva *et al.*, 2003). Kumar *et al*. (2006) also studied the cerium based catalyst for wet oxidation of diluted AA with the concentration of 5 g/l of AA at different temperatures. The manganese (Mn) and cerium (Ce) was equal to molar. The catalyst loading was 5 g/l and airflow rate was maintained at 0.25-0.3 LPM.

The maximum removal under atmospheric pressure was only 16% after 30 hours at 368 K comparing to the pressurised reactor (14 kg/cm^2) which achieving 86.12% COD reduction after 6 hours at 453 K. Oliviero *et al*. (2000) studied the ruthenium supported on cerium for the treatment of aqueous solution of AA (52 mmol/l) at 433 K and 20 bar for 3 hours. This ceria gave high surface area to insure oxygen activation when AA was adsorbed. The conversion of AA was 100%. The conversion of AA into formic acid and acetic acid did not exceed 40% for the carbon supported catalyst because the low AA adsorption affinity. The wet oxidation treatment is an effective for wastewater containing AA with 2-50 g/l of COD. However, it requires elevated temperature to maintain its high removal efficiency.

2.2.4 Esterification

The treatment methods for wastewater containing AA with various concentrations such as biological treatment, adsorption and wet oxidation have shown the respective shortcomings despite its high efficiency. Furthermore, some of these methods are not appropriate for the targeted wastewater containing AA with the concentration of 4-10 wt%. The limitation of these methods was included in Table 2.2. Esterification of the wastewater containing carboxylic acid with alcohol has been reported as a promising to convert carboxylic acid to a valuable product while purifying the wastewater (Bianchi *et al*., 2003 and Ragaini *et al*., 2007).

Table 2.2: Treatment method for the wastewater containing AA

Treatment	**AA concentration**	**Removal efficiency**	**Drawbacks**	**Reference**
Anaerobic digestion	100-1500 mg/l	>99%	Extremely long residence time	Stewart *et al.*, 1995
	3000 mg/l	95%		Demirer and Speece, 1998
	0.66%	~100%		Bhattacharyya *et al.*, 2013
Adsorption	50-500 mg/l	36.23 mg AA /g adsorbent	Large amount of adsorbent usage	Kumar *et al.*, 2009
	720 mg/l	727 µmol AA /g adsorbent		Mao and Fung, 1997
Wet oxidation	1000 mg/l	97.7%	Effective for 2-50 g/l of COD	Silva *et al.*, 2003
	5000 mg/l	86.12% COD removal	Need high temperature and pressure.	Kumar *et al.*, 2006

Bianchi *et al*. (2003) has implemented the esterification method to recover diluted acetic acid (6 wt%) using n-butanol and 2-ethyl-1-hexanol with Amberlite 200 as catalyst at 372 K for 6 hours. In equimolar condition of acid and alcohol, the efficiency was only 3.4% but when double phase was generated by increasing the volume alcohol, the efficiency increased to 67.9%. Ragaini *et al.* (2005 and 2007) also studied on diluted acetic acid (6-15%) with 2-ethyl-hexanol and Amberlyst 15 was used as the catalyst. The system used was completed with evaporation and condensation with double phase reactant. The conversion achieved was up to 70%. The efficiency of the reaction with double phase reactant was increased because the reaction took place in organic phase. The presence of upper phase where acetic acid was able to migrate and react with alcohol and the water produced migrated to the lower phase.

Previous study has used alcohol in excess in order to achieve high conversion by generating double phase. This can overcome the problems due to the easily leached catalyst active sites and the hydrophilic properties of the reactants. Yagyu *et al.* (2013) studied the single layer of aqueous esterification which adding acetone to form homogeneous mixture. The hydrophobic catalyst (polymer supported sulfonic acid, PS-SO_3H) was used. The reaction proceeded for the 50% acetic acid with equimolar of ethanol. The toluene was used as solvent. The ester yield was 45% after 4 hours. The addition of salt (calcium chloride) increased the yield to 94% after 72 hours. The study also was carried out under solvent free condition. Higher ester yield 76% was achieved in the organic phase as compared to the ester yield in the aqueous phase which was only 7%.

Saha *et al.* (2000) and Arpornwichanop *et al.* (2008) studied the aqueous esterification of acetic acid with butanol using hybrid reactive distillation column to avoid water effect on the catalyst and the reaction. These methods minimize downstream separation process and possessed promising result in the recovery of carboxylic acid from wastewater. The conventional distillation or membrane pervaporation needed a concentrated aqueous acetic acid because the dilute carboxylic acid would increase the reboiler heat duty. The required concentration was up to 65% to achieve the same conversion and yield as obtained in the reaction with pure acetic acid.

2.3 CATALYST FOR ESTERIFICATION

Esterification is the chemical process for making esters which are compounds of the chemical structure R-COOR’, where R and R’ are either alkyl or aryl groups. The common method to prepare esters is to heat a carboxylic acid with alcohol while removing the water that is formed. The chemical structure of the alcohol, the acid and the acid catalyst used in the esterification process affect the reaction (Yadaw, 2010 and Rahman *et al.,* 2012). The esterification reaction is started when the carboxylic acid accepts a proton from proton donor (catalyst). Then, alcohol molecule attacks the protonated carbonyl group to give a tetrahedral intermediate. Proton is lost at one oxygen atom and gained at another to form another intermediate and further loses a molecule of water to gives a protonated ester. Lastly, a proton is transferred to a water molecule to give the ester. This mechanism shows in Figure 2.1.

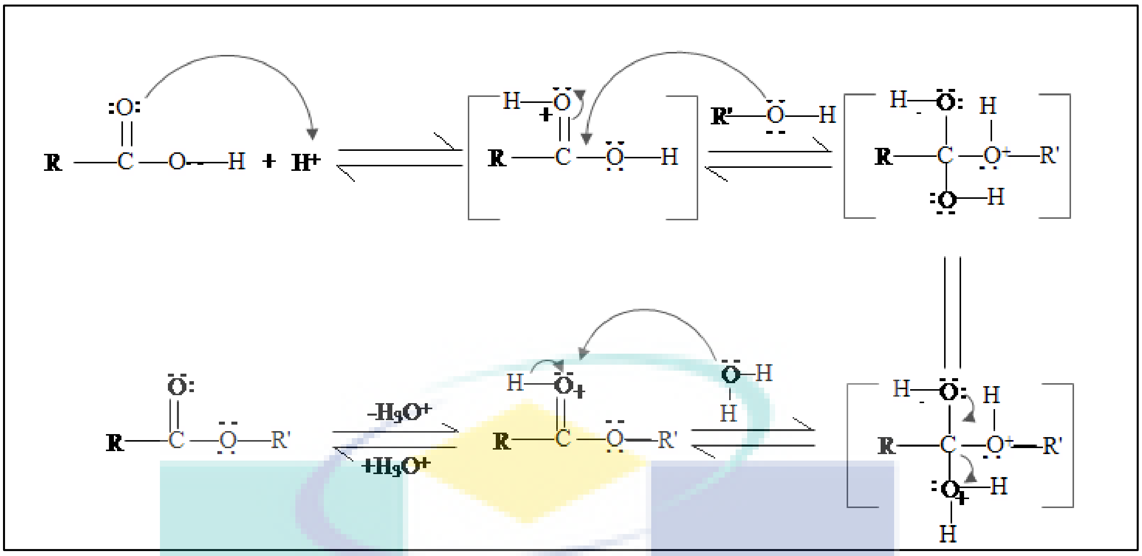

Figure 2.1: Esterification reaction mechanism

Catalyst is required by the esterification to accelerate the process by promoting the protonation of carbonyl oxygen on carboxylic acid group. Protonation then activates the nucleophilic attack by an alcohol to form tetrahedral intermediate. The intermediate will yields ester by disproportion the group (Liu *et al.*, 2005). This esterification processes are commonly synthesised through liquid phase reaction which catalysed either homogeneous (strong mineral acid) or heterogeneous (acidic ion exchange resins) catalyst. These catalysts are Brønsted acid or Lewis acid catalyst type. The Brønsted acid catalysts such as sulphuric acid and hydrochloric acid are usually used to catalyse long fatty acid or tertiary acid due to the sterically hindered substance. The Lewis acid catalyst type is preferred to avoid alcohol dehydration or racemisation and to create the condition that compatible with acid labile group (Hoydonckx *et al.*, 2004).

2.3.1 Homogeneous Catalyst

Homogeneous catalyst is soluble in reaction mixture and widely used in industrial because the economic consideration (Das and Parida, 2006). These catalysts have strong catalytic effect and provide distinguish performance in the reaction rate (Izci and Bodur, 2007 and Ju *et al.*, 2010). Other advantages of using homogeneous catalyst include negligible in mass transfer resistance because of high degree of dispersion and high selectivity towards product (Dunnewijk *et al.*, 2004). Liu *et al.*

(2006) claimed that, the homogeneous catalytic activity was greater because the same phase as reaction mixture has provided higher acid density and free protons availability.

Homogeneous catalyst can be classified in to real homogeneous catalyst and soluble-metal-particle catalyst. The true homogeneous catalyst has single type active site while metal-particle typically consists of multiple types of active site on the metallic surface. These classes of catalyst affect catalyst activity, selectivity, stability, lifetime and recovery. On the other hand, the soluble-metal-particle catalyst with multiple active sites was referred as soluble heterogeneous catalyst based on the Schwartz's modern definition (Widegren and Finke, 2002). It includes polyoxometalates such as phosphotungstic acid and phosphomolybdic acid) (Craig and Christina, 1995).

Despite of the good activity of homogeneous catalyst, it promotes side reactions, necessitates the neutralisation at the end of the process due to its corrosive nature and requires downstream separation.

2.3.2 Heterogeneous Catalyst

Heterogeneous acid catalyst is defined as solids or mixtures of solid used to accelerate chemical reaction without undergoes any transformation but sometimes there are changes in structure and compositions as a result from interaction with reaction mixture (Boreskov, 2003 and Campanati *et al.*, 2003). The catalyst is developed to overcome the shortcoming of homogeneous catalyst (Rattanaphra *et al.,* 2011). These insoluble non-corrosive catalysts are recyclable. It possess higher local concentration of H^+ ions, eases the separation from reaction medium, reduces secondary reaction and minimise waste stream (Silva and Rodrigues, 2005).

Heterogeneous Catalysed for AA Esterification

The ion exchange resin is widely used compared to the other solid catalyst because of it properties which are non-corrosive and easy to separate from reaction mixture. Many studies have been done using ion exchange resin for esterification process (Sharma *et al.*, 2014). Sert *et al*. (2013) and Karakus *et al*. (2014) studied the comparison of the performance between ion exchange resin (Amberlyst 15, Amberlyst 131 and Dowex 50Wx-400) in the esterification of acrylic acid with n-butanol and isobutyl alcohol respectively. The reaction was at temperature of 338 to 358 K, $M_{acid:alcohol}$ of 1:1 to 1:3 and catalyst loading of 10 to 20 g/l. The catalyst activity was depended on the degree of swelling that could enhance the internal mass transport. The gel type, Dowex 50Wx-400 was more effective than the macroreticular catalyst (Amberlyst). However, Amberlyst 131 had given the highest conversion due to the variation of H^+ concentration.

Catalytic activity for different ion exchange resin was also studied by Komoń *et al.* (2013) for the esterification of acrylic acid with 2-ethyl-hexanol at temperature of 333 to 373 K, $M_{acid:alcohol}$ of 7:1-1:7 and catalyst loading of 1-10 wt%. The Amberlyst 70 has achieved highest conversion, 76% as compared to others (Amberlyst 39, Amberlyst 46 and Amberlyst 131) after 6 hours. The reaction mixture was highly polar due to the alcohol and water formed. The swollen catalyst had made the accessibility of the reactants to the active sites easier. Amberlyst 70 had achieved the highest yield because of its acidic strength that was enhanced by chlorine atom in the resin matrix.

Ostaniewicz-Cydzik *et al.* (2014) studied the esterification of AA with methanol using Amberlyst 15 as catalyst in a batch reactor at temperature of 323 to 363 K, $M_{acid:alcohol}$ of 1:2 and 1:3 and catalyst loading of 1 to 3.5 wt%. The catalyst was adsorbed the water (by products) and hence decreasing the reaction rate which giving the conversion of 50% only after 6 hours.

Esterification process is widely used in batch reactor and there is increasingly interest to improve process. Sert and Atalay, (2014) studied on pervaporation-esterification of AA with n-butanol at temperature of 338 to 358 K, $M_{acid:alcohol}$ of 1:4 and 1:8 and catalyst loading of 10 to 20 g/l. Amberlyst 131 was used as catalyst. The continuously removing water from the reactant mixture had increased the conversion because the equilibrium has shifted to the product side. The maximum conversion was 96.3% after 6 hours. This method was proven successful for removing by product (water) because of low energy requirement and able to separate azeotropic mixture. This method also relied on the solubility and transport rate.

Strohlein *et al.* (2006) studied the esterification of AA and methanol in a chromatopraphic reactor using Amberlyst 15 as stationary phase at 333 K and $M_{acid:alcohol}$ of 1:2 and 1:3. The simulated moving bed reactor (SMBR) was viable option to overcome the drawbacks of the conventional production process because the optimal point has yielded the conversion of 98% with complete separation of reaction products at low operating temperature.

Several studies have been done for esterification of AA using different heterogeneous catalyst and compared it with the ion exchange resin. Chen *et al.* (1999) compared the organic resin with HPA supported on cesium (CsHPA) and different solid oxides for esterification of AA with butanol. The reaction were carried out at 353 K, $M_{acid:alcohol}$ of 1:1 and catalyst loading of 0.25 to 1 wt%. The conversion of Nafion was 61.1%. It was the highest followed by the conversion of the reaction catalysed by Amberlyst (33.6%), CsHPA (19%), sulphated zirconia (14.2%), Amberlite (10%), HY (2.3%) and H-mordenite (2.3%). The activity of CsHPA was retained after the addition of water because of the hydrophobic nature of the catalyst surface.

Altiokka and Ödeş, (2009) also studied the comparison of resin (Amberlyst 15 and Amberlyst 36) with CsHPA for esterification of AA with propylene glycol at temperature of 333 to 358 K, $M_{acid:alcohol}$ of 1:1 and catalyst loading of 3.11, 5.06 and 8.46 wt%. The Amberlyst 36 has the highest reaction rate followed by Amberlyst 15 and CsHPA. However, CsHPA possessed highest selectivity of 100% compared to the selectivity of the Amberlyst 15 and Amberlyst 36, which were 74% and 49% respectively. Dupont *et al.* (1995) also studied the HPA as catalyst but using activated carbon as support for esterification of AA with butanol. The reaction was under a flow condition. The activity of catalyst reduced to 13% from 95% after 670 minutes for the recycled catalyst because of dissolution of support in reaction medium.

Saha and Sharma, (1995) studied on the esterification reaction of AA with cyclohexene using different catalyst which were cation exchange resin (Indion 130), acid treated clay (Engelhard F-24), Amberlyst 15 and Amberlite IR-200 in the autoclave and packed distillation column reactor. The reaction were carried out at temperature of 343 to 373 K, $M_{acid:alcohol}$ of 1:1 to 1:5 and catalyst loading of 5 to 15 wt%. The conversion of the reaction catalysed by Engelhard F-24 and Amberlite IR-120 were only 10% and 13% respectively. These conversions were relatively low than the conversion achieved by Indion 130 and Amberlyst 15 which were 50% and 46% respectively. The higher degree of swelling was in Indion 130 and Amberlyst 15 which enhanced the accessible of the reactants. The addition of 1 wt% of water resulted in a sharp decreased of reaction rate because of water molecule permeated easily to the pores of the ion exchange resin and attached to the 4 active sites (sulphonic acid groups).

Essayem *et al.* (2007) studied on the effect of promoters (manganese and ferum) towards sulfated zirconia in the esterification of acrylic acid with butane at temperature of 343 K, $M_{acid:alcohol}$ of 1:0.9 and catalyst loading of 11 g. The sulphated zirconia was as active as resin and more selective. Nevertheless, the catalyst was deactivated rapidly. The promoter did not increase the reaction rate but improved the resistance to deactivation which avoided the formation by passivating the surface or neutralizing the sites responsible for the poisoning.

The different type of heterogeneous catalyst and its performance in the esterification of AA are summarised in Table 2.3.

Table 2.3: Heterogeneous catalyst for the esterification of AA with different alcohol

Alcohol	**Reaction time (hour)**	**Temperature (K)**	**Molar ratio ($M_{acid:alcohol}$)**	**Catalyst loading**	**Catalyst/ conversion (%)**	**References**
Cyclohexane	6	343-373	1:1-1:5	5-15 wt%	Indion 130/ 95.8 Engelhard F 24/ NA Amberlite- IR-120/ 52.7 Amberlyst 15/92.9	Saha and Sharma, 1995
Butanol	~11	353	1:1.35 and 1:0.75	NA*	HPA supported by activated carbon/ 94	Dupont *et al.*, 1995
1-butanol	5	353	1:1	0.25-1 wt%	CsHPA/19 Nafion-H/ 61.1 Amberlyst 15/ 33.6 Sulphated zirconia/ 14.2 Amberlite 200C/ 10 HY/ 2.3 H-mordenite/ 2.3 Nafion-SiO_2/ 26.3	Chen *et al.*, 1999
Methanol	~2	333	1:0.4	NA*	Amberlyst 15/98	Strohlein *et al.*, 2006
1-butene	4	343	1:0.9	11 g	ZS/ 58 ZFS/24 ZMS/54 ZMFS/62	Essayem *et al.*, 2007

Table 2.3: Continued

Alcohol	Reaction time (hour)	Temperature (K)	Molar ratio (M $_{acid:alcohol}$)	Catalyst loading	Catalyst/ conversion (%)	References
Propylene glycol	7	333-358	1:1	5.54 wt%	Amberlyst 15/ 45	Altiokka and Ödeş, 2009
	4			5.57 wt%	Amberlyst 36/ 45	
	3			4.73 wt%	CsHPA/ 4	
2-ethyl hexanol	6	333-373	7:1-1:7	1-10 wt%	Amberlyst 39/ 68.9	Komoń *et al.*, 2013
					Amberlyst 46/ 64.5	
					Amberlyst 70/ 76	
					Amberlyst 131/62.2	
n-butanol	4	338-358	1:1-1:3	10-20 g/l	Amberlyst 15/ 24.1	Sert *et al.*, 2013
					Amberlyst 131/ 43.3	
					Dowex 50Wx-400/ 36.1	
Isobutyl alcohol					Amberlyst 15/ 21.1	Karakus *et al.*, 2014
					Amberlyst 131/ 37.2	
					Dowex 50Wx-400/ 32.8	
n-butanol	NA*	323-363	1:2 and 1:3	1-3.5 wt%	Amberlyst 15/ 50	Ostaniewicz-Cydzik *et al.*, 2014

*NA denotes not available

Heterogeneous Catalysed for the Esterification of Other Carboxylic Acid

Ion exchange material was widely used as heterogeneous catalyst for the esterification reaction because of its special characteristics such as insoluble, good selectivity and specificity. Park *et al.* (2009) studied the water effect on the esterification of oleic acid with methanol catalysed by Amberlyst 15. The reaction was carried out in a batch reactor at temperature of 333 to 353 K and $M_{acid:alcohol}$ of 1:3 and 1:6. The conversion was 91% after 6 hours for the reaction without water. The catalytic activity was decreased rapidly even though the water content was only 1 wt% of oleic acid because water had poisoned the catalyst active sites.

Pappu *et al.* (2012) studied the effect of carbon number in alcohol for the esterification of butyric acid catalysed by cation exchange resin at temperature of 373 to 423 K, $M_{acid:alcohol}$ of 1:4 to 1:6 and catalyst loading of 4 to 12 wt%. The reaction rate was decreased with the increasing of alcohol carbon chain length because the polarity and steric effect of alcohol had decreased the accessibility of OH group.

Liu *et al.* (2006) studied the effect of carbon number in carboxylic acid for the esterification with methanol using SAC-13. The reactions was at temperature of 333 K, $M_{acid:alcohol}$ of 1:2, catalyst loading of 1.09 g and reaction time of 1 hour. The carboxylic acid reactivity was decreased with increasing alkyl chain because the inductive effect and steric effect. The inductive effect facilitates the protonation of the carbonyl oxygen but it also lower the electrophilicity of the carbonyl carbon which increased the energy needed for the nucleophilic attack.

Oguzhan, (2014) studied the esterification of oleic acid with methanol catalysed by Amberlyst 46 at temperature of 323 to 373 K, $M_{acid:alcohol}$ of 1:1 to 1:9 and catalyst loading of 0 to 15 wt% . The conversion was 98.6% after 2 hours and the catalyst can be reused for ten times with less than 2% of activity loss. The conversion was decreased at high molar ratio because the increasing amount of alcohol prevents the interaction between reactants and blocked the catalyst active site.

Marchetti and Errazu, (2008) compared the esterification oleic acid using different catalyst and alcohol at 328 K, $M_{acid:alcohol}$ of 6.13:1 and catalyst loading of 2.6 wt%. The conversion of enzyme Lipozyme was the highest compared to the other catalyst. The initial reaction rate seems higher when present of small amount of water but the catalyst might deactivated and shift the reaction towards reactant when the reaction produced more water. The addition of triglycerides allowed a higher conversion because the water produced was small compared to the reaction volume. The solubility of alcohol and oleic acid also affected the reaction.

Tetravalent metal acid (TMA) is one of the inorganic ion exchange with robust properties in thermal stability, chemical resistivity and ion exchange characteristics. These catalysts react as cation exchange using its' hydroxyl groups (H and –OH). Zirconium phosphate is important class in TMA which has been widely studied (Feng *et al.,* 2006; Jayswal and Chudasama, 2007; Patel *et al.,* 2008, and Thakkar and Chudasama, 2009). It is a promising heterogeneous catalyst since it is thermal stable, tolerate to water and active in esterification reaction. It can be reused after recovering by a simple filtration (Kamiya *et al.,* 2004 and Sinhamahapatra *et al.,* 2010). Kamiya *et al.* (2004) studied the esterification reaction of acetic acid with ethanol in batch reactor using zirconium phosphate as catalyst at temperature of 343 K, $M_{acid:alcohol}$ of 1:1 and catalyst loading of 0.8 g. The conversion was 20% after 2 hours. The catalyst was water tolerant and can be reused up to 5 times. There are two different sites which may responsible for catalytic activities which are hydroxyl groups (Brønsted sites) and Lewis acid sites. The catalytic activity was not all controlled by hydroxyl group and the Lewis acid sites also play a role in the catalytic reactions. A large amount of water was being absorbed on the catalyst which shows that the zirconium phosphate was hydrophilic but the limited of acid sites was surrounded by hydrophobic surface which avoids the water attacks (Alberti *et al.,* 2001, and Asghari and Yoshida, 2006).

Expanded polystyrene (EPS) is popular in packaging or insulating material in various industry which global consumption exceeds 3 million ton with increased approximately 6% because its characteristics such as lightweight, low thermal conductivity, chemical resistance, dimensional stability, buoyancy, low cost, hygienic appearance and high impact resistance (Sekharan *et al*., 2012). This material only use one time and disposed as bulky waste in large quantity which became serious environmental issues. The EPS usually end up in landfills or incinerated. Due to high cost of disposal and growing public opposition in land filling, there are more strategies of recycling EPS. The reduction in effective methods for recycling EPS will have huge impact in environment (Inagaki *et al*., 1998; Landim *et al.*, 2007; Bhutta *et al*., 2010; Morales *et al.*, 2010 and Sekharan *et al*., 2012). Several techniques have been applied to recycle EPS which are the material, chemical and thermal recycling. Material recycling is to reuse the material which has been used in plastic processing industries. Thermal recycling is to get thermal energy but require high calorie incinerator and produced harmful gas (dioxin and hydrogen chloride). Chemical recycling is a method to convert into styrene or hydrocarbures but usually involve hazardous solvents. Sulfonation process is one of the new efficient techniques to recycle EPS. This process is done by converting the used EPS into the functional polymer which are more valuable than virgin polymer or hydrocarbures (Bekri-Abbes *et al*., 2008 and Poletto *et al*., 2010).

Huang *et al*. (2014) studied on the esterification of citric acid with n-butanol using sulfonated and carbonized SEP as catalyst. The conversion was 94.8% after 4 hours at temperature of 423 K, $M_{acid:alcohol}$ of 0.05:0.2 and catalyst loading of 0.6 g. The catalyst can be reused for five times without any significant reduction. Grossi *et al*. (2010) also used SEP as the heterogeneous catalyst in study about esterification of oleic acid and ethanol. The catalyst was synthesised using simple sulfonation method. Almost 100% yield was achieved after 8 hours at $M_{acid:alcohol}$ of 0.00745:2.19 and catalyst loading of 25 mg. The high yield was not only depended on the acid sites but also resulted from the water adsorption by the sulfonated SEP during the reaction.

Zatta *et al*. (2011) studied on raw halloysite as catalyst for the esterification reaction between lauric acid and alcohol (methanol and ethanol) at temperature of 433 K, $M_{acid:alcohol}$ of 1.35:1 to 1:12 and catalyst loading of 0 to 15 wt%. The increasing amount of catalyst was increased the number of active sites which gave the positive effect on conversion. The conversion was increased with molar ratio. Nevertheless, the conversion was decreased at the molar ratio of 1:12 due to the presence of water or the effect of fatty acid dilution. There were gradually decrease in the reusability catalyst due to the increased particle size and the lower surface area.

Operating conditions for heterogeneously catalysed esterification of other carboxylic acid with different alcohol has been summaries in Table 2.4.

Table 2.4: Heterogeneous catalyst for the esterification of other carboxylic acid with different alcohol

Catalyst	Alcohol	Acid	Reaction time (h)	Temperature (K)	Molar ratio ($M_{acid:alcohol}$)	Catalyst loading	Conversion (%)	References
Zirconium phosphate	Ethanol	Acetic acid	2	343	1:1	0.8 g	20	Kamiya *et al.*, 2004
SAC-13	Methanol	Acetic, propionic, butyric, hexanoic and caprylic acid	1	333	1:2	1.09 g	NA*	Liu *et al.*, 2006
Zeolite	Ethanol, Methanol and butanol	Oleic acid	4	328	6.13:1	2.6 wt%	23	Marchetti and Errazu, 2008
Dowex Monosphere 550A							15	
Lipozyme							95	
SEP	Ethanol	Oleic acid	8	NA*	0.00745:2.19	25 mg	~100	Grossi *et al.*, 2010
Amberlyst 15	Methanol	Oleic acid	6	333-353	1:3 and 1:6	NA*	91	Park *et al.*, 2009
Raw hallosite	Methanol	Lauric acid	2	433	1.35:1-1:12	NA*	95	Zatta *et al.*, 2011
	Ethanol						87	
Amberlyst 15, Amberlyst 36, Amberlyst BD 20 and Amberlyst 70	Methanol, Ethanol, propanol, butanol and ethyl hexanol.	Butyric acid	3	373-423	1:4-1:6	4-12 wt%	NA*	Pappu *et al.*, 2012

Table 2.4: Continued

Catalyst	Alcohol	Acid	Reaction time (h)	Temperature (K)	Molar ratio ($M_{acid:alcohol}$)	Catalyst loading	Conversion (%)	References
SEP	n-butanol	Citric acid	4	423	0.05-0.2	0.6 g	94.8	Huang *et al.*, 2014
Amberlyst 46	Methanol	Oleic acid	2	323-373	1:1-1:9	0-15 wt%	98.6	Oguzhan, 2014

*NA denotes not available

2.3.3 Biocatalyst

Lipase or triacylglycerol acylhydrolase is a commercial enzyme that used as catalyst in esterification reaction between carboxylic acid and alcohol, hydrolysis of ester and transesterification between ester and acyl group (Shin *et al*., 2002). This enzyme used in esterification to produce products such as emulsifiers, surfactants and flavour ester. Lipase usually used in the organic synthesis but needs to immobilize to make it more effective (Kartal *et al*., 2011). The immobilize lipase usually used nanostructured materials which high surface area, volume ratio that improve enzyme loading and catalytic efficiency. The main problem is to recover the immobilize lipase that limited which used magnetic nanoparticles. The alternative support is covalent binding, entrapment and adsorption (Jiang *et al*., 2008).

Studies have been reported on the esterification of AA using lipase (Novozym 435) as catalyst to produce sugar ester. Park *et al*. (2004) studied on the esterification of β-methylglucoside (β-MG) with AA in different solvent (1,4-dioxane,acetonitrile, acetone, t-butannol and t-amyl alcohol) at temperature of 318 to 328 K, concentration of β-MG of 30 to 60 g/l, $M_{sugar:AA}$ of 1:3 to 1:5 and enzyme concentration of 1 to 5% w/v. 60 g/l of β-MG was used for the effective and short reaction time. The maximum conversion was 59.3% at temperature of 323 K after 12 hours. The catalyst had been removed from reaction mixture by evaporation at 333 K under reduced pressure. Tsukamoto and Franco, (2009) studied on the esterification of D-fructose with AA in tert-butanol as solvent. The reaction were carried out at temperature of 318 to 338 K, $M_{sugar:AA}$ of 1:1 to 1:5 and enzyme loading of 0.7 to 2.1 g. The initial rate and sugar ester yield was affected by the solubility of sugar and solvent used

Several studies have been done using biocatalyst for the esterification for the other carboxylic acid. Zaidi *et al.* (2002) studied the esterification of fatty acid (butanoic acid and oleic acid) with n-butanol and oleyl alcohol using nylon-immobilized lipase in n-hexane. The reaction was carried out at 277 to 333 K and catalyst loading of 25 to 100 g/l. The yield was nearly 100% after 10 hours of reaction. The substrate acidity was influencing the enzyme activity. The acid and alcohol had inhibiting effect on the enzyme catalytic function due to the decreasing pH of the reaction mixture and competitive inhibition by the reactants which act as dead-end inhibitor. The reaction rate was faster when more nucleophile of alcohol.

Raita *et al*. (2011) studied the esterification of fatty acid with ethanol catalysed by cross-linked protein coated myrocrystalline (CL-PCMC) lipase in tert-butanol. The highest yield was >95% after 6 hours at temperature of 323 K, $M_{acid:alcohol}$ of 1:4 and catalyst loading of 20 wt%. The increasing yield due to nucleophile concentration can be explained by the sensitivity of biocatalyst to the nucleophile (ethanol) in the reaction. The addition of solvent increased the yield because of the stabilization of lipase from nucleophilic inactivation by linear low molecular weight alcohols.

Rahman *et al*. (2012) studied on the esterification of various fatty acids with oleyl alcohol catalysed by tetraethylammonium amino acid ionic liquid coated lipase (ILs) in hexane. The catalyst was favoured for fatty acid with medium chain length especially lauric acid with yield up to 87% after 1 hour at temperature of 323 K, $M_{acid:alcohol}$ of 1:2 and catalyst loading of 15 mg because the longer chain were the excellent acyl donor. The enzyme activity was decreased with the relatively long chain because of the bulky chain moiety, hindered the nucleophilic attack and restrain the molecule from free rotation in enzyme’s acyl binding site.

Operating conditions for biocatalyst catalysed esterification of carboxylic acid with different alcohol has been summaries in Table 2.5.

Table 2.5: Biocatalyst for the esterification of carboxylic acid with different alcohol

Carboxylic acid	**Alcohol/ substrate**	**Solvents**	**Catalyst**	**Temperature (K)**	**Molar ratio ($M_{acid:alcohol}$)**	**Catalyst loading**	**Reaction time (h)**	**Yield (%)**	**References**
Butanoic acid and oleic acid	n-butanol and oleyl alcohol	n-hexane	nylon-immobilised lipase	277-333	1:1	25-100 g/l	10-12	~100	Zaidi *et al.*, 2002
Acrylic acid	β-methylglucoside	1,4-dioxane, acetonitrile, acetone, t-butanol and t-amyl	Novozym 435	318-328	1:3-1:5	1-5% w/v	12	59.3	Park *et al.*, 2004
Acrylic acid	D-fructose	Tert-butanol	Novozym 435	318-338	1:1-1:5	0.7-2.1g	NA*	NA*	Tsukamoto and Franco, 2009
Fatty acid	Ethanol	Tert-butanol	CL-PCMC lipase	323	1:4	20%	6	>95	Raita *et al.*, 2011
Adipic acid, lauric acid, myristic acid, stearic acid and oleic acid	Oleyl alcohol	hexane	ILs	323	1:2	15 mg	1	87	Rahman *et al.*, 2012

*NA denotes not available

2.4 REACTION KINETICS FOR HETEROGENEOUSLY CATALYSED ESTERIFICATION REACTION

Kinetics of catalytic reaction is one of the key to understand the rate behaviour of the catalytic reactions and the reaction mechanism in development of reactor design (Johannessen *et al.*, 2000). The kinetics also helps to select the optimum condition to get the maximum yield. Kinetics is needed in analysing the reaction process and controlling the reaction parameters (Johannessen *et al.*, 2000; Sayyed Hussain *et al.*, 2010; Tesser *et al.*, 2010 and Shi *et al.*, 2011). The reaction phases also need to be considered such as used heterogeneous catalyst which has multiphase catalytic reactions. The interphase mass transfer steps need to be included in overall reactions (Chaudhari *et al.*, 2001). The reaction mechanism can be elucidated using different type of kinetic model. The model must fit with the experimental data, have random residuals, least sum of squares and give positive activation energy (Teo and Saha, 2004).

2.4.1 Pseudo-Homogeneous (PH) Model

The model does not include the adsorption effect which the reactant and product adsorbed and desorbed without any resistance. This model usually successful used in polar reaction (Yadav and Thathagar, 2002 and Yixin *et al*., 2009). The general rate equation is shown in Eq. (2.1).

$$-r_A=-\frac{dC_A}{d_t}=k_f\left(C_AC_B-\frac{C_EC_W}{K_{eq}}\right) \tag{2.1}$$

where subscripts *A*, *B*, *E*, and *W* are acid, alcohol, ester and water respectively. The k_f is forward reaction rate, *C* is concentration and K_{eq} is an equilibrium constant. Arrhenius law is used to determine the activation energy for temperature dependency of rate constant (Izci and Bodur, 2007 and Shi *et al.*, 2011).

Altiokka and Ödeş, (2009) had compared the performance of Amberlyst 15 and Amberlyst 36 for the esterification of acrylic acid with propylene glycol at temperature of 333 to 358 K and catalyst loading of 3.11, 5.06 and 8.46 wt%. Amberlyst 15 was chosen as the best catalyst for the kinetic study in a batch reactor at different temperatures and initial reactant molar ratios. The simultaneous dimerisation/polymerisation of acrylic acid and products, in addition to the reversible esterification reaction, was considered in the PH kinetic equations development. The activation energy was 80.37 kJ/mol. A reasonably good agreement between the predicted and experimental concentration profile was found. It was also concluded that the high selectivity of hydroxypropyl acrylate only can be maintained at low conversion levels of acrylic acid.

The reaction kinetics of neopentyl glycol esterification with propionic acid was studied in a batch reactor at temperature of 373 to 408 K and catalyst loading of 0.29 wt%. The reaction was catalysed by a heterogeneous resin (DOWEX 50WX2). The kinetic parameters, pre-exponential factors and activation energies were estimated for the PH model and their reliability was studied using the Markov chain Monte Carlo (MCMC) method. It was proven that the most reliable kinetic parameters were determined by taking the side reactions (monoester esterification and disproportionation) into account. This kinetic model had coefficient of determination (R^2) around 0.97 indicated good agreements between the measured and calculated concentrations in different circumstances (Vahteristo *et al*., 2007).

The esterification reactions of lactic acid with iso-butanol and n-butanol had been studied by Yixin *et al.* (2009) in the presence of acid ion-exchange resin Weblyst D009 at temperature of 333 to 363 K, $M_{acid:alcohol}$ of 1:1 to 1:4 and catalyst loading of 1.5 to 6 wt%. Experimental data was correlated by using the PH, Langmuir-Hinshelwood and Eley-Rideal models. It was found that these three models were comparably accurate if the nonideality of the liquid phase was taken into account by using activities instead of molar fractions. Nevertheless, PH model was preferred due to its simple mathematical form with the R^2 was approximately 1. The activation energy was 54.3 kJ/mol.

Kara and Erdem, (2011) studied on the sulfonic acid functionalized magnetic-poly (divinylbenzene-4-vinylpyridine) microbeads (m-poly (DVB-4VP)) as heterogeneous catalyst for the esterification between propionic acid and methanol. The catalytic activity was compared with commercial Amberlyst 15 and Dowex 50WX2. The reaction was carried out in flask with temperature controlled by shaking water bath. The reaction were carried out at temperature of 313 to 348 K, $M_{acid:alcohol}$ of 1:1, catalyst loading of 0.5 wt% and 1,4-Dioxane as solvent. The conversion of Amberlyst 15 and Dowex 50WX2 were 15% and 30% respectively. However, the esterification conversion catalysed by m-poly (DVB-4VP-20%SO_3H) was 46%. The kinetics was followed PH second order kinetic and the activation energy was 38.5 kJ/mol.

The kinetics of catalytic esterification of amyl alcohol with acetic acid was carried out in a pulse fixed-bed vertical flow type micro reactor at temperature of 423 to 523 K over 20 and 30 wt% of 12-tungstophosphoric acid (TPA) loaded on tin oxide (SnO_2). The kinetics was monitored using 0.01, 0.03, 0.06 and 0.08 g catalyst and $M_{acid:alcohol}$ of 1:1 to 1:5. It was found that the catalytic activity mainly depended on the TPA coverage and the highest activity corresponding to the catalyst with 20 wt% TPA. This may be attributed to the highest surface area and the maximum number of Brønsted acid sites of the catalyst. The reasonably fit between the experimental data and PH kinetic model support that the esterification reaction obeyed the first order kinetics in all cases. The mechanism of the reaction occurs through the protonation of the acetic acid by the Brønsted acid sites. Subsequently the protonated acetic acid intermediate reacts with amyl alcohol to form the corresponding ester and water. The reusability study proved that the catalyst was stable and active (Rahman and Khder, 2008).

Brahmkhatri and Patel, (2011) studied the esterification of oleic acid and methanol catalysed by supported TPA which anchored to SBA-15. The esterification was carried out at temperature of 303 to 323 K, $M_{acid:alcohol}$ of 1:6 to 1:60 and catalyst loading of 25 to 150 mg. The catalyst activity was comparable to sulphuric acid. Kinetic studies was showed that the reaction was followed the PH model. The reaction was found to follow the first order and the activation energy was 44.6 kJ/mol. Meanwhile, the kinetic for the esterification of lauric acid and 1-butanol catalysed by TPA supported by MCM-41 at 343 to 373 K, $M_{acid:alcohol}$ of 1:1 to 1:3 and catalyst loading of 100 to 200 mg followed the PH second order model. The activation energy was 78 kJ/mol (Brahmkhatri and Patel, 2012).

Srilatha *et al*. (2012) studied on the esterification of rice bran fatty acid with methanol catalysed by cesium-exchange TPA at temperature of 313 to 338 K, $M_{acid:alcohol}$ of 1:5 to 1:25 and catalyst loading of 0.01 to 0.08 g/cm^3. The kinetic studies were well described by PH and followed first order reaction. The activation energy was 37.09 kJ/mol.

The esterification of oleic acid in subcritical methanol using zinc acetate has been studied using batch-type autoclave. The reactions were carried out at temperature of 433 to 493 K, pressure of 3 to 10 Mpa, $M_{acid:alcohol}$ of 1:1 to 1:10 and catalyst loading of 1 wt%. The reaction was not influenced much by pressure since the reactants were soluble. Conversion reached 95% at 493 K but only 60% at 333 K due to the hydrophobic nature of supercritical methanol. At high temperature, the low polar of oleic acid can be well soluble in supercritical methanol and form a single phase to promote the esterification reaction. The experiment data was best fitted with PH kinetic equation with the reaction order of 2.2. The activation energy was lower than previous research which 32.62 kJ/mol due to the promoting effect of subcritical methanol and the catalyst (Song *et al*., 2009).

Gan *et al.* (2010) studied the waste cooking oil (WCO) esterification in three neck flask with reflux condenser at 700 rpm, 100 g of WCO. The ferric sulphate conversion was 97.22% after 4 hours for catalyst loading of 2 wt%, temperature of 368 K and $M_{oil:alcohol}$ of 1:10. The reaction kinetics followed the PH model when the catalyst loading was 2 wt% and below because the catalyst was dissolved in methanol and water. The metal salt will form complexes $(Fe\ (H_2O)_6]^{3+}$) in transition metal ion driven the esterification process. The higher catalyst loading not followed the PH phase because of the catalyst was super-seeded due to the two phase reaction mixtures.

Carbon based is promising solid catalysts which have chemical inertness, superior mechanical and thermal stability. Sulfonated mesoporous carbon was used for the esterification of oleic acid with methanol in 20 ml autoclave at temperature of 338 K, catalyst loading of 50 mg, 1 g oleic acid and 8 ml methanol. The catalytic activity was higher than Amberlyst 15 because the catalyst had good dispersion in methanol although the strong acid density was much lower (five times turnover frequency). The kinetic study showed the good correlation with pseudo-first order model because of the amount of methanol was 66 times of oleic acid (Geng *et al*., 2011).

Shu *et al*. (2011) studied on the esterification using carbon based catalyst that prepared by sulfonation of carbonize vegetable oil asphalt and petroleum asphalt at temperature of 453 to 493 K, $M_{acid:alcohol}$ of 1:21 and catalyst loading of 0.5 wt%. The kinetic was studied for the simultaneously reaction of esterification and transesterification. Although the kinetic was controlled by mass transfer but due to reaction in high pressure with stirring, the immiscibility between reactant was improved. The reaction was followed the PH second order model where chemical reaction controlled the kinetics since the mass transfer was neglected.

Geng *et al*. (2012) studied on the esterification of oleic acid with methanol catalysed by Ph-SO_3H modified mesoporous carbon at temperature of 338 K, 1 g of acid, 8 ml of alcohol and catalyst loading of 20 mg. The catalyst was synthesised by covalent grafting of Ph-SO_3H groups on mesoporous carbon via the diazonium salt. The sulphuric acid was used for sulfonation. The catalyst had three times rates constant and eight times turnover frequency compared to Amberlyst 15 for the same conditions in the esterification of oleic acid with methanol in autoclave. The kinetic data was fitted the pseudo-first order equation. The catalyst activity was similar to the sulphuric acid.

Rattanaphra *et al*. (2011) studied on the esterification of myristic acid with methanol using sulphated zirconia which prepared by solvent free method. In kinetic study, the parameters that had been investigated were temperature (393-443 K), catalyst loading (1-3 wt%) and molar ratio of oil to methanol (1:4-1:20). The modelling that fitted the data was second order PH model which gave correlation between 0.952-0.990. The activation energy was much lower from the previous study which was 22.51 kJ/mol.

Propyl sulfonic acid functionalized SBA-15 mesoporous catalyst (HSO_3SBA-15) was adopted by Hermida *et al*. (2011) for the monoglyceride synthesis through the glycerol esterification with lauric acid under reduced pressure to continuously removed water formed. Effects of various reaction parameters such as reaction temperature (413–

433 K), catalyst loading (1–5 wt%) and glycerol/lauric acid molar ratio (2:1 and 4:1) on lauric acid conversion and products selectivity were studied and correlated with reaction scheme and kinetic model. The reaction pathways were deemed to follow irreversible parallel reactions that involved a series of glycerol esterification with lauric acid reactions that occurred at the same time to form monoglyceride, diglyceride and triglyceride. These reactions could be modelled as irreversible parallel reactions and the kinetic data were successfully fitted to a PH second order kinetic model. The apparent activation energy for monoglyceride formation using a catalyst loading of 5 wt% and glycerol/lauric acid molar ratio of 4:1 was found to be 42 kJ/mol. The HSO_3SBA-15 catalyst could be reused up to four times without significant loss of catalytic activity.

Adam *et al.* (2012) used L-(N-α-acetylphenylalanine)-ruthenium (III) complex (RHAPhe-Ru) immobilized on silica for the production of ethyl acetate. It gave the conversion of 82% and selectivity of 100%. The reaction was carried out in the 50 ml bottom flask with stirrer and condenser. The catalyst loading was 0.10 g, temperature was 358 K, $M_{acid:alcohol}$ was 1:1 and the duration for reflux was 9 hours. The reaction followed the PH second order rate equation. The terminal –Cl in the catalyst formed hydrogen bond with hydroxyl group of acid. The carbonyl group in acetic acid interacted with ruthenium and formed six member rings (transition state). The transition state created partial positive charge on carbonyl group which would be easily attacked by alcohol to form ester. The activation energy of the reaction was 82.2 kJ/mol.

Sarkar *et al.* (2010) studied on the esterification of oleic acid with ethanol catalysed by mesoporous SnO_2/WO_3 (SW) as catalyst. The reaction took place in flask with reflux condenser, thermometer and sampling system. The system was placed in the oil bath. The efficiency of the catalyst was similar to H_2SO_4 with conversion up to 90% after 2 hours of reaction at temperature of 353 K, 0.1 g of SW and $M_{acid:alcohol}$ of 1:120. While non-catalyse reaction only produced 10% conversion even after 12 hours. The kinetic order of the reaction was pseudo-first order which depend on the concentration of oleic acid and catalyst. The concentration of ethanol considered constant. The activation energy was 39.5 kJ/mol.

There is an increasing interest in loading organophosphonic acids on zeolite because of their structural variety and great economic importance recently. Chen *et al.* (2011) investigated the esterification reaction of n-butyl acetate production using PA/NaY (PA = 1-hydroxyethylidenediphosphonic acid) in a flask fitted with a stirrer and a thermometer. The kinetic data were generated by varying the molar ratio, $M_{acid:alcohol}$ of 1:2 to 1:6 and temperature of 393 to 403 K. Kinetic models for the esterification reaction catalysed by PA/NaY were established, and the results were found that the second order PH mechanism was better at describing the kinetics of this esterification than the Langmuir Hinshelwood mechanism. It was found that the activation energies of the forward and reverse reactions were 34.18 kJ/mol and 57.70 kJ/mol, respectively. With the loading of PA on zeolite, the reactants and products were not adsorbed on the catalyst surface during the reaction and hence diverse from the typical reaction mechanism of the pure zeolite for esterification reaction (Schildhauer *et al.*, 2009).

The kinetic model used depending on the reactant used, reaction condition and the type of catalyst. The PH model that used to elucidate the reaction mechanism are summarised in Table 2.6.

.

Table 2.6: Summaries of PH kinetic modelling

Catalyst	Acid	Alcohol	Molar ratio ($M_{acid:alcohol}$)	Temperature (K)	Catalyst loading	Ea (kJ/mol	Reaction order	References
Dowex 50WX 2	Propionic acid	Neopentyl glycol	NA*	373-408	0.29 wt%	NA*	NA*	Vahteristo *et al.*, 2007
Tin oxide supported TPA	Acetic acid	Amyl alcohol	1:1-1:5	423-523	0.01-0.08 g	NA*	1	Rahman and Khder, 2008
Amberlyst 15 and Amberlyst 36	Acrylic acid	Propylene glycol	NA*	333-358	3.11, 5.06, and 8.46 wt%	65-103	NA*	Altiokka and Ödeş, 2009
Zinc acetate	Oleic acid	Methanol	1:1-1:10	433-493	1 wt%	32.62	2.2	Song *et al.*, 2009
Weblyst D009	Lactic acid	Iso-butanol	1:1-1:4	333-363	1.5-6 wt%	65.57	NA*	Yixin *et al.*, 2009
		n-butanol	1:1:1:3			54.34		
Ferric sulphate	Fatty acid	Methanol	1:6-1:15	303-333	0-4 wt%	NA*	NA*	Gan *et al.*, 2010
SW	Oleic acid	Ethanol	1:120	353	0.1 g	39.5	1	Sarkar *et al.*, 2010
TPA anchored to SBA-15	Oleic acid	Methanol	1:6-1:60	303-323	25-150 mg	44.6	1	Brahmkhatri and Patel, 2011
PA/NaY	Stearic acid	n-butanol	1:2-1:6	393 -403	1 g	34.18	2	Chen *et al.*, 2011
Sulfonated	Oleic acid	Methanol		338	50 mg		1	Geng *et al.*, 2011
$HSO_3SBA-15$	Lauric acid	Glycerol	1:2-1:4	413-433	1-5 wt%	42	2	Hermida *et al.*, 2011
M-poly (DVB-4VP)	Propionic acid	Methanol	1:1	318-348	0.5 wt%	38.5	2	Kara and Erdem, 2011

Table 2.6: Continued

Catalyst	**Acid**	**Alcohol**	**Molar ratio ($M_{acid:alcohol}$)**	**Temperature (K)**	**Catalyst loading**	**Ea (kJ/mol**	**Reaction order**	**References**
Sulfonated	Fatty acid	Methanol	1:21	453-493	0.5 wt%	NA*	2	Shu *et al.*, 2011
RHAPhe-Ru immobilized on silica	Acetic acid	Ethanol	1:1	358	0.1 g	82.2	2	Adam *et al.*, 2012
TPA anchored to MCM-41	Lauric acid	1-butanol	1:1-1:3	343-373	100-200 mg	78	2	Brahmkhatri and Patel, 2012
Ph-SO3H modified mesoporous carbon	Oleic acid	Methanol	1 g acid: 8 ml alcohol	338	20 mg	NA*	1	Geng *et al.*, 2012
Cesium exchange TPA	Fatty acid	Methanol	1:5-1:25	313-338	0.01-0.08 g/cm^3	37.09	1	Srilatha *et al.*, 2012
Sulphated zirconia	Myristic acid	Methanol	1:4-1:20	393-443	1-3 wt%	22.51	2	Rattanaphra *et al.*, 2011

*NA denotes not available

2.4.2 Eley-Rideal (ER) Model

The model involve a single site mechanism and indicates the reaction between one reactant adsorbed on the catalyst surface and its other reactant in bulk region (Ju *et al.*, 2010; Miao and Shanks, 2011, and Akyalçın and Altiokka, 2012). The rate equations are shown in Eq. (2.2) and (2.3).

$$-r_A = \frac{k_f\left(C_A C_B - \frac{C_E C_W}{K_{eq}}\right)}{1 + K_A C_A + K_W C_W} \tag{2.2}$$

$$-r_A = \frac{k_f\left(C_A C_B - \frac{C_E C_W}{K_{eq}}\right)}{1 + K_B C_B + K_E C_E} \tag{2.3}$$

where K is the adsorption constant.

Sulphated zirconia can be applied in acidic catalyst reaction. Sert and Atalay, (2009) studied on the same catalyst for the reaction of acetic acid with butanol. The reaction were carried out at temperature of 328 K to 343 K, $M_{acid:alcohol}$ of 1:1, catalyst loading of 3 g/L and stirring rate of 800 rpm. The sulphated zirconia was prepared by impregnating zirconia with sulphuric acid. The kinetic study was observed that equilibrium constant weakly depends on the temperature and the reaction enthalpy was -18.7 kJ/mol. The non-catalyse reaction was followed the second order rate equation and the activation energy was 58 kJ/mol. The experimental data for catalysed reaction was followed the ER modelling mechanism with the assumption of the adsorbed reactants was reacted with another in the fluid. The activation energy was reduced from 58 to 49.2 kJ/mol.

In recent years, the esterification reaction was used to pre-treat the cheaper feedstock before it was employed for the transesterification reaction for biodiesel production. This can be done by means of an esterification reaction of the FFA with methanol, catalysed by acidic ion exchange resins such as Amberlyst 15. Tesser *et al.* (2010) carried out the above mentioned reaction by reacting acidified soy bean oil in a batch stirred tank reactor and a tubular packed bed loop reactor (PBLR). Data collected in a batch reactor were better interpreted with ER kinetic model with R^2 of 0.912 as compared with PH model with R^2 of 0.8. According to this model, the reaction occurs between the oleic acid adsorbed on the catalyst surface and methanol from the bulk. The triglycerides produced were considered as non-adsorbing compound. The kinetic model developed on the basis of batch runs was able to simulate the behaviour of PBLR, providing the external mass transfer resistance calculated by Nitta correlation, was properly accounted for.

2.4.3 Langmuir Hinshelwood Hougen Watson (LHHW) Model

Model represents the rate determining step which both reactants adsorbed on the catalyst surface first before the reaction occurred (Ju *et al*., 2010; Akbay and Altiokka, 2011). The general reaction rate is shown in Eq. (2.4).

$$-r_A=\frac{k_f(C_A C_B-(\frac{C_E C_W}{K_{eq}})}{(1+\sum K_i C_i)^2} \tag{2.4}$$

where *Ki* adsorption constant for species *i* and *Ci* is bulk concentration of species *i*.

Sert *et al*. (2013) studied on the esterification of AA and BuOH catalysed by Amberlyst 131. The reaction were carried out at temperature of 338 to 358 K, $M_{acid:alcohol}$ of 1:1 to 1:3 and catalyst loading of 10 to 20 g/l. The data for kinetic was not controlled by diffusion because the conversion increased with increasing temperature. The activity coefficients were calculated using UNIQUAC method for the non-ideal behaviour. The kinetic data were correlated with LHHW which gave the smallest mean relative error and the activation energy was 57.4 kJ/mol.

Altiokka and Ödeş, (2009) studied the esterification of AA with propylene glycol with the presence of Amberlyst 15 as catalyst at temperature of 333 to 358 K, $M_{acid:alcohol}$ of 1:1 and catalyst loading of 3.11, 5.06 and 8.46 wt%. The reaction rate was highly sensitive to temperature which accepts that the reaction was controlled by surface reaction. The reaction was fitted with LHHW model with 95% confidence interval. The activation energy was 80.37 kJ/mol.

In the production of biodiesel, the waste cooking oil (WCO) is the cheap source for raw material. The acid-alkali process has been developed in producing biodiesel. In esterification process, the free fatty acid must be reduced below than 1%. Gan *et al.* (2009) studied the esterification of WCO with methanol by using supported ferric sulphate on carbon ($Fe(SO_4)_3/C$) at temperature of 338 to 368 K, $M_{acid:alcohol}$ of 1:9 to 1:21 and catalyst loading of 0 to 7.5 wt%. The function of carbon was to adsorb the colour of WCO. The model that could be described the reaction satisfactorily was LHHW model. Assumptions were considered to follow the model which were neglected the non-catalysed reactions, sites at catalyst surface were the same, surface reaction with rate controlling step and adsorption and desorption of reactants and product were fast and at equilibrium.

Mesoporous silica materials supported organic acid such as sulfonated SBA-15 is an attractive heterogeneous acid catalyst due to its high surface area, good control of the acid moieties, no significant Lewis acidic sites and good stability without swelling in organic solvents. Miao and Shanks, (2011) investigated the difference in reaction mechanism between homogeneous and supported propylsulfonic acid for the esterification reaction of acetic acid with methanol. The heterogeneous catalyst, propylsulfonic acid functionalized SBA-15 (HSO_3SBA-15) was prepared by co-condensation method. In isothermal batch experiments at temperature of 323 K, $M_{acid:alcohol}$ of 1:2 and catalyst loading of 0.25 to 1 wt%, the apparent reaction orders using the heterogeneous catalyst were determined to be 0.72 for methanol and 0.87 for acetic acid. Reactant adsorption studies showed that pre-adsorption of acetic acid hindered the reaction rate, while pre-adsorption of methanol or acetic acid with methanol increased the reaction rate. This indicated that acetic acid adsorbs more strongly than methanol over the heterogeneous acid catalyst. The experimental results demonstrated that the esterification reaction followed a dual-site LHHW type reaction mechanism, which required both the adsorption of acetic acid and methanol over HSO_3SBA-15. In contrast, esterification reaction with the homogeneous catalyst followed an Eley–Rideal mechanism.

Kinetics of the zeolite BEA catalysed the esterification of 1-octanol with hexanoic acid and its side reaction, the etherification of 1-octanol, was determined by

Schildhauer *et al.* (2009) using a stirred glass flask equipped with reflux cooler at 433 K and catalyst loading of 2.75 g/l. Both reactions can be described using a LHHW type approach accounting for the reversibility of the esterification reaction. The adsorption of water was 38 times stronger than that of 1-octanol while the adsorption of hexanoic acid, ester and ether were negligible. Removal of water in the reaction system would lead to higher activity but lower selectivity due to the ether formation from the 1-octanol. The formation of octene was not considered in the kinetic model as it was found that octene was formed in a consecutive reaction by ether splitting and could be neglected in the kinetic experiments.

The LHHW that used to elucidate the reaction mechanism are summarised in Table 2.7.

Table 2.7: Summaries of LHHW kinetic modelling

Catalyst	**Acid**	**Alcohol**	**Molar ratio ($M_{acid:alcohol}$)**	**Temperature (K)**	**Catalyst loading**	**Ea (kJ/mol)**	**Reaction order**	**References**
Amberlyst 15	Acrylic acid	Propylene glycol	1:1	333-358	3.11,5.06. 8.46 wt%	80.37	NA*	Altiokka and Ödeş, 2009
Fe2(SO_4)$_3$/C	Fatty acid	Methanol	1:9-1:21	338-368	0-7.5 wt%	18.59	NA*	Gan *et al.*, 2009
Zeolite BEA	Hexanoic acid	1-octanol		433	2.75 and 4.85 g/l		NA*	Schildhauder *et al.*, 2009
HSO3 SBA-15	Acetic acid	Methanol	1:2	323	0.25-1 wt%	44.8	1	Mio and Shanks, 2011
Amberlyst 131	Acrylic acid	Butanol	1:1-1:3	338-358	10-20 g/l	57.4	NA*	Sert *et al.*, 2013

*NA denotes not available

2.5 LITERATURE REVIEW SUMMARY

Acrylic acid (AA) has high demand in chemical industry because the product especially acrylates has high commercial value due to its properties. In acrylic acid manufacturing, the wastewater containing very low concentration of acrylic acid which very toxic to living things. The common practice to treat this wastewater is by incineration but used substantial energy and not environmental friendly. There are others methods to treat this wastewater. The anaerobic digestion can achieved up to 100% removal but need extremely long residence time. The adsorption also can removed AA with high efficiency but needs large amount of adsorbent which not economical. While the wet oxidation treatment is used when the concentration AA in wastewater is not suitable for anaerobic digestion or adsorption. Since AA is thermally stable and it’s poorly oxidised below 523 K. High temperature and pressure needed to achieve the high efficiency. So, esterification is used to treat this type of wastewater by producing ester while purify the wastewater. Several studies have implemented the esterification to treat the wastewater containing carboxylic acid and have promising result. The catalyst is needed for this type of treatment. There are two types of catalyst which are homogeneous and heterogeneous catalyst. The heterogeneous catalyst is preferred because it can overcome the drawback of homogeneous catalyst usage. Reaction kinetics is important to understand the behaviour and mechanism of the reaction. To elucidate the reaction, the experimental data is fitted with different types of kinetic model including PH, ER and LHHW.

CHAPTER 3

RESEARCH METHODOLOGY

3.0 INTRODUCTION

The present chapter includes the materials, apparatus, and equipment used for the catalyst synthesis, characterisation and catalytic activity testing throughout the study of the esterification of the pure and dilute acrylic acid with butanol. All the experimental procedures are also delineated.

3.1 MATERIALS

The chemicals used in the present study are listed in the Table 3.1 with its brand, purity, and functions. All these chemicals were used without further purification.

Table 3.1: List of chemical

Chemicals	Assay (%)	Supplier	Function
1-butanol	99.8	Sigma Aldrich	As a reactant
Acrylic acid	99	Aldrich	As a reactant
Amberlyst 15	NA*	Sigma Aldrich	catalyst
Ammonium molybdate tetrahydrate	81-83	Merck	As a reactant for catalyst synthesis
Argentums nitrate	99.8	R&M chemicals	As an indicator
Barium chloride	100.02	Fisher	As an indicator
Butyl acrylate	≥99.5(GC)	Fluka	As a standard for GC-FID analysis
Compressed Air	99.99	Air product	To initiate flame in FID
Helium gas	99.99	Air product	As a mobile phase and carrier for GC-FID analysis
Hydrochloric acid	37	Merck	As a reactant for catalyst synthesis
Hydrogen gas	99.99	Air product	As an inert gas for GC-FID
n-hexane	98	Merck	As a solvent for GC-FID analysis
Nitric acid	65	R&M chemicals	As a reactant for catalyst synthesis
Nitrogen gas	99.99	Air product	As a makeup for GC-FID
Phenolphthalein	NA*	Emory Laboratory Chemicals	As an indicator
Potassium hydrogen phthalate	99.5	Merck	For standardise KOH solution
Potassium hydroxide	85	Merck	For IEC analysis
Sodium chloride	100.1	Fisher	For IEC analysis
Sodium dihydrogen phosphate	99	Systerm	As a reactant for catalyst synthesis
Sodium hydroxide	99	R&M chemicals	As a reactant for catalyst synthesis
Starch		Sigma Aldrich	As a reactant for catalyst synthesis
Sulphated zirconia	NA*	NA*	Catalyst
Sulphuric acid	96	Fisher	As a reactant for catalyst synthesis
Waste expanded polystyrene	NA*	NA*	As a reactant for catalyst synthesis
Zirconium hydroxide	97	Aldrich	As a reactant for catalyst synthesis
Zirconyl chloride octahydrate	98	Sigma Aldrich	As a reactant for catalyst synthesis
ZSM-5 zeolite	NA*	Alfa Aesar	catalyst

*NA denotes not available

3.2 APPARATUS AND EQUIPMENT

3.2.1 Catalyst Characterisation

The sulfonated expanded polystyrene (SEP) were examined using Scanning Electron Microscopy (SEM), thermogravimetric analyser, Fourier Transform Infrared Spectroscopy (FT-IR) and gas pycnometer for its morphology, thermal stability, functional groups and density.

3.2.2 Esterification Reaction Studies

The catalysts were tested through esterification reaction carried out in a three necked flask equipped with condenser, temperature controller and temperature probe. Figure 3.1 shows the experimental setup and Table 3.2 shows the function of each part in the set up.

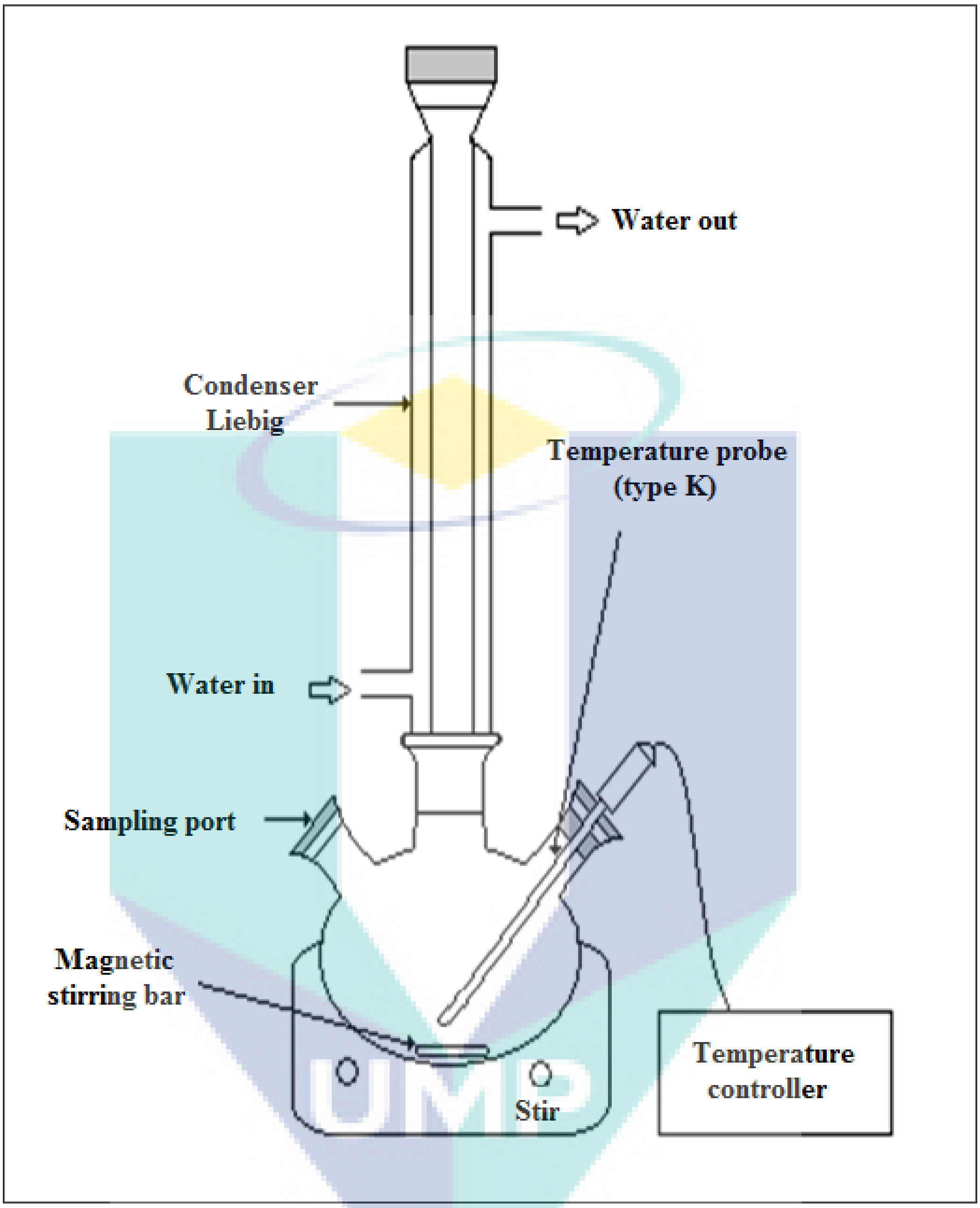

Figure 3.1: The experimental setup for esterification reaction studies

Table 3.2: List of main components in the experimental setup for the esterification reaction studies

Component	Description	Function
Rotamantle	Equipment with heating and stirring which hold the 3-necked round flask. The heating system was connected to the temperature controller.	To supply heat required for reaction and to provide magnetic field to stir the reaction mixture.
Temperature controller	Proportional-integral-derivative (PID) controller with on/off system.	To control and maintain the temperature during reaction.
3-necked round flask	A round bottom flask with capacity of 500 ml with three openings. The condenser was connected to the opening in the middle. One of the side opening was used to locate the temperature probe while the other one was used for product sampling	As batch reactor.
Liebig condenser	Glass condenser with the length of 50 cm.	To condense the reaction mixture vapour during reaction
Temperature probe	K-type probe.	To measure the temperature.
Magnetic stirring bar	3cm in length.	To stir the reaction mixture continuously.

3.2.3 Sample Analysis

The samples from esterification of acrylic acid (AA) with butanol (BuOH) were analysed using gas chromatography Agilent HP 1200 equipped with flame ionisation detector (FID). The column used was DB-200 column (Agilent) with length of 30 m, diameter of 0.32 mm and inner diameter of 0.25 μm.

3.3 EXPERIMENTAL PROCEDURES

3.3.1 Catalyst Preparation

A number of catalysts which were reported with high water tolerance have been prepared using different methods. These catalysts were screened based on its activity in the esterification of AA and BuOH.

Zirconium Phosphate

Amorphous zirconium phosphate was prepared using sol gel method. Zirconium chloride octahydrate ($ZrOCl_2.8H_2O$) solution was added dropwise into the solution of sodium dihydrogen phosphate at the pH range of 1-2 and 343 K. The molar ratio between zirconium chloride octahydrate and sodium dihydrogen phosphate (ZCO/SDP) was 2 M. The gelatinous precipitates were continuous stirred for 1 hour. Then, the solution was filtered and washed with ultrapure water to remove the chloride ions. The chloride ions were determined by dropping 0.1 M argentums nitrate into the solution. The precipitate was dried at room temperature before it was sieved. The materials were converted to acid form by treating 1 g of material with 10 ml of 1 M nitric acid for 30 minutes. The acid treatment was repeated for five times. The material was washed to remove adhering acid and dried at room temperature.

Sulphated Zirconia

The sulphated zirconia was calcined at 773 K for 5 hours before it was used.

Sulfonated Carbon

The 25 g of starch was gradually added to 75 ml of concentrated sulphuric acid (H_2SO_4) (96 vol%). The solution was stirred vigorously and heated for 2 hours. The solution was dried at 373 K and 623 K for 24 hours. After drying, the solid was washed with distilled water to remove the sulphate ion which can be traced using 0.1 M barium chloride ($BaCl_2$). The catalyst was dried again at 373 K and 623 K for 24 hours before used.

Molybdenum Zirconia

1 cm^3 of aqueous solution of ammonium molybdate tetrahydrate ($(NH_4)_6Mo_7O_{24}.4H_2O$) was impregnated on 1 g of zirconium (IV) hydroxide ($ZrOH_4$). The solution was dried at 393 K for 48 hours. Then, the catalyst was calcined in air for 3 hours at 773 K.

Zeolite ZSM-5

The catalyst was calcined at 823 K for 4 hours before it was tested in the esterification reaction.

Sulfonated Expanded Polystyrene

The 1 g of expanded polystyrene was reacted with 20 ml of concentrated H_2SO_4 (96 vol%) at 378 K for 2 hours. The brown slurry was transferred into 100 ml of deonised water. The slurry was filtered and washed with 50 ml of 0.1 M sodium hydroxide (NaOH). Then, the slurry was first washed using hydrochloric acid (HCl) solution in volume ratio of 1:50 before it was washed using an excess of deionised water. Lastly, it was dried at 343 K.

3.3.2 Catalyst Characterisation

Scanning Electron Microscopy (SEM)

The morphology of the catalyst was determined by scanning electron microscope (Model Leo Supra 50VP equipped with an Oxford INCA 400 Energy Dispersive X-ray Microanalysis (EDS) system). The plate containing sample was placed in the electron microscope for analysis with magnification of 1000x, 2000x and 5000x.

Thermogravimetric Analysis (TGA)

The thermogravimetric analysis was carried out using themogravimetric analyser (Q500) at a heating rate of 283 K/min with the maximum temperature of 1223 K. The sample was placed on the pan and weigh before it was burned in the atmospheric of nitrogen.

Fourier Transmitter Infrared (FTIR)

The FT-IR spectroscopic analysis was measured using Perkin Elmer (model spectrum 100) spectrophotometer. The spectrum was recorded using pellet technique. The sample was mixed and ground with potassium bromide (KBr) before it was pressed to a pellet under hydraulic pressure. The pellet was then used to record the IR spectrum from the wavenumber of 4000-400 cm^{-1} under atmospheric conditions with a resolution of 1 cm^{-1}.

Density

The density of the catalyst was measured using gas pycnometer (Micromeritics Accu pyc II 1340). The density and volume were determined by the pressure change of helium.

Ion exchange capacity (IEC)

0.1 g of catalyst was immersed in 100 ml of 0.1 M NaCl solution for 24 hours. The NaCl solution was then titrated with 0.1 M KOH with phenolphthalein as indicator. The KOH solution was standardised by titrated 0.7-0.9 g of potassium phthalate in 50 ml deionised water. The ion exchange capacity in milliequivalents/gram was calculated using Eq. (3.1).

$$IEC=\frac{V_{KOH}\times M_{KOH}}{Mass_{catalyst}} \tag{3.1}$$

where V is volume and M is molarity.

Catalyst Reusability

After the esterification reaction, the SEP was separated from the reaction mixture by filtration and washed with BuOH. The SEP was dried for 24 hours at 343 K before it was reused again.

Catalyst Regeneration

The used catalyst (SEP) was immersed in H_2SO_4 with different concentration for 24 hours at room temperature. The catalyst was then washed with water and dried.

3.3.3 Esterification Reaction Study

The BuOH was first charged into the flask in the esterification reaction experimental setup. After the required temperature was obtained, AA and the catalyst were charged and the reaction time was started. Sample was taken at certain time interval and kept in the ice bath to cease the reaction before analysing using GC. The total amount of sample taken was less than 10% of the total volume (30 ml) of the reaction mixture.

Effect of Mass Transfer

The kinetic studies were carried out under the operating conditions which were not limited by mass transfer effects. External mass transfer is the diffusion of the reactant from bulk fluid to the external surface of the heterogeneous catalyst across the boundary layer surrounding the catalyst (Fogler, 2008). The effect of external mass transfer resistance was examined by varying the stirring speed from 0 to 600 rpm. The reaction was not limited by external diffusion if the Mears Criterion (C_M) as shown in Eq. (3.2) was less than 0.15.

$$C_M = \frac{r_{A(obs)}\rho_b R_c n}{K_C C_{Ab}} < 0.15 \qquad (3.2)$$

where $r_{A(obs)}$ is the observed reaction rate of species A, ρ_b is the bulk density of catalyst, R_c is the catalyst radius, n is the reaction order, K_c is the mass transfer coefficient and C_{Ab} is the bulk concentration of limiting reactant.

The K_c was calculated using Eqs. (3.3-3.6)

$$K_c = \frac{2D_{AB}}{d_p} + 0.31 N_{sc}^{-\frac{2}{3}} \left(\frac{\Delta\rho \mu_c g}{\rho_c^2}\right)^{\frac{1}{3}} \tag{3.3}$$

$$D_{Am}\mu_m^{0.8} = \sum_{\substack{j=1 \\ j\neq A}}^{n} x_j D_{Aj} \mu_j^{0.8} \tag{3.4}$$

$$D_{AB}^0 = \frac{1.173x10^{-8} (\Phi_B M_B)^{\frac{1}{2}} T}{\mu_B V_A^{0.6}} \tag{3.5}$$

$$N_{sc} = \frac{\mu_c}{\rho_c D_{AB}} \tag{3.6}$$

where D_{AB} is the diffusivity of solute A in solution, d_p is the diameter of catalyst particle size, N_{sc} is the Schmidt number, $\Delta\rho$ is the different between density solution and density catalyst, μ_c is the viscosity of solution, g is the gravitational acceleration, ρ_c is the catalyst density, D_{Am} is the diffusivity of solute in mixture, μ_m is the viscosity of mixture, x_j is the mole fraction, D_{Aj} is the diffusivity of A in j, μ_j is the viscosity of j, $D_{AB}^0$is the diffusivity based on molarity, Φ_B is the association parameter of solvent, M_B is the molecular weight of solvent B, T is the temperature , μ_B is the viscosity of B and V_A is the specific molar volume of limiting reactant.

Internal mass transfer or pore diffusion is the diffusion of reactant from the external surface into and through the pores within the catalyst to the catalytic surface of the pores, in which the reaction occurs. It is affected by the particle size of the catalyst, pore size, temperature, catalyst composition, and reaction medium (Ali *et al.,* 2007; Fogler, 2008 and Raweewan *et al.*, 2011). Weisz-Prater Criterion (C_{WP}) as shown in Eq. (3.7) should be less than 1 to ensure an internal diffusion free reaction region.

$$C_{WP} = \frac{r_{A(obs)}\rho_c R_c^2}{D_{eff} C_{li}} < 1 \tag{3.7}$$

where D_{eff} is the effective diffusivity and C_{li} is the limiting reactant concentration in mixture.

Effect of Important Operating Parameters

The yield and conversion of reaction were measured at different operating parameters. These parameters included catalyst loading, molar ratio, initial water content and temperature as shown in Table 3.3.

Table 3.3: Important operating parameter study and its' range

Parameter	Range
Catalyst loading	0-15 wt% of acid
Molar ratio	1:1-1:7 (excess BuOH) 1:1-3:1 (excess AA)
Initial water content	0-90 wt% of acid
Temperature	313- 373 K

3.3.4 Sample Analysis using GC

The compositions of the samples taken during the study of esterification reaction between AA and BuOH were analysed using GC-FID with the injector and detector block temperature at 503 K (with 1:10 split ratio) and 523 K respectively. The oven was maintained isothermal at 308 K for 5 minutes and the oven temperature was then increased to 473 K at a rate of 10 K/min. The carrier gas (Helium) flowed at a flow rate of 36.8 cm^3/s. Figure 3.2 shows one of the chromatograms for acrylates analysis.

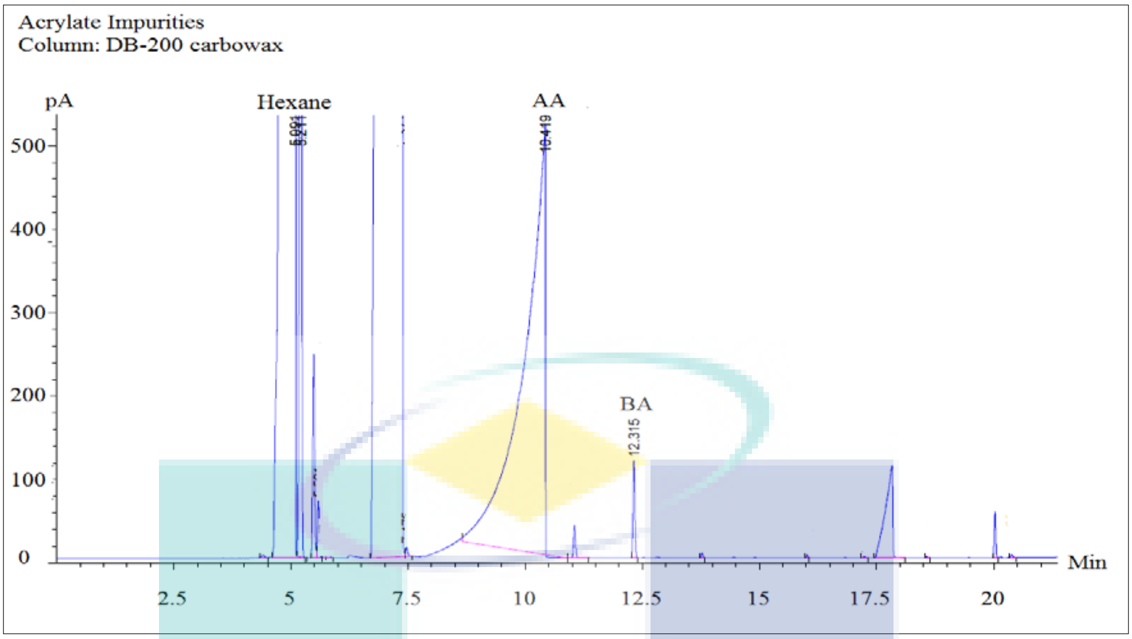

Figure 3.2: Chromatogram obtained from GC-FID analysis

The standard calibration curves of butyl acrylate (BA) and AA were required to obtain the concentration of these components in the samples. The analytical standard or HPLC standard of each component was used to generate the calibration curve. The standard calibration curves were included in Appendix A and B for AA and BA. In order to ensure the consistent and persistently GC performances, the BA standard solutions were injected before the samples were analysed. The Eqs. (3.8-3.9) are used to calculate the BA yield and AA conversion respectively.

$$yield\,(\%)=\frac{mol_{BA}}{mol_{AA^0}}\times 100\% \tag{3.8}$$

$$conversion\ (\%)=\frac{mol_{AA^0}-mol_{AA}}{mol_{AA^0}}\times 100\% \tag{3.9}$$

where AA, AA^0 and BA are the acrylic acid, initial acrylic acid and butyl acrylate respectively. The example calculation of yield and conversion are in Appendix G.

3.4 KINETIC MODELLING

In the present study, the kinetic data of esterification of AA with BuOH were correlated with pseudo-homogeneous (PH), Eley-Rideal (ER), and Langmuir-Hinshelwood-Hougen-Watson (LHHW) kinetic models. The kinetic data comprised of the rate of AA consumed and the rate of BA produced. For a batch system, it was calculated based on the concentration profile generated from the study of the temperature effect using Eqs. (3.10-3.11).

$$r_{AA}=\frac{dC_{AA}}{d_t} \tag{3.10}$$

$$r_{BA}=\frac{dC_{BA}}{d_t} \tag{3.11}$$

where r is the reaction rate and t is the time.

Pseudo-homogeneous (PH) concentration based model is derived by assuming that there is no sorption effect which every single active site on the catalyst particles is in contact with the surrounding bulk liquid (Schimdt-Traub and Gorak, 2006). Eq. (3.12) shows the PH model in concentration based while Eq. (3.13) shows the activity based PH model.

$$r_{AA}=-k_f\left(C_{AA}C_{BuOH}-\frac{1}{Keq}C_{BA}C_w\right) \tag{3.12}$$

$$\frac{r_{AA}V}{N_T}=-k_f\left(\alpha_{AA}\alpha_{BuOH}-\frac{1}{Keq}\alpha_{BA}\alpha_w\right) \tag{3.13}$$

where k_f is the forward rate constant, K_{eq} is the equilibrium constant, V is the volume, N_T is the total mole, α is the activity and the subscripts of AA, BuOH, BA and W are the acrylic acid, butanol, butyl acrylate and water respectively.

Eley-Rideal (ER) model was derived by assuming the reactant approach the surface and react with chemisorbed reactant without being adsorbed itself

(Chorkendorff and Niemantsverdriet, 2003). Eq. (3.14) and Eq. (3.15) show the concentration and activity based Eley-Rideal (ER) model respectively.

$$r_{AA}=\frac{-k_f(C_{AA}C_{BuOH}-\frac{1}{K_{eq}}C_{BA}C_w)}{(1+K_{AA}C_{AA}+K_wC_w)} \tag{3.14a}$$

$$r_{AA}=\frac{-k_f(C_{AA}C_{BuOH}-\frac{1}{K_{eq}}C_{BA}C_w)}{(1+K_{BuOH}C_{BuOH}+K_{BA}C_{BA})} \tag{3.14b}$$

$$\frac{r_{AA}V}{N_T}=\frac{-k_f\left(\alpha_{AA}\alpha_{BuOH}-\frac{1}{K_{eq}}\alpha_{BA}\alpha_w\right)}{(1+K_{AA}\alpha_{AA}+K_w\alpha_w)} \tag{3.15a}$$

$$\frac{r_{AA}V}{N_T}=\frac{-k_f\left(\alpha_{AA}\alpha_{BuOH}-\frac{1}{K_{eq}}\alpha_{BA}\alpha_w\right)}{(1+K_{BuOH}\alpha_{BuOH}+K_{BA}\alpha_{BA})} \tag{3.15b}$$

where K is the adsorption constant.

Langmuir-Hinshelwood-Hougen-Watson (LHHW) was derived by assuming all species are adsorbed accommodated with the surface before the reaction take places. This reactant reacts in the chemisorbed state on the surface (Chorkendorff and Niemantsverdriet, 2003). Eq. (3.16) and Eq. (3.17) show the concentration and activity based LHHW model respectively.

$$r_{AA}=\frac{-k_f(C_{AA}C_{BuOH}-\frac{1}{K_{eq}}C_{BA}C_w)}{(1+K_{AA}C_{AA}+K_{BuOH}C_{BuOH}+K_{BA}C_{BA}+K_wC_w)^2} \tag{3.16}$$

$$\frac{r_{AA}V}{N_T}=\frac{-k_f\left(\alpha_{AA}\alpha_{BuOH}-\frac{1}{K_{eq}}\alpha_{BA}\alpha_w\right)}{(1+K_{AA}\alpha_{AA}+K_{BuOH}\alpha_{BuOH}+K_{BA}\alpha_{BA}+K_w\alpha_w)^2} \tag{3.17}$$

where K_{eq} was calculated using Eq. (3.18) and α_i was calculated using UNIFAC method.

$$K_{eq}=\frac{k_f}{k_r} \tag{3.18}$$

where k_r is reverse rate constant.

The theoretical developments in the molecular thermodynamics of liquid solution behaviour are often based on the concept of local composition, presumed to account for the short range order and non-random molecular orientations that result from differences in molecular size and intermolecular forces, alternatively correlative methods, UNIFAC (UNIQUAC Functional-group Activity coefficient) was employed to provide fitted component-specific and model parameters as shown in Eq. (3.19).

$$\alpha_i = \gamma_i x_i \tag{3.19}$$

where γ_i is the liquid activity coefficient for component i and x_i is the concentration of each component. The UNIFAC model splits the activity coefficients for each species in the system into two components; the combinatorial component, γ_i^c and the residual component, γ_i^r as shown in Eq. (3.20).

$$ln\gamma_i = ln\gamma_i^c + ln\gamma_i^r \tag{3.20}$$

The UNIFAC program written in Microsoft Excel is included in Appendix C.

CHAPTER 4

RESULTS AND DISCUSSION

4.1 CATALYST SCREENING

Several potential acidic catalysts were tested in the esterification of acrylic acid (AA) with butanol (BuOH) at the stirring rate of 600 rpm, temperature of 353 K and $M_{AA:BuOH}$ of 1:1. The catalyst loading of 40 wt% was used for all type of catalysts except 10 wt% for SEP. Figure 4.1 compares the yield profiles of the non-catalysed and catalysed reactions. The inset of the Figure 4.1 clarifies the yield profile of the non-catalysed system and the reaction system catalysed by sulfonated carbon and zeolite ZSM-5. The esterification is a recovery AA from wastewater by converted AA into ester while purifying wastewater. The 75% of yield is high compared to previous studies. The yield can be increased by continuously withdrawal the reaction products (Chen *et al.*, 1999; Essayem *et al.*, 2007; Altiokka and Ödeş, 2009; Sert *et al.*, 2013 and Karakus *et al.*, 2014).

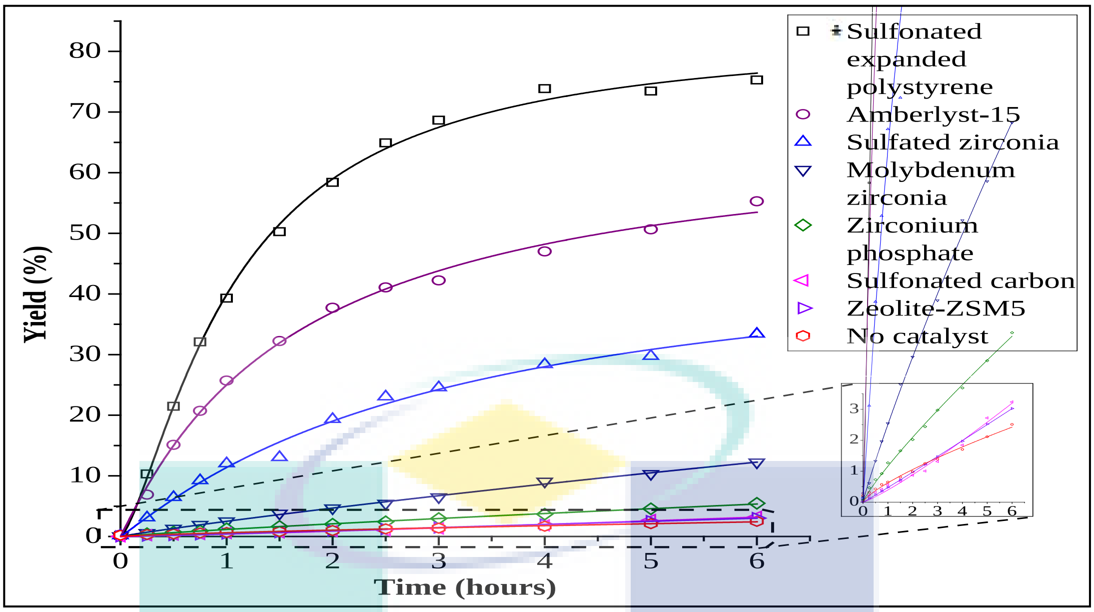

Figure 4.1: Catalyst screening for the esterification of AA with BuOH at the stirring rate of 600 rpm, $M_{AA:BuOH}$ of 1:1, temperature of 353 K and catalyst loading of 40 wt% (* catalyst loading of 10 wt%)

Considering the non-catalysed reaction as the basis of comparison, the increment in yield for the reactions catalysed by sulfonated carbon and zeolite ZSM-5 was negligible. The yield increases significantly in the presence of the zirconium phosphate, molybdenum zirconia, sulphated zirconia, Amberlyst 15 and sulfonated expanded polystyrene (SEP) as catalyst. The catalytic activity of the different type of catalysts follows the order of: SEP > Amberlyst 15 > sulphated zirconia > molybdenum zirconia > zirconium phosphate > sulfonated carbon > zeolite ZSM-5. The higher catalytic activity of the catalyst was attributed to the superior proton source and efficient proton donor. Proton was required during the esterification process to protonate the AA to oxonium ion. Nucleophilic attack occurred when the oxonium ion was attacked by BuOH to form butyl acrylate (BA) and water (Åkerman *et al*., 2011 and Bhorodwaj *et al*., 2011). The catalyst activity of SEP was higher than Amberlyst 15 because of its higher ion exchange capacity (IEC), 8.23 meq/g comparing to the IEC of Amberylst 15, 4.39 meq/g. Higher IEC indicates that SEP was a better proton source and donor (Komoń *et al*., 2013 and Osorio-Viana *et al*., 2013).

The reusability studies were carried out to examine the SEP activity and stability. Figure 4.2 has proven that the SEP can be recovered by simple filtration. The

BA yield decreases for about 10% when the catalyst reused for 2nd time. Nevertheless, the yield reduction was not significant when the catalyst is used in the 4th consecutive run. The reused catalyst has reduced the acid site concentration because the hydrolysis of sulfonic group in the water as shown in Figure 4.5 (Andrijanto *et al.*, 2012 and Jiang *et al*., 2013).

In view of SEP activity and stability, it was chosen as the catalyst for the esterification of AA with BuOH. It was characterised and tested at different operating conditions in the following sections.

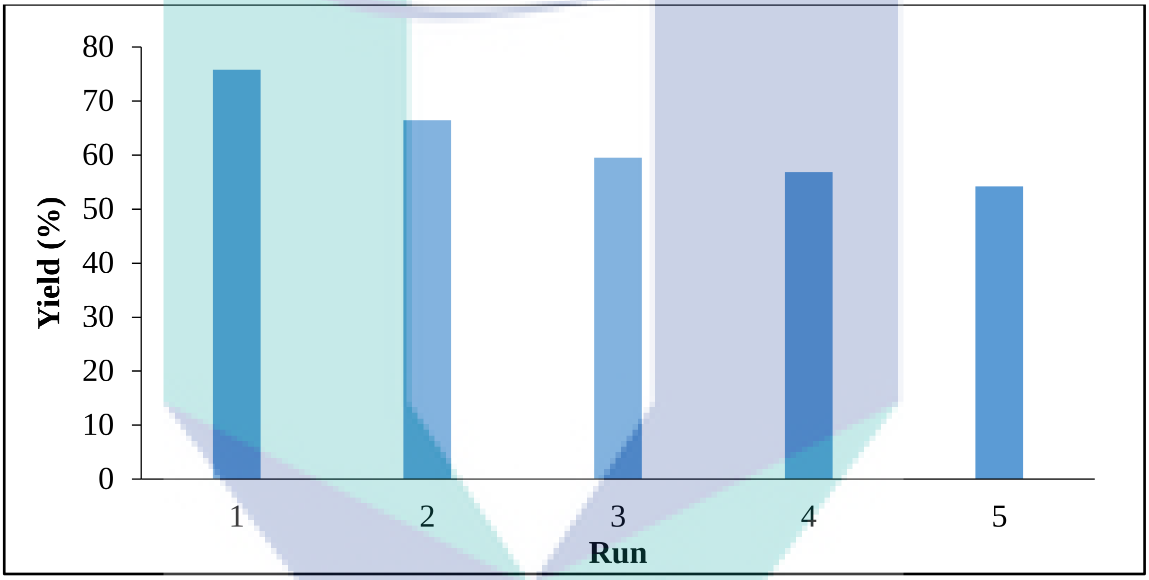

Figure 4.2: Reusability study of SEP. Reaction conditions: temperature of 353 K, $M_{AA:BuOH}$ of 1:3, catalyst loading of 10 wt%, reaction time of 6 hours and stirring rate of 400 rpm

4.2 CHARACTERISATION OF SEP

The chosen catalyst, SEP was characterised to gain insights of the physical and chemical properties. The sulfonation of expanded polystyrene (EPS) is by electrophilic aromatic substitution, sulphur trioxide. The heated concentrated sulphuric acid is generated sulphur trioxide. The benzene (aromatic substrate) in polystyrene is attacked by sulphur trioxide to produce sulfonated expanded polystyrene (EPS) (Mulijani *et al.*, 2014). The reaction pathway is shown in Appendix F. The catalyst was characterised using SEM, TGA, FTIR and gas pycnometer. The swelling effect was also examined.

4.2.1 SEM

The fresh SEP was agglomerate, irregular shape and dark brown in colour. The SEM micrograph under magnification of 2000x and 5000x were shown in Figure 4.3 (a) and (b) respectively. The SEP with rough surface exhibits minute cracks and pores which allows the reactant penetration and gives higher surface area.

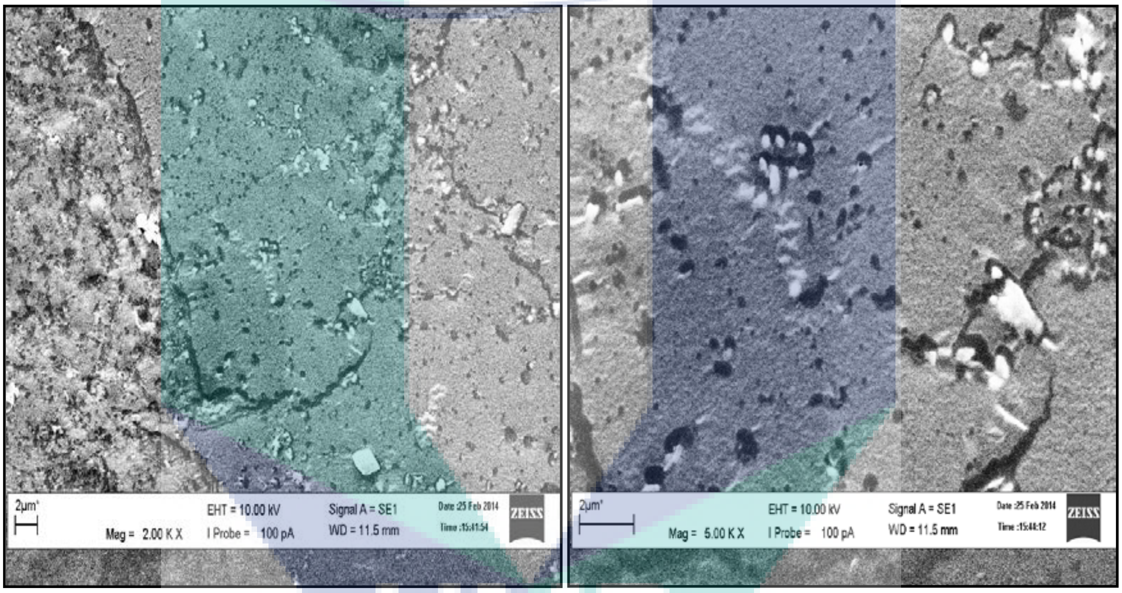

(a) (b)

Figure 4.3: SEM micrograph of fresh SEP under magnification of, a) 2000x and b) 5000x.

4.2.2 Thermal Analysis

Figure 4.4 depicts that the weight loss occurs in three regions. Approximately 20% of weight was lost from 313-403 K because of the elimination of moisture. The decomposition of sulfonic groups has caused a weight loss of 40% from 443-573 K while the destruction of polymer has resulted a weight loss of 15% from 573-1173 K. The SEP was less thermal stable than the Amberlyst 15 in which the sulfonic acid decomposes at lower temperature due to the different chemical environment of the group in the main line of polymer. The structure of Amberlyst 15 was cross-linked by divinylbenzene (Wang *et al*., 2012).

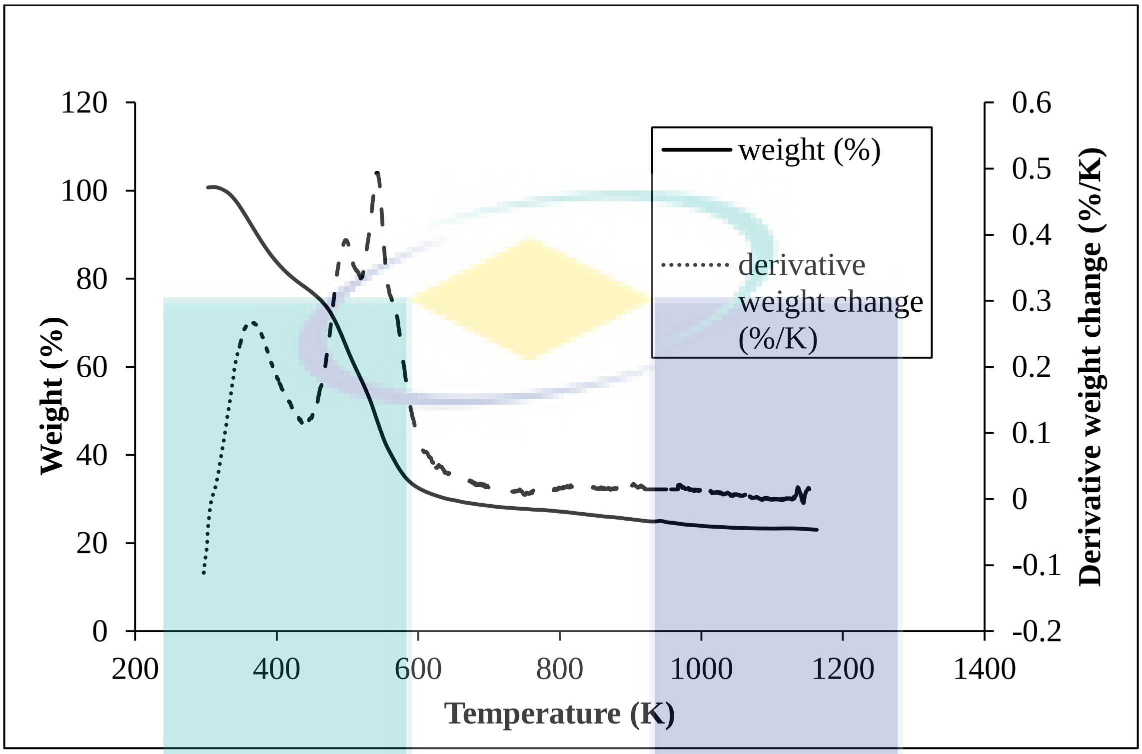

Figure 4.4: The thermogravimetric curve of SEP

4.2.3 Fourier Transform Spectroscopy

FT-IR spectrum in Figure 4.5 shows a broad band centered at 2928 cm^{-1} which attributing to the O-H stretching vibration sulfonic acid group. There was an intense band around 1700 cm^{-1} which might due to the deformation vibration of O-H groups. A sharp peak at 1124 cm^{-1} indicates the S=O stretching vibration of sulfonic acid group. The peaks at 1022 and 992 cm^{-1} represent the symmetric and asymmetric stretching vibration of the sulfonic group respectively. Comparing the spectrum, the bands (stretching vibrations associated with sulfonic group) do not exist in the polystyrene. Absence of this spectrum confirms that the waste polystyrene was successfully sulfonated. The band intensity of used SEP is slightly reduced because of its lower IEC, 7.79 meq/g comparing to the fresh SEP with the IEC of 8.23 meq/g. The SO_3H groups were leached from the used SEP.

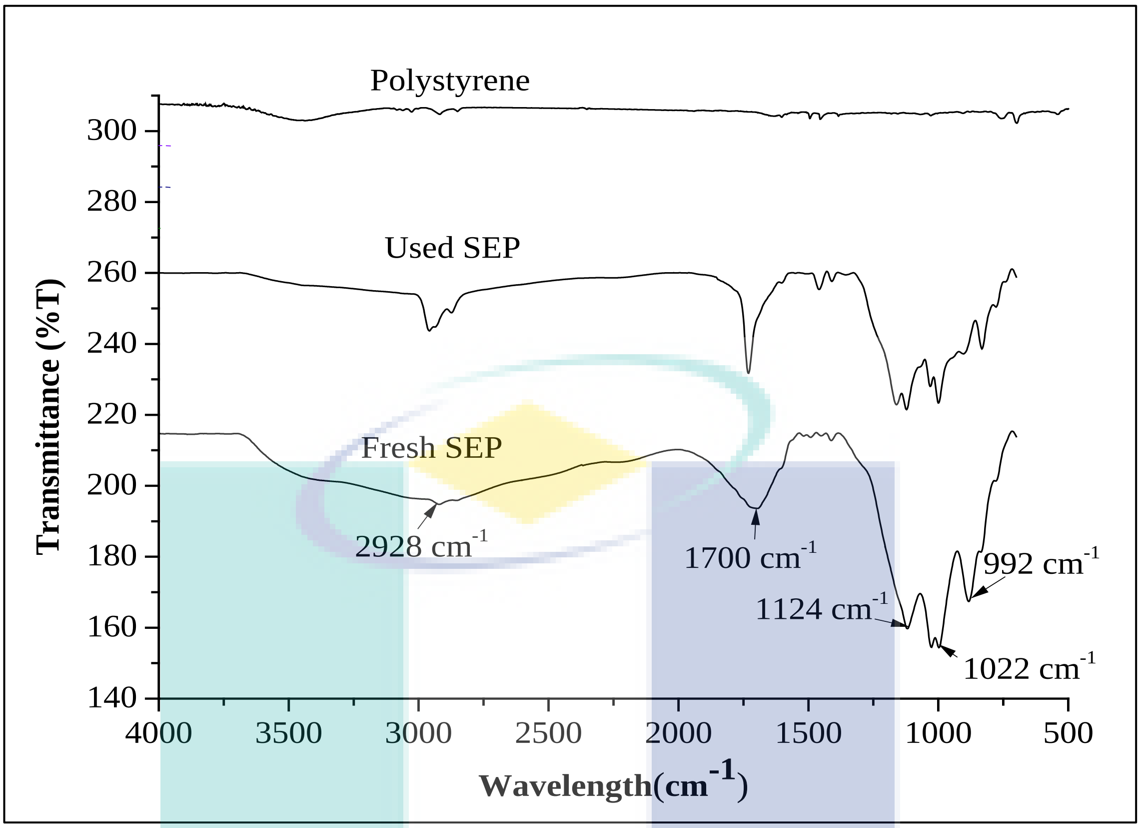

Figure 4.5: FT-IR spectra of waste polystyrene, used and fresh SEP

4.2.4 Density

Density is one of the important features of the catalyst. It is a required data when calculating the Mears and Weisz-Prater Criterion to examine the mass transfer effect. The SEP density is 1.2790 g/cm^3. The total pore volume of SEP is 0.22 cm^3/g. The porosity (ε) is 0.28 by using Eq. (4.1).

$$\varepsilon_{SEP} = \frac{V_{pore}}{V_{SEP}} \tag{4.1}$$

where *V* is the volume.

4.2.5 Swelling Effect

Swelling effect is a measure of the enlargement of catalyst that absorbs solvent. The swelling ability is a prerequisite for gel type catalyst (Chakrabarti *et al.*, 1993). It can be determined by Eq. (4.2). This effect is important to estimate the ‘true radius’ for calculating Weisz-Prater Criterion.

$$swelling(\%) = \frac{swollen\ volume\ (cm^3)}{initial\ volume\ (cm^3)} \times 100\% \tag{4.2}$$

Figure 4.6 shows the effect of swelling for the used catalysts in different reaction mixtures. The fresh SEP in dark brown colour changed to a lighter brown colour after the catalyst was swollen. The change in colour was in consonance with the reduction of IEC as the initial water concentration in the reaction mixture increases (as shown in Figure 4.17). The decline in IEC is ascribed to the substantial amount of water molecules that dissociate the active sites. The swelling effect has transformed the smaller pores in the catalyst to macro pores and hence allowing easy access of the reactants to the acid sites (Sani *et al.*, 2013). The SEP loses its shape after the reaction in the reaction mixture with initial water concentration of 90 wt% because the polymer matrix was rupture. The swelling effects are 740% in BuOH and 550% in the reaction mixture with the $M_{AA:BuOH}$ of 1:3.

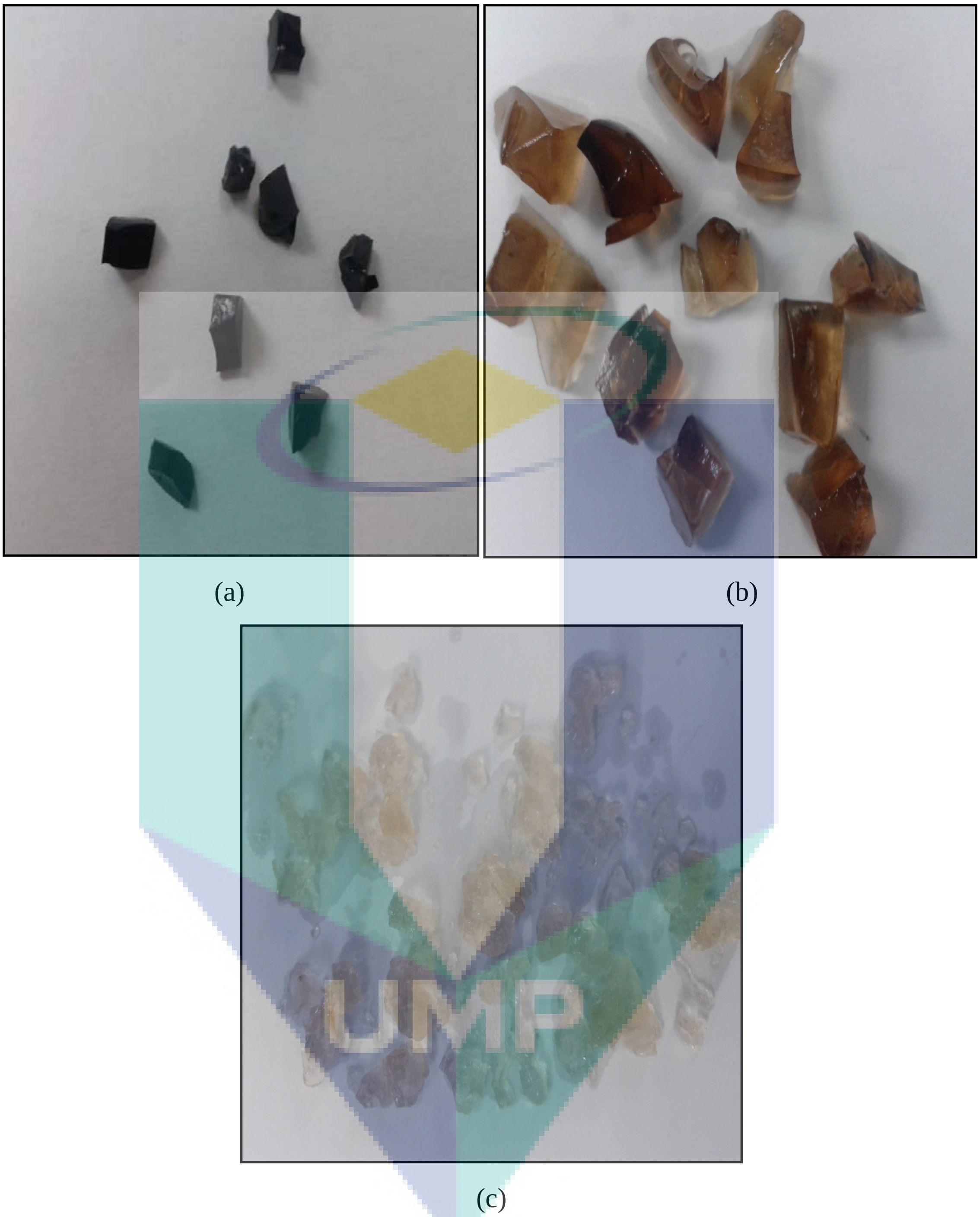

(a)

(b)

(c)

Figure 4.6: Swelling effect of (a) Fresh SEP, (b) Used SEP in the reaction mixture with 10-70 wt% of water and (c) Used SEP in the reaction mixture with 90 wt% of water

4.2.6 SEP Regeneration

The used SEP in the reaction mixture with the initial water concentration of 50 wt% with IEC of 3.42 meq/g was filtered and washed before it was regenerated using H_2SO_4. Different concentration of H_2SO_4 was to determine the best concentration for regenerate SEP. The increasing concentration of H_2SO_4 reduced the swelling effect (as shown in Figure 4.7) and hence declining the IEC of the regenerated SEP as shown in Figure 4.8. The access of the solution with higher H_2SO_4 concentration to the active sites of used SEP was restricted. Therefore, the degree of regeneration was reduced. The regeneration using 10 and 20 wt% of H_2SO_4 has higher IEC compared to the fresh SEP may be because the $–SO_3H$ groups not attached to benzene ring along the polymer backbone or some of SEP is reverted back to EPS during the synthesis SEP (Kucera and Jancar, 1998 and Mulijani *et al.*, 2014).

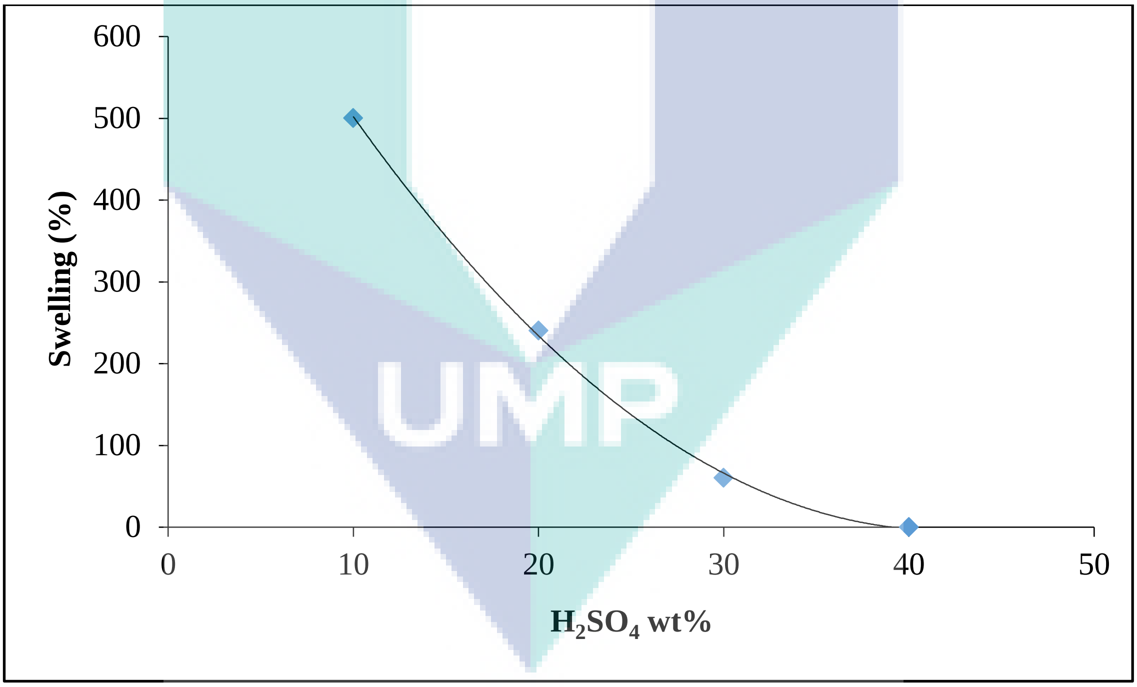

Figure 4.7: Swelling effect of the catalyst regenerated using the solutions with different H_2SO_4 concentration

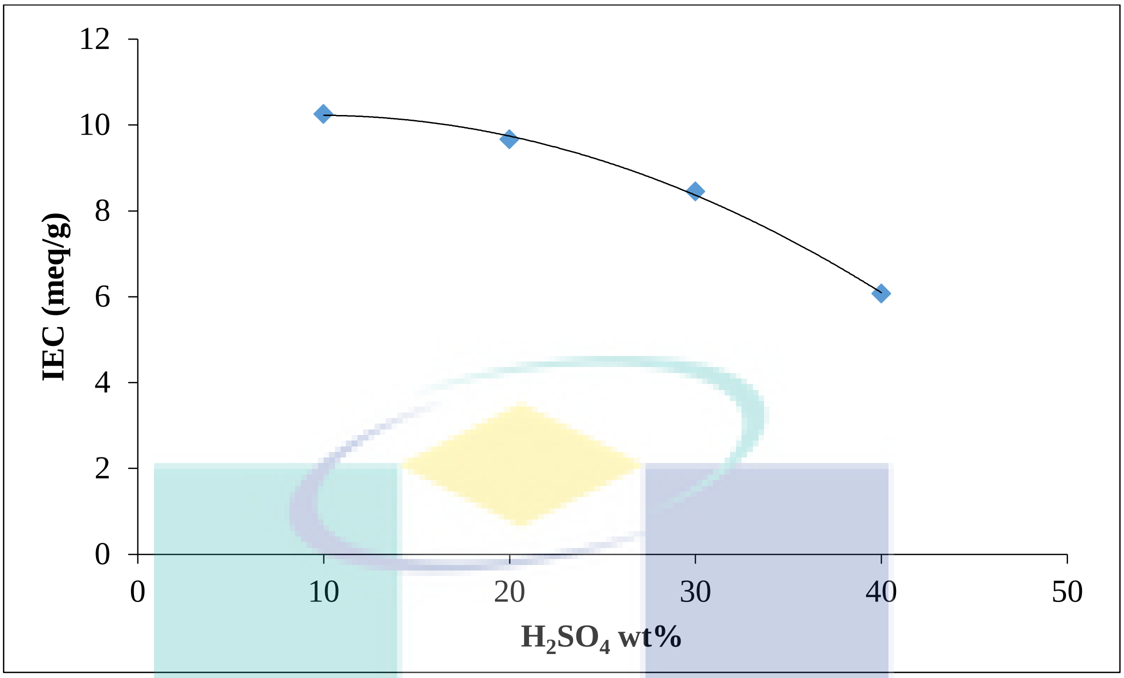

Figure 4.8: IEC of the regenerated SEP using the solutions with different H_2SO_4 concentration

4.3 STUDIES ON THE EFFECT OF IMPORTANT REACTION OPERATING PARAMETERS

The conversion and yield of esterification of AA and BuOH are affected by the parameters such as stirring rate, temperature, molar ratio of acid to alcohol and catalyst loading. A set of optimised parameters is required to develop an efficient process with high yield under the mild condition (Ju *et al*., 2010).

4.3.1 Effect of Mass Transfer

The mass transfer effect must be eliminated to ensure that the reaction was controlled by surface reaction during the measurement of apparent reaction kinetics (Ali *et al*., 2007 and Deborath *et al*., 2014).

The external diffusion does not control the overall reaction unless the stirring speed was very low and the viscosity is high (Lilja *et al*., 2005; Ali *et al*., 2007; Patricia *et al*., 2007 and Toor *et al*., 2011). In the present study, the external mass transfer was eliminated by varying the stirrer speed from 0 to 600 rpm and other parameters were kept constant.

Figures 4.9 (a) and (b) depict that the introduction of stirring to the reaction had successfully eliminated the external diffusion limitation. The yield of BA and conversion of AA had significantly increased in the stirred reaction medium. Nevertheless, the yield of BA and conversion of AA do not change significantly at different stirring speeds because of the absence of the resistance of the fluid layer surrounding the catalyst surface (Forni, 1999, and Silva and Rodrigues, 2005).

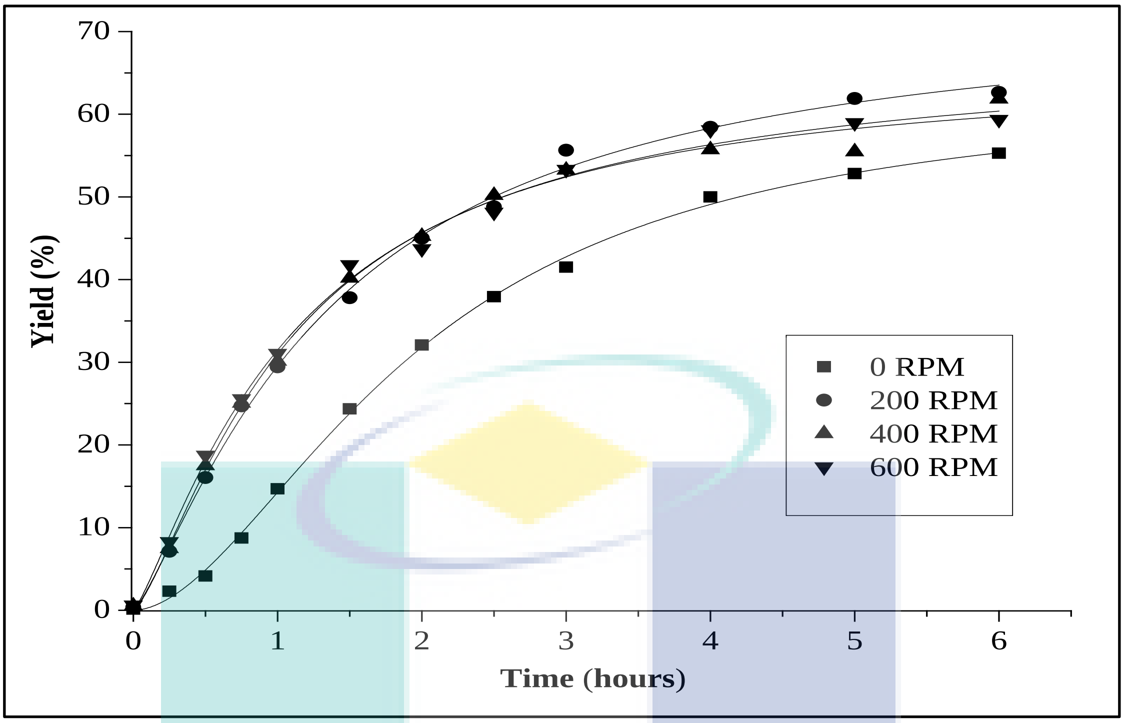

(a)

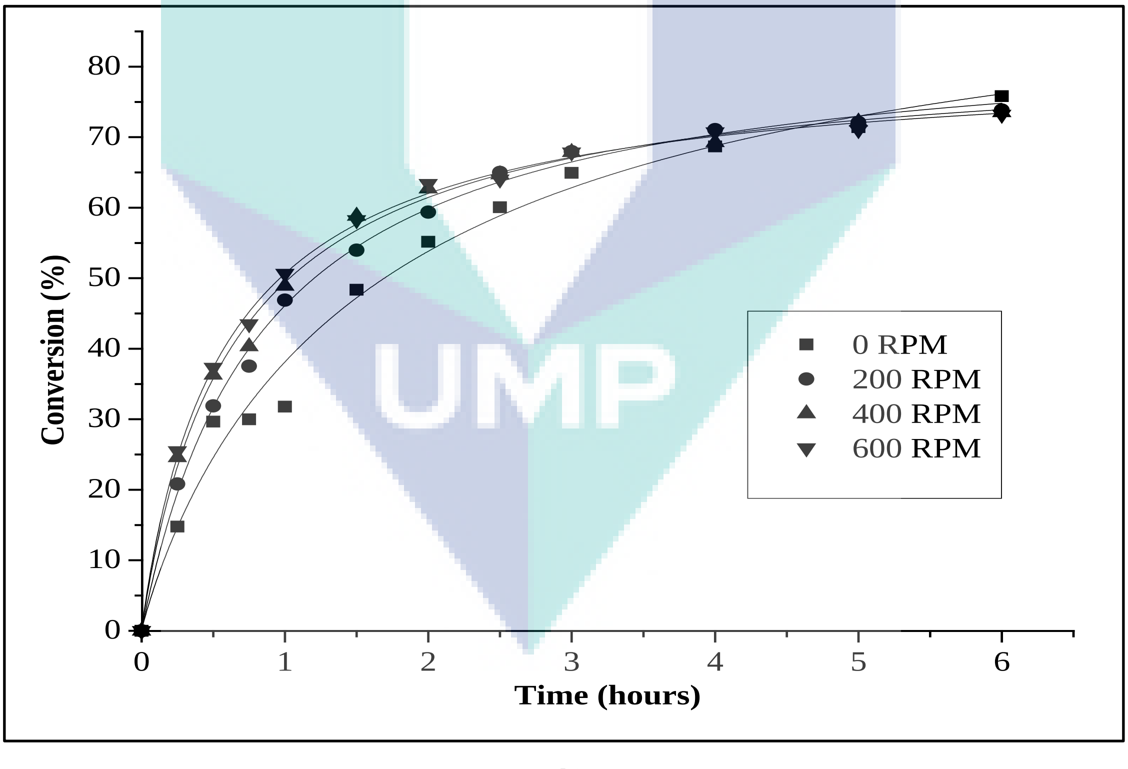

(b)

Figure 4.9: (a) Yield of BA and (b) Conversion of AA at different stirring speeds. Reaction conditions: $M_{AA:BuOH}$ of 1:1, catalyst loading of 10 wt% and temperature of 353 K

The elimination of external mass transfer was determined by Mears Criterion (C_M). The value of C_M must be less than 0.15. The C_M was calculated using Eq. (3.2) and the details of the calculation is shown in Appendix D. The values of C_M in Table 4.1 shows all the C_M values are less than 0.15, signifying that the diffusions of reactants from the bulk fluid through the fluid layer are extremely fast.

Table 4.1: The corresponding C_M values for the reactions carried out at different stirring speeds

No.	Stirring speed (rpm)	C_M	C_{WP}
1	0	0.004404	0.003352
2	200	0.004092	0.003114
3	400	0.003897	0.002966
4	600	0.003849	0.002929

Even though a stirring speed as low as 200 rpm could minimise the external diffusion limitation, the stirring speed of 400 rpm was chosen for the subsequent studies to guarantee the reaction was free from the external diffusion resistance.

The internal diffusion was not solely controlled by catalyst particle size but also the catalyst composition, reaction medium and temperature (Ali *et al.*, 2007). Delhomme, (2011) stated that the increase catalyst concentration could provide interfacial area to minimise the internal diffusion effect in the case which the catalyst was unavailable at different sizes. The SEP cannot be sieved into smaller size because it was a gel type catalyst. It was completely swelling in the reactants and hence making the reactants access to the active sites easily (Patricia *et al.*, 2007). The Weisz Prater Criterion (C_{WP}) for the reactions at different catalyst loadings, initial reactant ratios and temperature were calculated using Eq. (3.7) to identify the internal diffusion free region. The details calculation for the C_{WP} was shown in Appendix E. The values of C_{WP} in Table 4.2 shows all the C_{WP} values were less than 1 which implying that the resistance to internal pore diffusion was sufficiently small and the internal diffusion can be negligible in the present kinetic study.

4.3.2 Effect of Initial Molar Ratio

The usage of excess alcohol can shift the reaction equilibrium towards ester formation and hence shortens the time required to achieve equilibrium conversion. However, the excess alcohol also could lead to an expensive product recovery process (Teo and Saha 2004; Lilja *et al*., 2005; Ali *et al.*, 2007; Patricia *et al*., 2007; Yixin *et al*., 2009 and Toor *et al.*, 2011). The effect of molar ratio was studied to determine the best molar ratio. The others parameters were remained constant.

Comparing with the reaction with the stoichiometric ratio of AA and BuOH both the BA yield and AA conversion increase in the reactions with excess alcohol, particularly for the reactions with $M_{AA:BuOH}$ of 1:3 and 1:5 as shown in Figure 4.10. The $M_{AA:BuOH}$ of 1:7 has negative effect to the yield and conversion because BuOH has blocked the active sites on the catalyst surface and subsequently prevent it from nucleophilic attack by shielding the protonated AA (Das and Parida, 2006). The reaction with excess of acid with $M_{AA:BuOH}$ of 3:1 has resulted the low yield and conversion. This can be attributed to the insufficient BuOH available for the nucleophilic attack. Therefore, the best $M_{AA:BuOH}$ was 1:3 considering the yield, conversion and product recovery process.

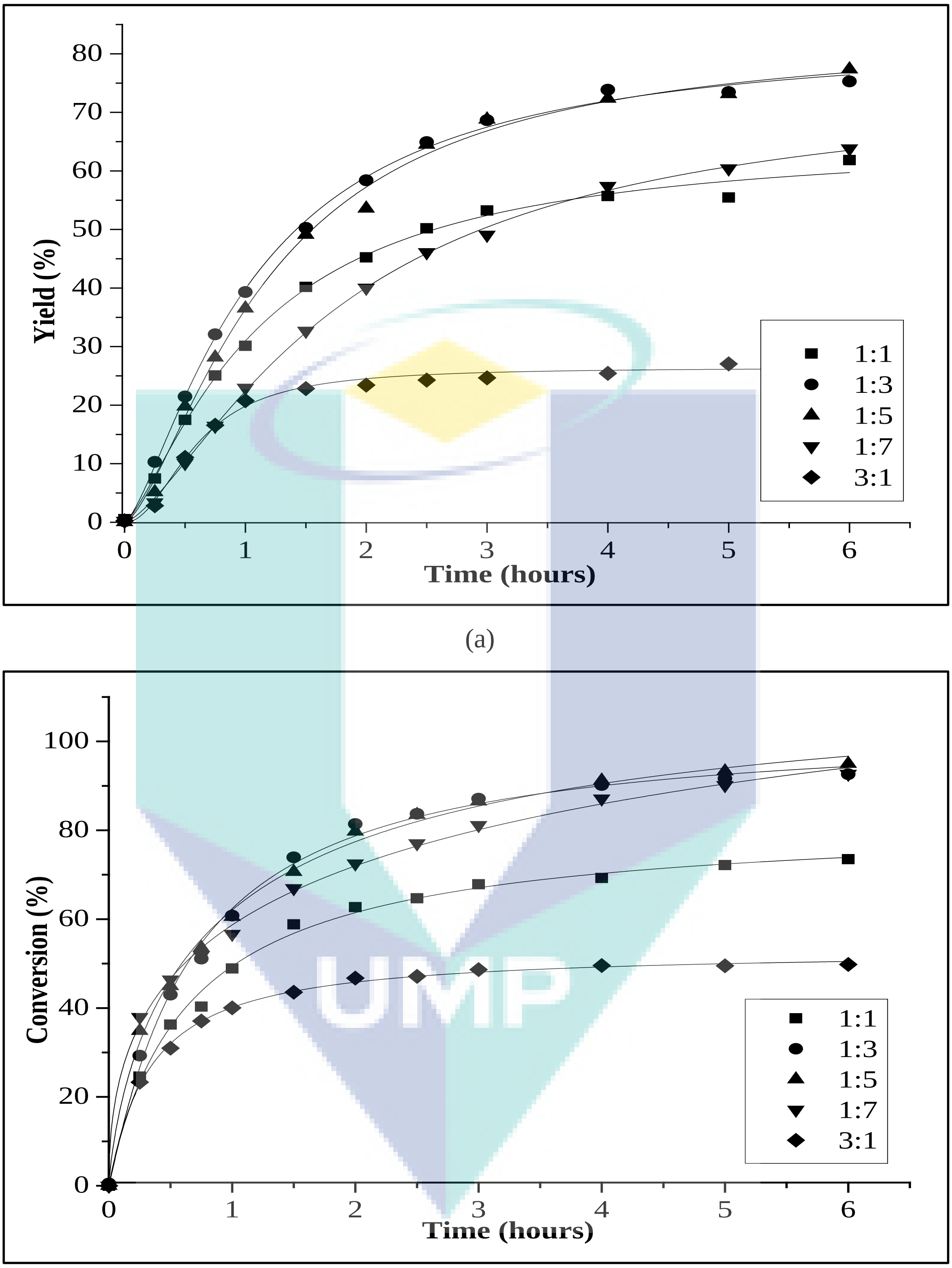

(a)

(b)

Figure 4.10: (a) Yield of BA and (b) Conversion of AA for the reactions carried out at different $M_{AA:BuOH}$ at the stirring speed of 400 rpm, catalyst loading of 10 wt% and temperature of 353 K

4.3.3 Effect of Catalyst Loading

The effect of catalyst loading on esterification between AA and BuOH was studied by varying the catalyst loading from 0 to 15 wt% (wt of catalyst/wt of AA). The other parameters were kept constant. Figure 4.11 shows that the increase in catalyst loading has led to the increase of yield and conversion. It is because of the increase of the catalyst active sites to promote the reaction (Das and Parida, 2006; Ali *et al*., 2007; Patricia *et al*., 2007; Ju *et al*., 2010 and Bhorodwaj *et al*., 2011). The yield and conversion after 6 hours for both the reaction with the catalyst loadings of 10 wt% and 15 wt% do not differ much since the reaction equilibrium was nearly achieved after 6 hours and the levelling off of the reaction rate because of excess catalyst sites rather than required by reactant molecules (Fogler, 2008; Rattanaphra *et al*., 2011 and Toor *et al*., 2011).

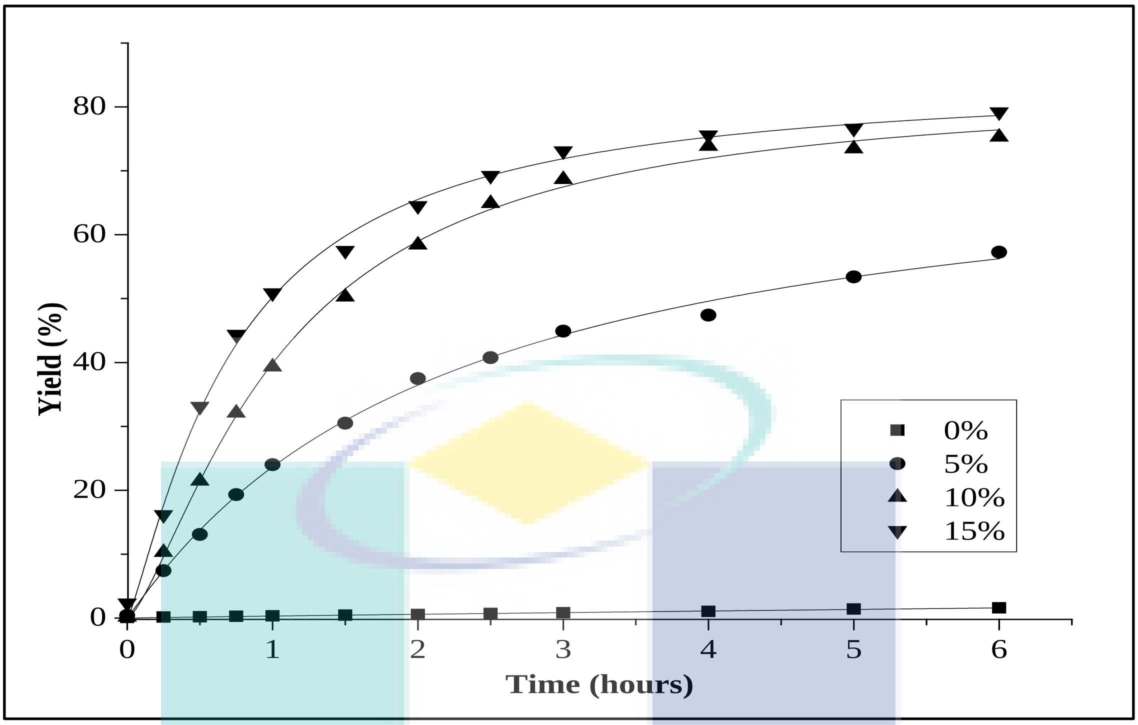

(a)

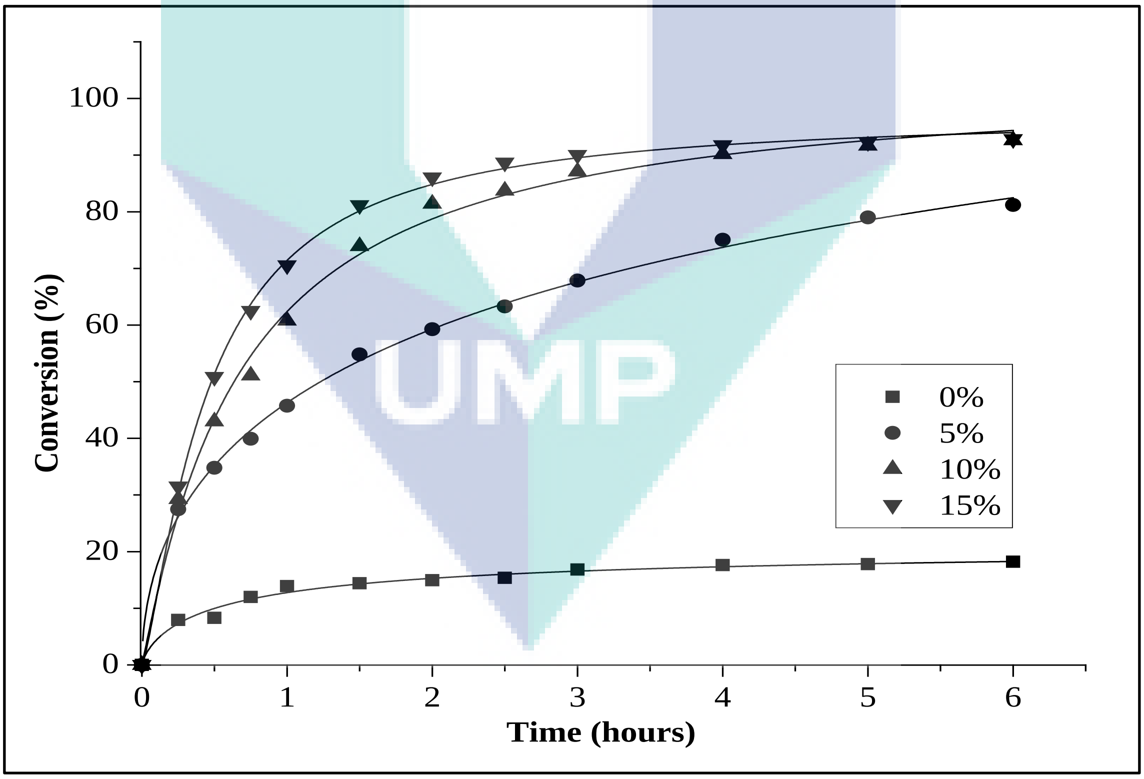

(b)

Figure 4.11: (a) Yield of BA and (b) Conversion of AA for the reactions carried out at different catalyst loadings. Reaction conditions: stirring speed of 400 rpm, $M_{AA:BOH}$ of 1:3 and temperature of 353 K

Figure 4.12 shows that the initial reaction rate was increasing linearly with the catalyst loading because number of active sites available for the reaction was proportional to the amount of catalyst (Kong *et al.*, 2011). The initial reaction rate was calculated using Eq. (4.3). The mathematical correlation as shown in Eq. (4.4) relates the initial reaction rate with the catalyst loading. This equation was only valid for the reaction carried out at the temperature of 353 K and the $M_{AA:BuOH}$ of 1:3.

$$r_o = \left(\frac{dC_{BA}}{dt}\right)_{t=0} \tag{4.3}$$

$$r_{BAo}\left(mol.L^{-1}.min^{-1}\right) = 0.0001 + 0.0028C_{cat}\left(mol.L^{-1}\right) \tag{4.4}$$

It was reported that a heterogeneous catalyst was not industrial practical if the amount required during the reaction was more than 10 wt% (Teo and Saha, 2004). Considering both the time taken to achieve equilibrium and the industrial practicability, the catalyst loading of 10 wt% was used in the subsequent studies.

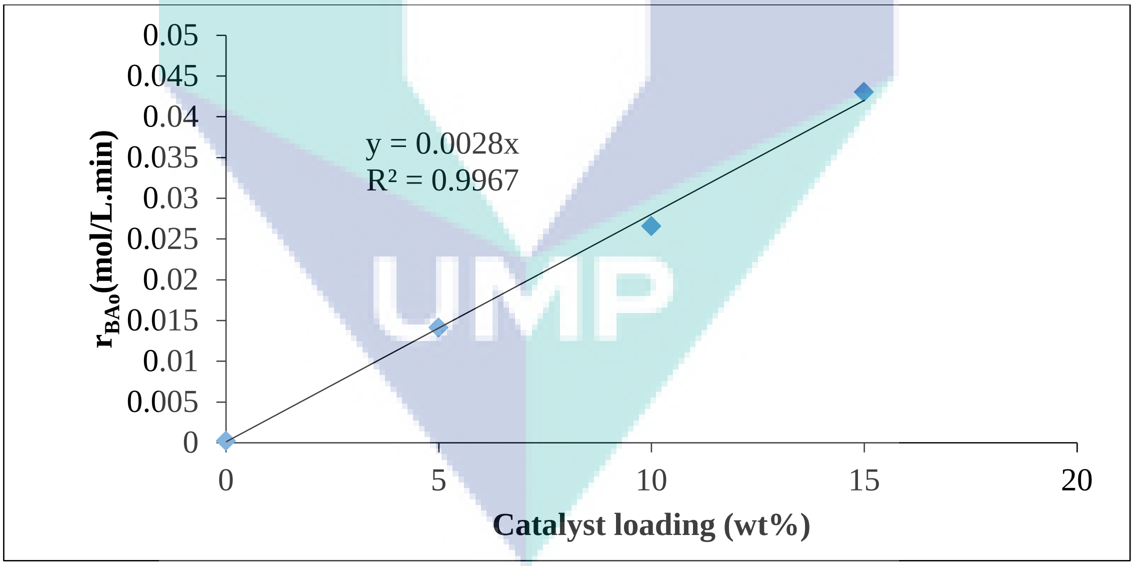

Figure 4.12: Effect of catalyst loading on the initial reaction rate. Reaction conditions: stirring speed of 400 rpm, $M_{AA:BuOH}$ of 1:3, and temperature of 353 K

4.3.4 Effect of Temperature

The effect of temperature was studied by varying the reaction temperature from 313-373 K while the other parameters were kept constant. Figure 4.13 (a) and (b) shows that the BA yield and AA conversion increase with the temperature. The BA yield decreased after certain durations (1-2 hours) for the reactions carried out at 363 K and 373 K but the AA conversion still increasing because the polymerisation of product and reactant took place (Yang *et al*., 2008). The reaction mixture also became more viscous indicated that polymerisation occurred (Kricheldorf, 1991). Figure 4.14 shows that the reaction rate increases exponentially with temperature indicating that the reaction controlled by surface reaction. The temperature rise causes more frequent collision of the reactants which resulting more successful collision to break the bonds to forms the ester (Ali *et al.*, 2007).

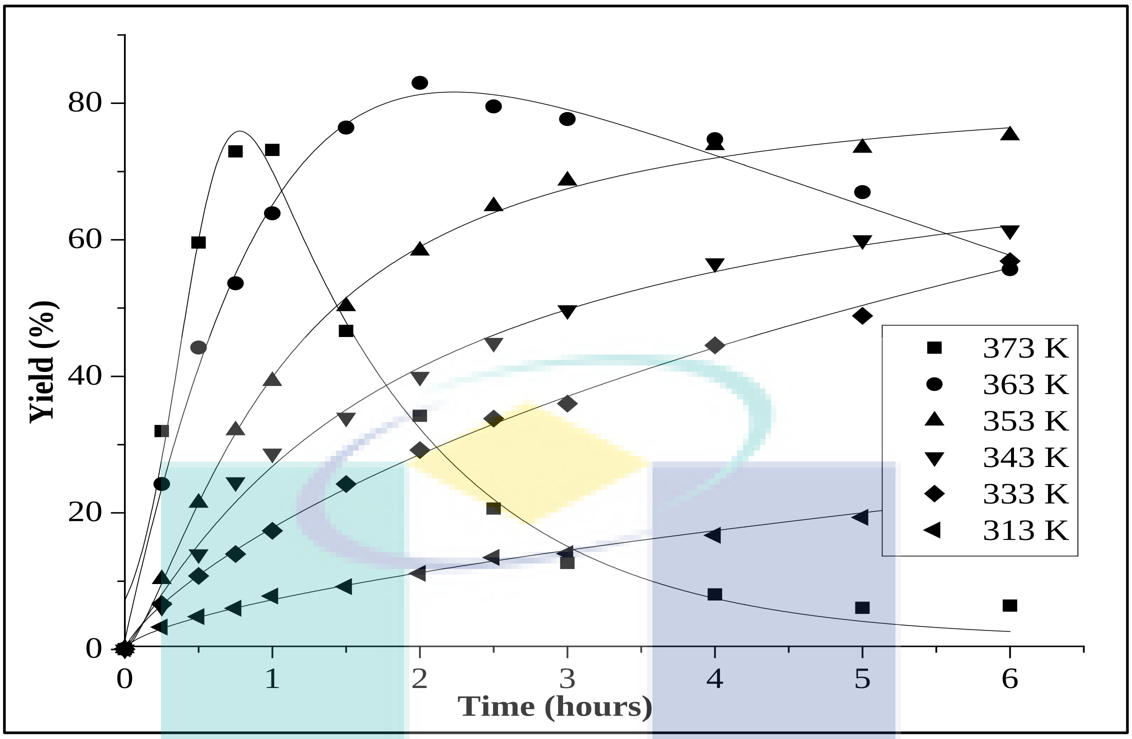

(a)

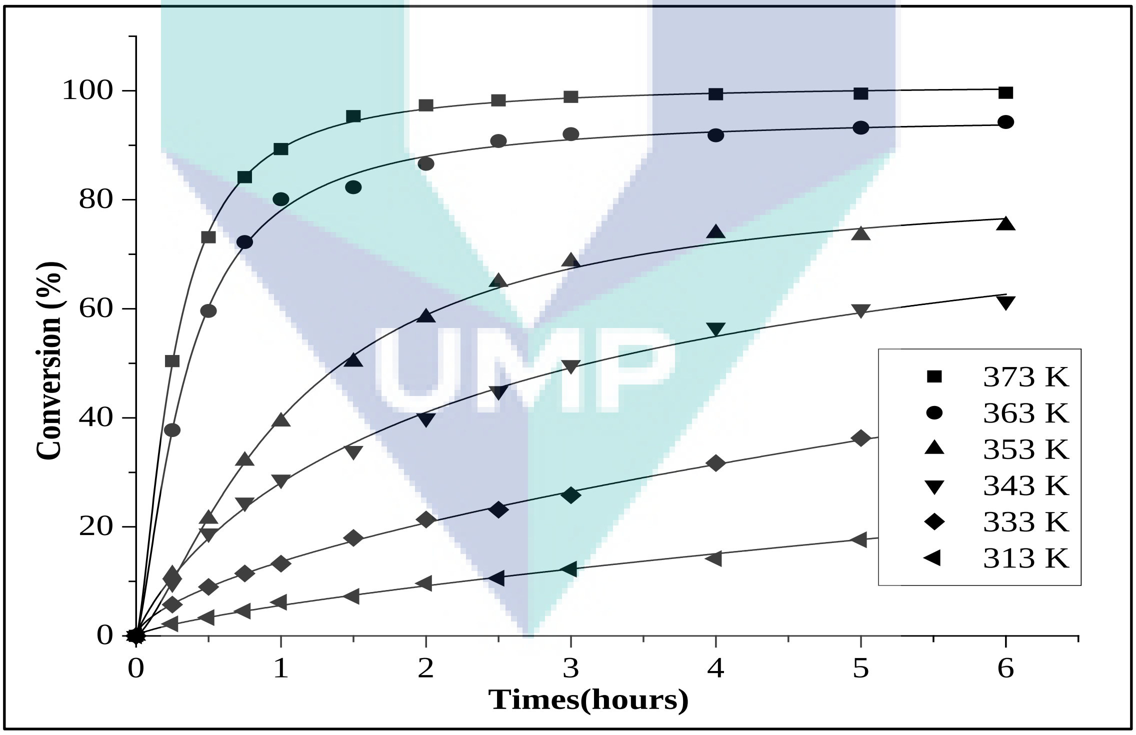

(b)

Figure 4.13: (a) Yield of BA and (b) Conversion of AA for the reaction carried out at different temperatures. Reaction conditions: stirring speed of 400 rpm, $M_{AA:BuOH}$ of 1:3 and catalyst loading of 10 wt%

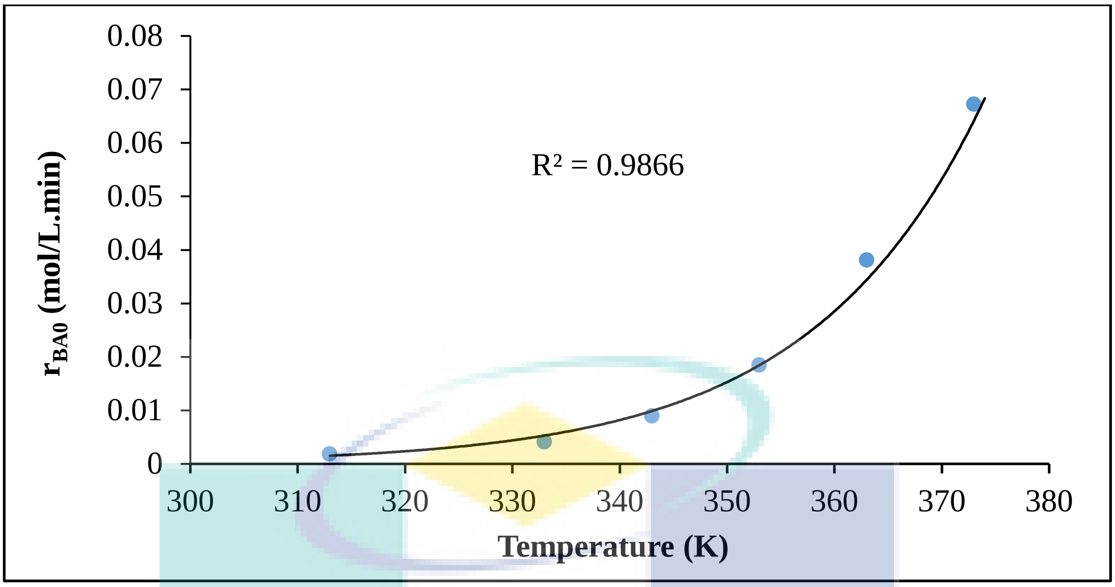

Figure 4.14: Effect of reaction temperature on initial reaction rate. Reaction condition: stirring speed of 400 rpm, initial $M_{AA:BuOH}$ of 1:3 and catalyst loading of 10 wt%

4.3.5 Effect of Initial Water Content

The initial water content in the reaction mixture was varied from 0 to 90 wt% to determine the stability of SEP under aqueous condition. Figure 4.15 shows that the yield of BA decreased with the increased of initial water content in the reaction mixture. The excess of water had shifted the reaction equilibrium to the reactant side and hence lower initial rate and BA yield were obtained. Figure 4.17 shown the declined of initial reaction rate with the increasing of initial water content in the reaction mixture. The increasing amount of water absorbed on the active sites of SEP has also blocked and hindered the other reactants to reach the active sites (Blagov *et al.*, 2005). Moreover, the poor accessibility of reactants may also due to the polymerisation as shown in Figure 4.16 (Park *et al.*, 2009). Figure 4.16 illustrates that the deposit of polymer on the catalyst surface has covered the minute cracks and pores on the used SEP. The degree of AA polymerisation is increased with the increased of initial water content in the reaction mixture (Kuchta *et al.*, 2000) and more deposit was found in the used catalyst of the reaction with initial content of 50 wt% (Figure 4.16(c)) comparing with the used catalyst of the reaction with initial water content of 10 wt% (Figure 4.16(b)). The AA will undergo a nucleophilic addition to the double bond of a second AA molecule. The increasing water will reduced the solubility of oxygen which is needed for inhibitor (MEHQ) to stop the polymerisation. Thus, diacrylic acid formation increases with increasing water content (Safety handling and storage of acrylic acid, 2012). The AA polymerisation mechanism shown in Appendix H.

The presence of excess water had also promoted desulfonation (deactivation) of the SEP because the interaction of water with sulfonic acid groups can be very detrimental. Figure 4.17 shown that the reduced of IEC with increasing of initial water concentration because the pores that serves as routes to interior active sites was clogging with polymerisation shown in Figure 4.16 (Miller *et al.*, 1981).

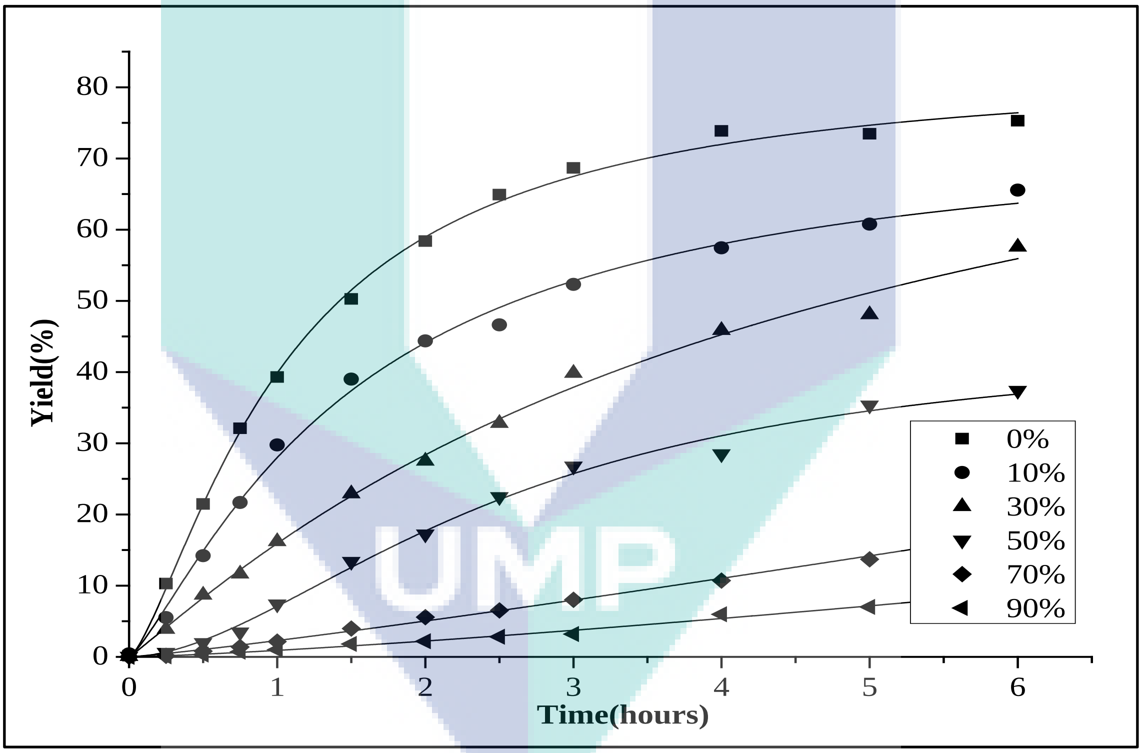

Figure 4.15: Effect of initial water content to the esterification of AA with BuOH. Reaction conditions: temperature of 353 K, $M_{AA:BuOH}$ of 1:3, catalyst loading of 10 wt%, stirring speed of 400 rpm

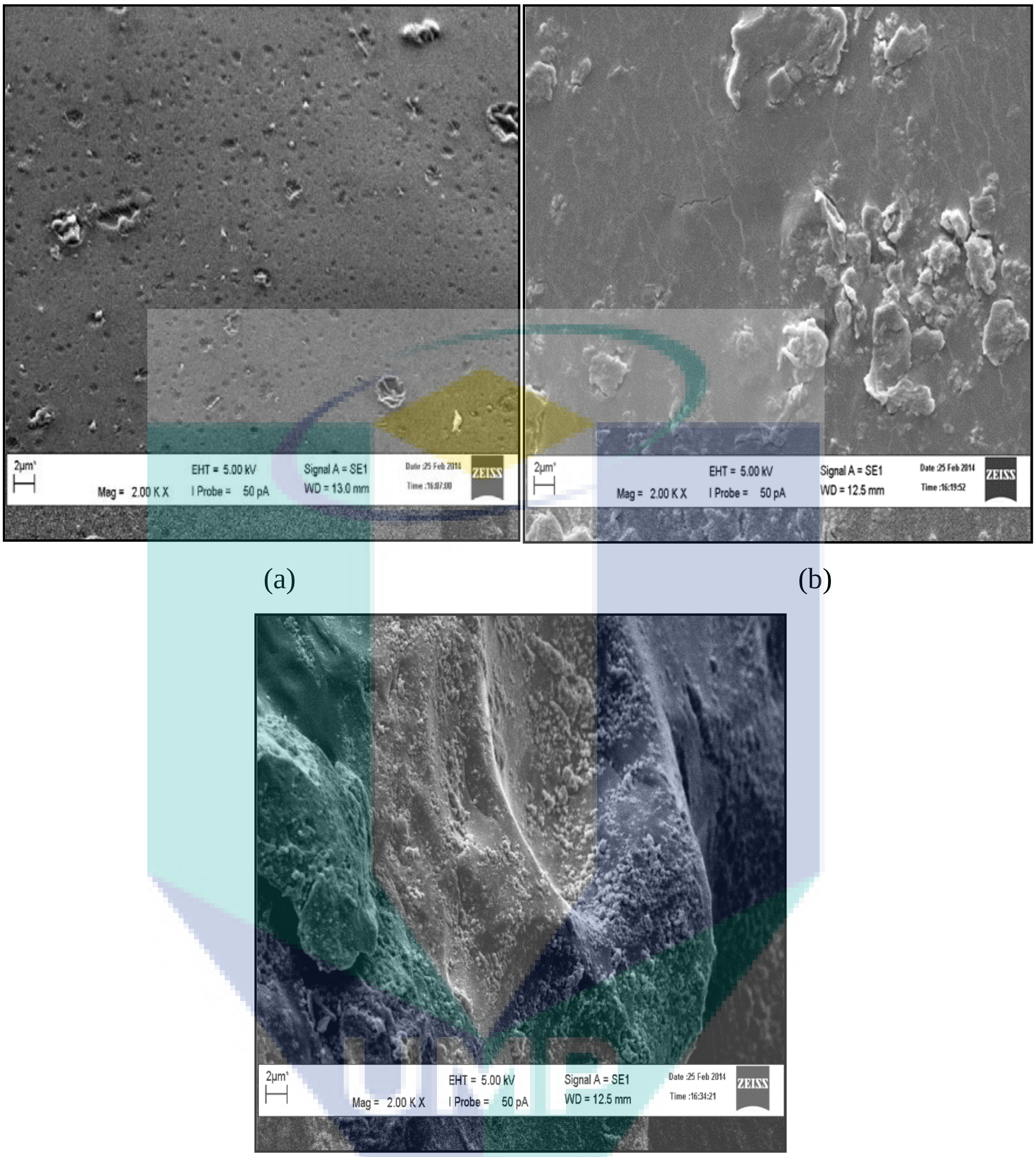

(a) (b)

(c)

Figure 4.16: SEM micrograph of the used SEP in the reaction mixture with different initial water contents of a) 0 wt%, b) 10 wt% and c) 50 wt%

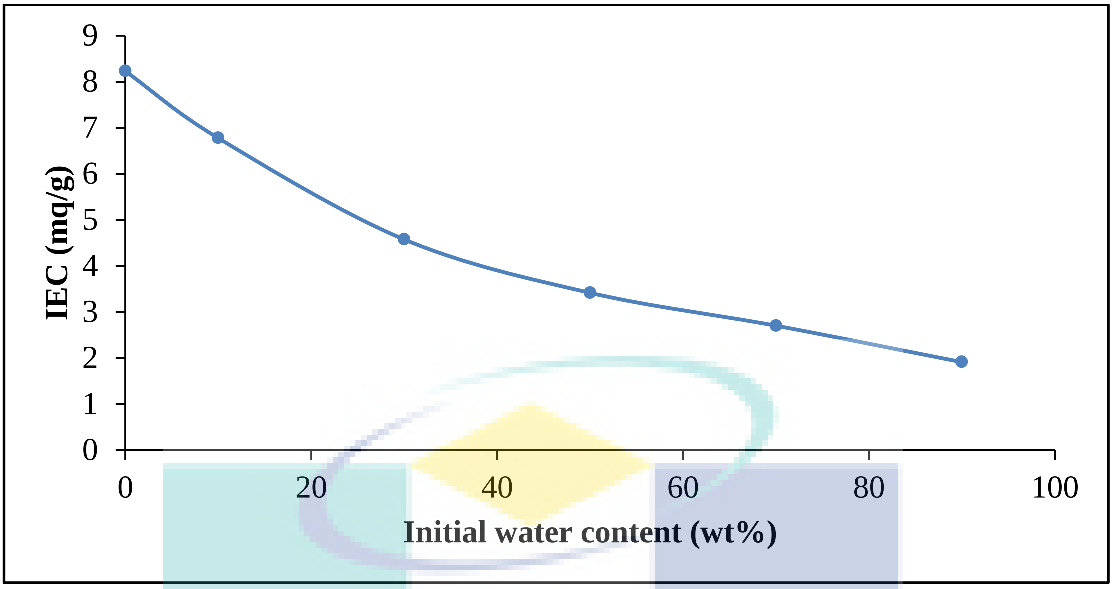

Figure 4.17: The IEC of SEP in different initial water concentration

Figure 4.18 shows the FT-IR spectra for fresh SEP and used SEP of the reaction with different initial water concentrations. The spectra shows slightly reduced on band intensity on stretching vibration of sulfonic acid at broad band centered at 2928 cm^{-1} in used SEP as initial water concentration increased. This supported by IEC in Figure 4.17.

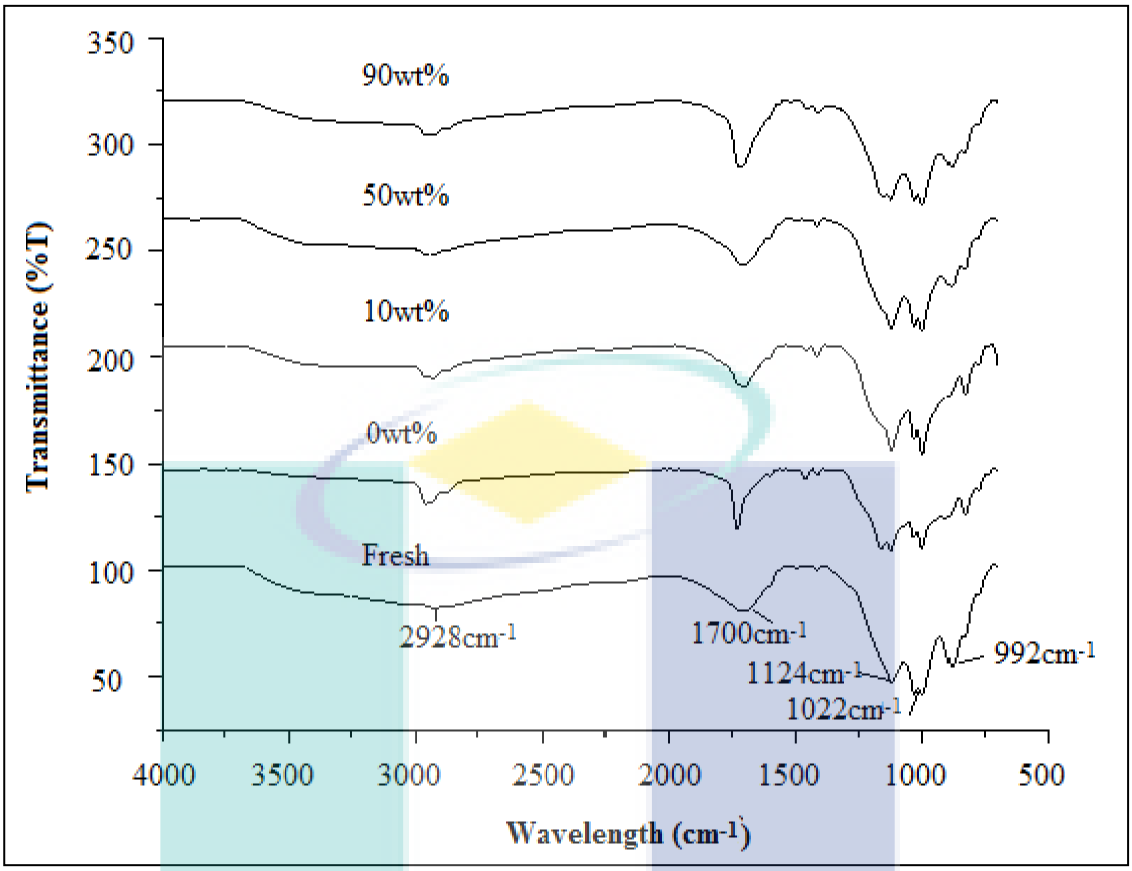

Figure 4.18: FT-IR spectra of fresh SEP and used SEP in the reaction mixtures with different initial water content

4.4 CHEMICAL EQUILIBRIUM STUDY FOR ESTERIFICATION OF AA WITH BUOH

The esterification of AA and BuOH is based on the following chemical equation:

$$\underset{AA}{CH_2CHCOOH}+\underset{BuOH}{C_4H_9OH}\leftrightharpoons\underset{BA}{CH_2CHCOO(CH_2)_3CH_3}+\underset{W}{H_2O} \tag{4.5}$$

The esterification process was limited by equilibrium conversion. The thermodynamic equilibrium constant of reaction, K_a was shown in Eq. (4.6).

$$K_a = exp\left(-\frac{\Delta G^o}{RT}\right) = \prod a_i^{v_i} = \prod_i (x_i\gamma_i)^{v_i} \tag{4.6}$$

where ΔG^o is the Gibbs energy, R is the gas constant, T is the temperature, v_i is the stoichiometric factor for *ith* component, γ_i is gamma of *ith* component, x_i is the mole fraction of *ith* component at equilibrium and a_i is the activity coefficient of *ith* component calculated by the UNIFAC model.

The equilibrium constant was calculated experimentally according the Eq. (4.7).

$$K_a = \frac{x_{BA} x_W \gamma_{BA} \gamma_W}{x_{AA} x_{BuOH} \gamma_{AA} \gamma_{BuOH}} = \frac{x_{BA}^2 \gamma_{BA} \gamma_W}{\left(x_{AA}^o - x_{BA}\right)\left(x_{BuOH}^o - x_{BA}\right)} \tag{4.7}$$

The apparent equilibrium constant of the reaction, K_x expressed in terms of mole fraction can be written as Eq. (4.8).

$$K_x = \sum x_i^{v_i} = \frac{x_{BA} x_W}{x_{AA} x_{BuOH}} = \frac{x_{BA}^2}{(x_{AA}^o - x_{BA})(x_{buOH}^o - x_{BA})} \tag{4.8}$$

The experimental data required to determine the equilibrium mole fraction of AA, BuOH, BA and W was generated at the reaction temperature of 313, 333, 343 and 353 K, molar ratio of 1:3, catalyst loading of 10 wt%, and stirring rate of 400 rpm. The activity coefficients corresponding to the experimental mole fraction of all components at equilibrium state were calculated using UNIFAC and shown in Table 4.2. The details of calculation are shown in Appendix C.

Table 4.2: Mole fraction and activity coefficient of component in the equilibrium state at various temperature

Temperature (K)	**Initial mol fraction, x_o**		**Mole fraction, x**				**Activity coefficient**			
	AA	BuOH	AA	W	BuOH	BA	AA	W	BuOH	BA
313	0.2500	0.7500	0.7940	0.1643	0.5920	0.1643	0.0603	0.5130	0.6367	0.4097
333	0.2500	0.7500	0.0270	0.1949	0.5831	0.1949	0.0191	0.6356	0.6303	0.4452
343	0.2500	0.7500	0.0177	0.2133	0.5557	0.2133	0.0123	0.7021	0.6052	0.4616
353	0.2500	0.7500	0.0100	0.2290	0.5320	0.2290	0.0068	0.7585	0.5832	0.4732

The thermodynamic and the apparent equilibrium constants calculated based on Eq. (4.7) and (4.8) is tabulated in Table 4.3 and plotted against temperature in Figure 4.19. K_a is more sensitive to temperature change.

Table 4.3: The apparent and activity based equilibrium constant (K_x and K_a respectively), the corresponding enthalpy of reaction and equilibrium conversion of AA (X_e)

Temperature (K)	K_x	ΔH_r^o **(kJ/mol)**	K_a	ΔH_r^o **(kJ/mol)**	X_e **(%)**
313	0.54	22.68	5.13	24.56	64.10
333	1.24	51.17	12.14	49.96	70.11
343	2.31	66.07	21.82	63.25	79.29
353	4.79	81.41	43.85	76.93	87.73

Table 4.4 shows the increasing equilibrium constant with an increase in temperature and the values of enthalpies are positive. This indicates that the esterification of AA with BuOH catalysed by SEP is endothermic in nature (Bart *et al.*, 1994 and Toor *et al.*, 2011).

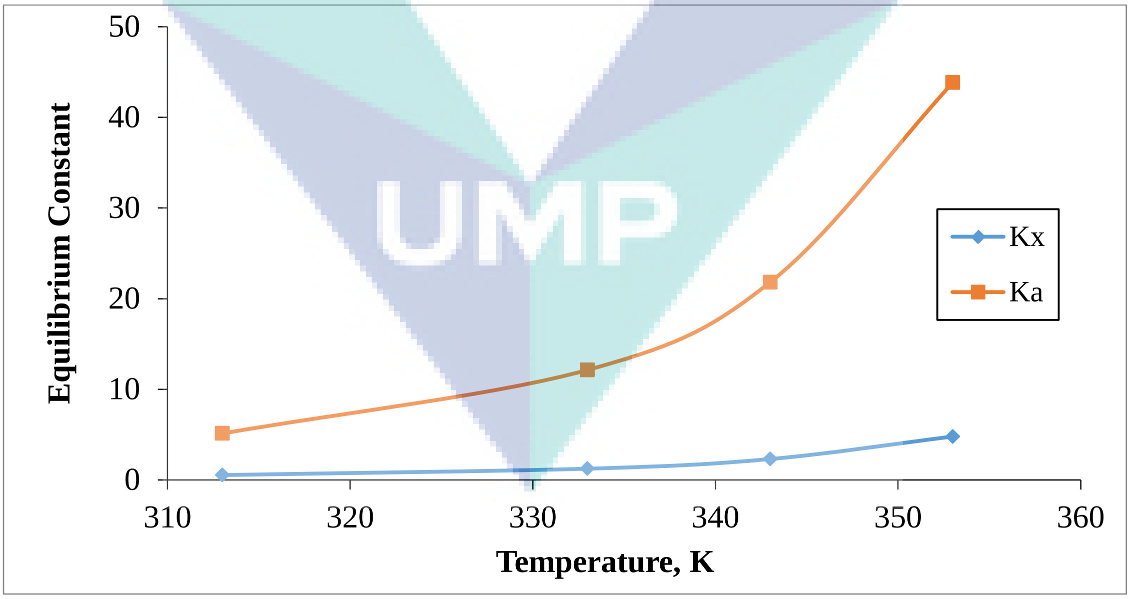

Figure 4.19: The temperature dependence of K_x and K_a equilibrium constants of the esterification of AA with BuOH. Reaction conditions: $M_{AA:BuOH}$ of 1:3, catalyst loading of 10 wt% and stirring speed of 400 rpm

The temperature dependence of the K_x and K_a can be described by Eq. (4.9).

$$K= exp\left(b_1+\frac{b_2}{T}+b_3T\right) \tag{4.9}$$

where b_i is the adjustable parameter of *ith* that can be fitted to the experimental data using the least squares method. The sum of squared between experimental and calculated values was evaluated for all the experiments points. The standard deviation as shown in Eq. (4.10) can be used as a measure of the quality of fit.

$$\sigma(K)=\sqrt{\sum_{i=1}^{N}\frac{\left(K_i^{exptl}-K_i^{calc}\right)^2}{n-m}} \tag{4.10}$$

Where n is the number of experimental points and m is the number adjusted parameters. The fitted parameters of Eq. (4.9) are tabulated in Table 4.4 with its standard deviation, $\sigma(bi)$.

Table 4.4: The b_i parameters and their standard errors, σ(*bi*)

i		K_x			K_a	
	1	2	3	1	2	3
b_i	-157.91	23250	0.26	-136.94	20210	0.24
σ(bi)	3.45	837.69	0.0062	12.94	2906.47	0.022

Based on the Van’t Hoff equation as shown in Eq. (4.11), the thermodynamics equilibrium, constant is related to standard enthalpy of reaction, ΔH_r^0.

$$\left(\frac{d\ lnK_a}{dT}\right)=\frac{\Delta H_r^0}{RT^2} \tag{4.11}$$

Eq. (4.12) is a combined Eq. (4.9) and (4.11) to calculate the enthalpy of reaction for both K_x and K_a. The enthalpy values calculated for the discrete temperatures are given in Table 4.4.

$$\Delta H_r^0 = -R\left(b_2 - b_3 T^2\right) \tag{4.12}$$

The estimated enthalpy of the reaction is compared with standard enthalpy of formation $\Delta_f H_i^0$ as shown in Eq. (4.13).

$$\Delta H_r^0 = \sum_{\text{product}} v_i \Delta_f H_i^0 - \sum_{\text{reactant}} v_i \Delta_f H_i^0 \tag{4.13}$$

The enthalpies of formation for each component in the liquid state at 298 K are given in Table 4.5. Considering that the temperature dependence of the enthalpy of reaction at 298 K, the calculated enthalpy based on Eq. (4.12) is 2.48 kJ/mol and 6.55 kJ/mol for K_x and K_a respectively. The enthalpy calculated based on K_x, 2.48 kJ/mol is in line with the enthalphy calculated using Eq. (4.13), 2.7 kJ/mol. This has validated the measured equilibrium data.

Table 4.5: Enthalpy of formation of the selected components

Compound	Enthalpy of formation (kJ/mol)
Acrylic acid	-383.8
1-butanol	-327.3
Butyl acrylate	-422.6
Water	-285.8

Source: CRC Handbook of Chemistry and Physics, 2000

4.5 KINETIC STUDY

4.5.1 Main Reaction (Esterification)

Based on the studies on the effect of important operating parameters, the esterification of AA with BuOH operated under the range of the operating condition for the present study was not affected by diffusion. Furthermore, the exponential increment of the reaction rate with the reaction temperature has proven the esterification of AA with BuOH catalysed by SEP was controlled by the surface reaction. Therefore, the experimental kinetic data was correlated to the surface reaction controlled kinetic models like PH, ER and LHHW models.

PH model is mostly adopted in the kinetic study because of its similarities to the homogeneous reaction which contains no adsorption terms for any reactant. This model is similar with power law model for homogeneous reaction. ER model delineates a reaction which the rate determining step is the reaction between one reactant adsorbed on the catalyst surface and it counterpart reactant in the bulk region. ER I model is derived based on the reaction mechanism in which adsorbed AA reacts with BuOH in the bulk region, while ER II model is derived based on the reaction mechanism in which adsorbed BuOH reacts with AA in the bulk region. While, LHHW model represents a reaction which the rate determining step being the reaction of both adsorbed reactants (AA and BuOH). The behaviour of liquid phase reactions may deviate from the ideal solution. The non-ideal arises due to the difference in size and polarity of the species. The activity coefficients were used to account for the non-ideal mixing behaviour of bulk liquid phase instead of molar fractions. The activity coefficients were calculated using UNIFAC group contribution method. The PH, ER I, ER II, and LHHW models in term of activity based are shown in Eq. (4.14-4.17) respectively.

$$r_{BA}=k_f\left(\alpha_{AA}\alpha_{BuOH}-\frac{1}{K_a}\alpha_{BA}\alpha_W\right) \tag{4.14}$$

$$r_{BA}=\frac{k_f(\alpha_{AA}\alpha_{BuOH}-\frac{1}{K_a}\alpha_{BA}\alpha_W)}{1+K_{AA}\alpha_{AA}+K_W\alpha_W} \tag{4.15}$$

$$r_{BA}=\frac{k_f(\alpha_{AA}\alpha_{BuOH}-\frac{1}{K_a}\alpha_{BA}\alpha_W)}{1+K_{BuOH}\alpha_{BuOH}+K_{BA}\alpha_{BA}} \tag{4.16}$$

$$r_{BA}=\frac{k_f(\alpha_{AA}\alpha_{BuOH}-\frac{1}{K_a}\alpha_{BA}\alpha_W)}{(1+K_{AA}\alpha_{AA}+K_{BuOH}\alpha_{BuOH}+K_{BA}\alpha_{BA}+K_W\alpha_W)^2} \tag{4.17}$$

The activity based equilibrium constant; K_a was adopted from section 4.4. The rate constant, k_f can be related to Arrhenius equation as shown in Eq. (4.18).

$$k_f=k_{f0}\,exp\left(\frac{-E_f}{RT}\right) \tag{4.18}$$

where k_{f0} is the pre-exponential factors for the reaction and E_f denote the activation energy of reaction.

Despite the use of MEHQ (180-200 ppm) as inhibitor, AA polymerisation still occurred when the reaction temperature was increased. Therefore, the instead of rate of reaction of the limiting reactant AA (r_{AA}), the rate of reaction of BA (r_{BA}) was used for correlated with kinetic models, r_{BA} was determined using Eq. (4.19).

$$r_i=\frac{dC_i}{dt} \tag{4.19}$$

where C_i is the concentration of component i and t is the reaction time. Figure 4.20 shows the parity plot of the experimental and predicted rate of reaction. Comparing to the predicted data of the PH model, the predicted data of the ER and LHHW models scatters nearer to the 45^o diagonal line signifying that ER and LHHW models could predict the rate of reaction with better accuracy.

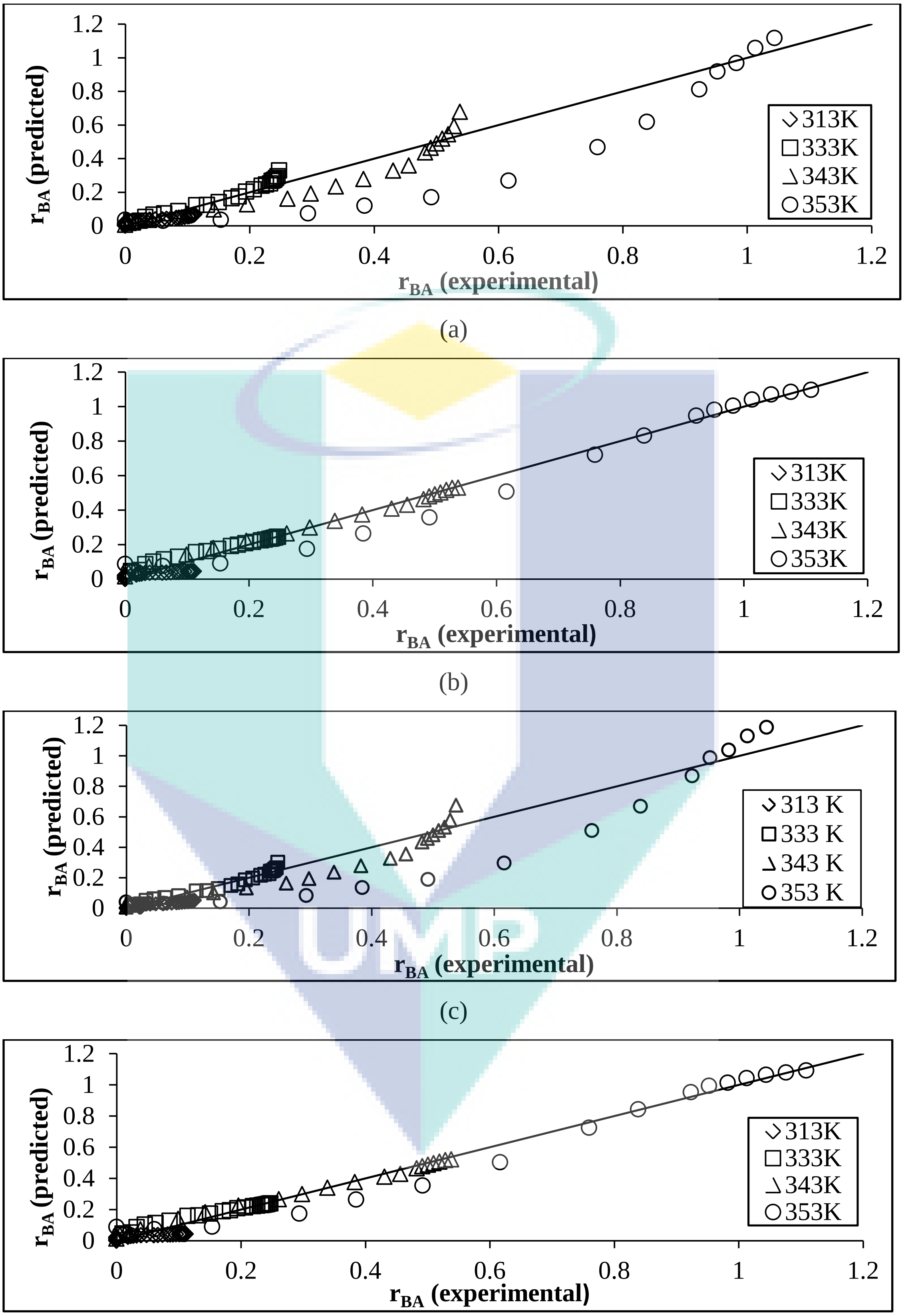

(a)

(b)

(c)

(d)

Figure 4.20: Parity plot of experimental and predicted rate of reaction using (a) PH model, (b) ER I, (c) ER II and (d) LHHW model

The kinetic parameters obtained with their standard errors, σ, are shown in Table 4.6. The ER I model with coefficient of determination, R^2 of closest to one, gave the best prediction indicating that the esterification of AA and BuOH catalysed by SEP occurred based on the ER mechanism. The AA was adsorbed onto SEP before reacting with BuOH in the bulk fluid. The adsorbed AA accepts a proton from SEP. BuOH molecule attacked the protonated carbonyl group to give a tetrahedral intermediate and water. A proton was lost at one oxygen atom and gains by another oxygen atom to form another intermediate which further loses a molecule of water that gives a protonated ester. A proton was transferred to a water molecule to give the butyl acrylate.

The apparent activation energy for the esterification of AA and BuOH catalysed by SEP was 73.6 kJ/mol. The same reaction studied by Sert *et al.*, (2013) using Amberlyst 131 has lower activation energy (57.4 kJ/mol) because the catalyst acidity used was lesser (Kong *et al.*, 2011). The activation energy was in between 72.8-77.8 kJ/mol, a range which was proposed by Fomin *et al.* (1991) in their study about esterification of acrylic acid catalysed by ion exchange resin.

Table 4.6 : Kinetic parameters of the models used to fit the experiment data

	Kinetic Parameter		**Adsorption Parameter**				
Model	K_{f0} (σ k_{f0}) (mol/L.hr)	Ef (σ Ef) (J/mol)	K_{AA} (σK_{AA})	K_{BuOH}(σK_{BuOH})	K_{BA}(σK_{BA})	K_W(σK_W)	**R^2**
PH	$1.39x10^{11}$ ($1.26x10^{11}$)	69420 (2597.54	-	-	-	-	0.92
ER I	$3.25x10^{12}$ ($2.36x10^{10}$)	73600 (20.86)	24.23 (0.23)	-	-	1.23 (0.12)	0.98
ER II	5.86x1012 (8.09x108)	77500 (0.40)	-	2.01 (0.0005)	0.26 (0.003	-	0.91
LHHW	$1.03x10^{14}$ ($7.97x10^{10}$)	74200 (2.22)	28.49 (0.03)	7.33 (0.01)	2.07 (0.02)	1.10 (0.02)	0.97

4.5.2 Side Reaction (Dimerisation)

The best fit model, ER I model was included into the batch reactor model to predict the concentration of components for determination of side reaction of the esterification reaction. The potential side reactions are the polymerisation of BA and AA. Some of dimer molecules will transform into polymer. Assuming each reaction was elementary, the chemical equations and corresponding reaction rates were shown in Eq. (4.20) and (4.21) respectively.

$$2AA \overset{k_2}{\rightarrow} dimer \tag{4.20 a}$$

$$2BA \overset{k3}{\rightarrow} dimer \tag{4.20 b}$$

$$r_{2,AA} = -k_2\left(\alpha_{AA}^2\right) \tag{4.21 a}$$

$$r_{3,BA} = -k_3\left(\alpha_{BA}^2\right) \tag{4.21 b}$$

where k_2 and k_3 are the rate constants for the polymerisation of AA and BA respectively. The reaction rate constants were related using Arrhenius equation. The constants, k_2 and k_3 were determined using the non-linear regression analysis in POLYMATH 6.10 program. Figure 4.21(a) shows the significant deviation of predicted and experimental concentration of AA concentration when the side reaction was not considered. Figure 4.21(b) shows the BA concentration was not significant for temperature 313 K to 353 K.

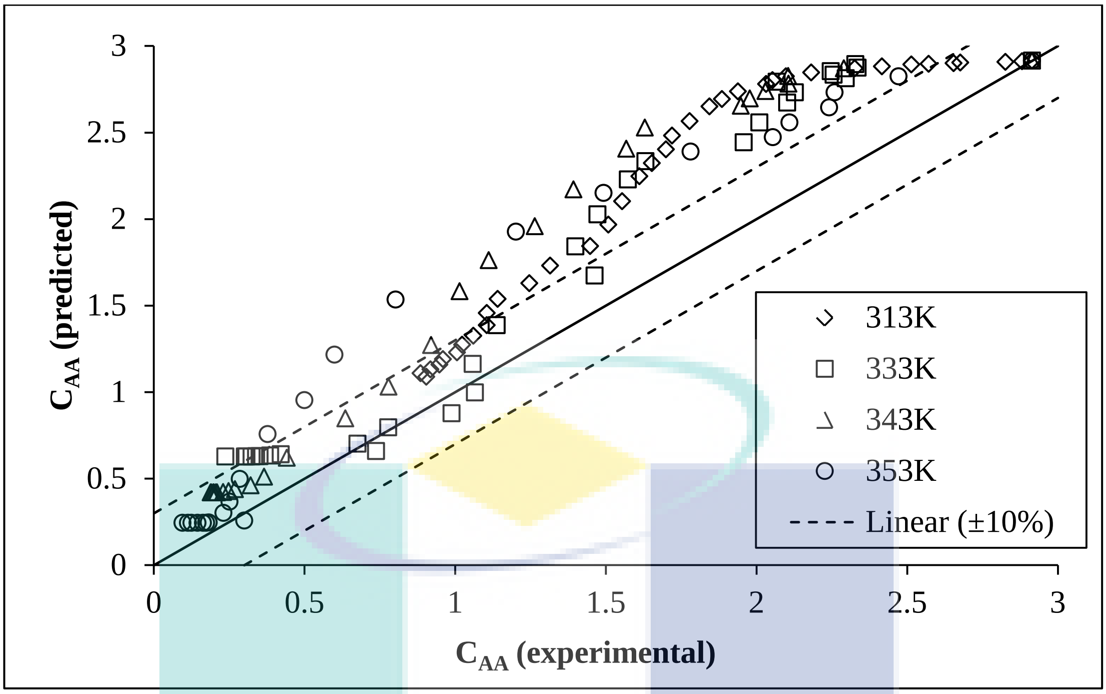

(a)

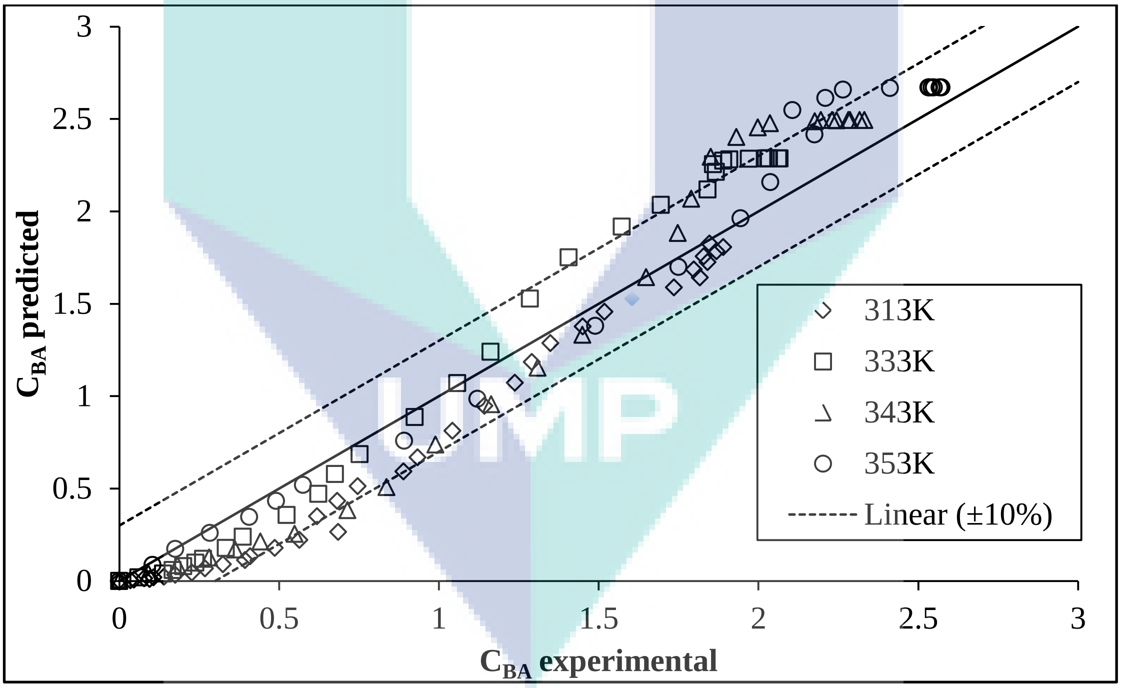

(b)

Figure 4.21: Parity plot of the experimental and predicted concentration of AA and BA without considered the polymerisation of AA and BA

The polymerisation of AA were related to the reaction temperature. The parity plot of the reaction rate of AA after considering the AA polymerisation was shown in Figure 4.22. The errors between predicted and experimental data are within ±10%. The polymerisation rate constant for AA was shown in Eq. (4.22).

$$k_2=3.018\times 10^{13}\,exp\left(\frac{-78640}{RT}\right) mol/L.hr \qquad (4.22)$$

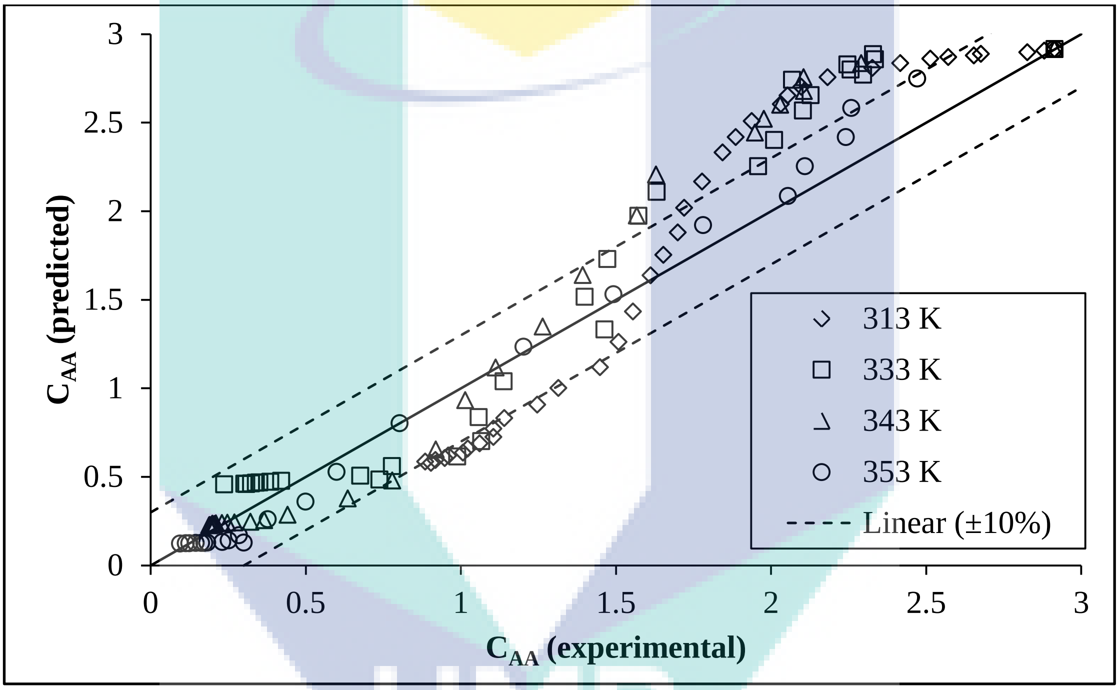

Figure 4.22: Parity plot of the experimental and predicted reaction rate of AA considering the polymerisation of AA

The reaction rate, Eq. (4.18) is obtained by solving the reactor design ordinary differential equations using Runge-Kutta method. Figure 4.23 shows the good agreement between the predicted and experimental concentration value for a reaction at an arbitrary operating condition.

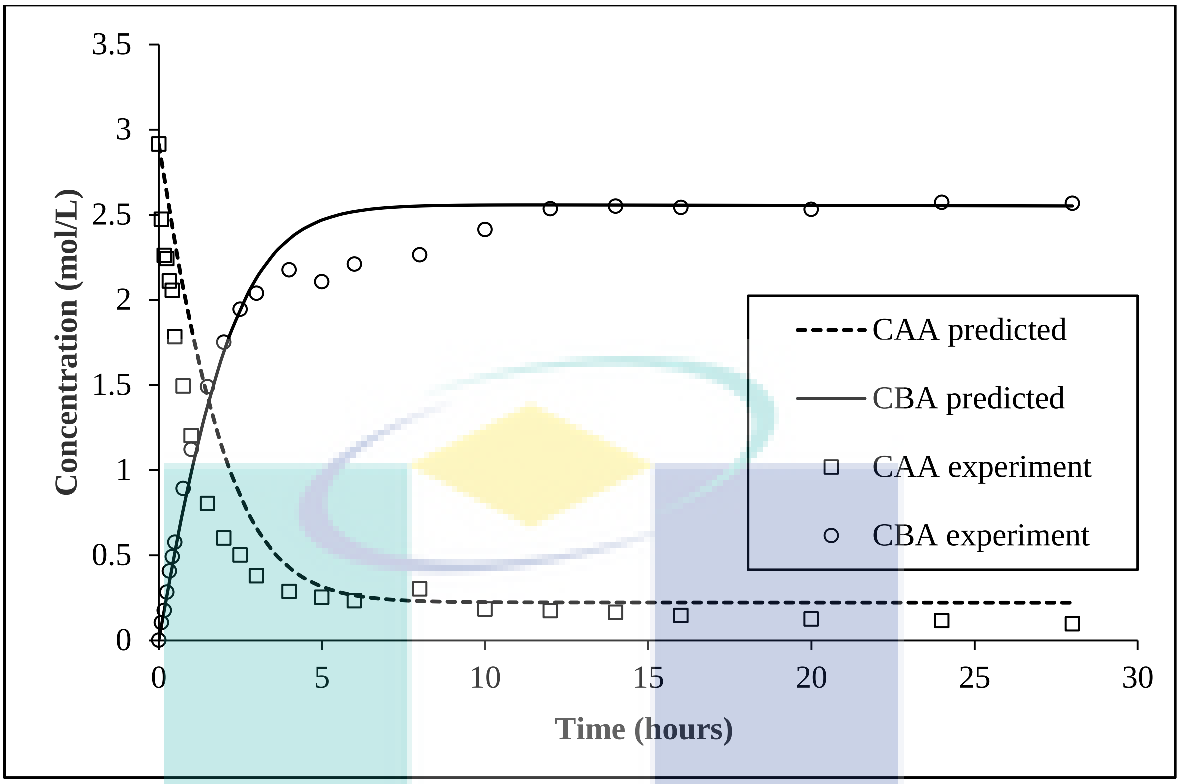

Figure 4.23: Comparison between experimental and predicted (with ER I model considering polymerisation of AA and BA) concentration profiles of AA and BA. Reaction conditions: $M_{AA:BuOH}$ of 1:3, temperature of 353 K, catalyst loading of 10 wt% and stirring speed at 400 rpm

CHAPTER 5

CONCLUSIONS AND RECOMMENDATIONS

5.1 CONCLUSIONS

The heterogeneous catalyst synthesised from waste polystyrene, SEP showed highest activity in the esterification of AA with BuOH comparing to the Amberlyst 15, sulfated zirconia, molybdenum zirconia, zirconium phosphate, sulfonated carbon and zeolite-ZSM5. The FT-IR spectra has validated that the expanded waste polystyrene was sulfonated successfully. The SEP was thermal stable up to 573 K and possessed rough surface with minute cracks that enabling the access of reactant to the active sites. The recyclability study has shown that the catalyst was reusable in the system with pure AA. Among the important operating parameters, the temperature has significantly affected the conversion of AA and yield of BA. The yield and conversion at optimum condition of $M_{AA:BuOH}$ is 1:3, catalyst loading is 10 wt% and temperature of 353 K were 75% and 92% respectively. The activity was reduced when initial water content in the reaction mixture increased because the increasing polymerisation which clogging the pore and hindered the reactants from access the active sites. The water molecule also shifts the equilibrium reaction to reactants side. Nevertheless, the catalyst can be regenerated easily using sulphuric acid.

The elimination of mass transfer effect is important to ensure that the reaction is controlled by surface reaction. The C_M and C_{WP} were 0.003849 and 0.002966 respectively at the stirring speed of 400 rpm and catalyst particle size of 0.4 mm. This indicated that the equilibrium and kinetic studies carried out at the stirring speed of 400 rpm, $M_{AA:BuOH}$ of 1:3 and catalyst loading of 10 wt% were not limited by external and internal diffusion. The esterification of AA with BuOH catalysed by SEP was proven as endothermic reaction.

The non-ideal PH, ER and LHHW models were correlated with the experimental data. The ER I model gave the best prediction with R^2 closest to one indicating that the esterification of AA and BuOH catalysed by SEP occurred based on ER mechanism. The activation energy is 73.6 kJ/mol. Taking into account the polymerisation of AA and BA into main reaction, the experimental data are more accurate because more closer predicted data.

5.2 RECOMMENDATIONS

Based on the present study, SEP is a potential catalyst for the esterification of AA with BuOH due to its high catalytic activity as compared to the others catalysts. A more comprehensive characterisation on its physicochemical properties such as surface area and acidity is required. Since SEP, suffered from the drawback of leaching when the initial water content in the reaction mixture increased, a thorough study to strengthen the bonding of sulfonic acid with the support should be carried out.

The reaction in the present study was also restricted by thermodynamic equilibrium and polymerisation. A reactor system with continuous water removal should be used to carry out the reaction in order to minimise the detrimental effect of the water and hence increasing the conversion and yield.

The present study has shown that the conversion of the esterification of AA with BuOH was high but the selectivity was relatively low. This was attributed to the polymerisation of AA. Optimisation study for the amount of the polymerisation inhibitor should be taken into account in the future.

REFERENCES

Adam, F., Hello, K. and Chai, S. 2012. The heterogeneous of I-phenylalanine-Ru(III) complex and its application as catalyst in esterification of ethyl alcohol with acetic acid. *Chemical Engineering Research and Design*. **90**: 633-642.

Akbay, E.Ö. and Altiokka, M.R. 2011. Kinetics of esterification of acetic acid with n-amyl alcohol in the presence of Amberlyst-36. *Applied Catalysis A: General*. **396**: 14-19.

Åkerman, C.O., Gaber, Y. and Ghani, N. 2011. Clean synthesis of biolubricants for low temperature applications using heterogeneous catalysts. *Journal of Molecular Catalysis B: Enzymatic*. **72**: 263-269.

Akyalçın, S. and Altıokka, M.R. 2012. Kinetics of esterification of acetic acid with 1-octanol in the presence of Amberlyst 36. *Applied Catalysis A: General*. **429-430**: 79-84.

Alberti, G., Cavalaglio, S., Marmottini, F., Matusek, K., Megyeri, J. and Szirtes, L. 2001. Preparation of a γ composite zirconium phosphate-silica with large specific surface and its first characterisation as acid catalyst. *Applied Catalysis A: General*. **218**: 219-228.

Ali, S.H., Tarakmah, Alia, Merchant, Sabiha Q. and Al-Sahhaf, Taher. 2007. Synthesis of esters: Development of the rate expression for the Dowex 50 Wx8-400 catalyzed esterification of propionic acid with 1-propanol. *Chemical Engineering Science*. **62:** 3197-3217.

Allison, M., Singh, K., Webb, J. and Grant, S. 2011. Treatment of acrylic acid production wastewater using a submerged anaerobic membrane bioreactor. *Proceedings of The Water Environment Federation,WEFTEC 2011: Session 101 Through Session*. **110**: 6554-6564.

Altiokka, M.R. and Ödeş, E. 2009. Reaction kinetics of the catalytic esterification of acrylic acid with propylene glycol. *Applied Catalysis A: General*. **362**: 115-120.

Andrijanto, E., Dawson, E.A. and Brown, D.R. 2012. Hypercrosslinked polystyrene sulphonic acid catalysts for the esterification of free fatty acids in biodiesel synthesis. *Applied Catalysis B: Environmental*. **115-116**: 261-268.

Arpornwichanop, A., Koomsup,S. and Assabumrungrat, S. 2008. Hybrid reactive distillation systems for n-butyl acetate production from dilute acetic acid. *Journal of Industrial and Engineering Chemistry*. **14**: 796-803.

Asghari, F.S . and Yoshida, H. 2006. Dehydratio of fructose to 5-hydroxymethylfurfural in sub-critical water over heterogeneous zirconium phosphate catalyst. *Carbohydrate Research.* **341**: 2379-2387.

Bajt, O., Sket, B. and Faganeli, J. 1997. The aqueous photochemical transformation of acrylic acid. *Marine Chemistry Journal* **58**: 255-259.

Bart, H.J., Reidetschlager, J., Schatka, K. and Lehman, A. 1994. Kinetics of Esterification of Levulinic Acid with n-Butanol by Homogeneous Catalysis. *Indian Engineering Chemical Response*. **33**: 21-25.

Bekri-Abbes, I., Bayoudh, S. and Baklouti, M. 2008. The removal of hardness of water using sulfonated waste plastic. *Desalination*. **222**: 81-86.

Bhattacharyya, D., Allison, M.J., Webb, J.R., Zanatta, G.M., Singh, K.S. and Grant, S.R. 2013. Treatment of an Industrial Wastewater Containing Acrylic Acid and Formaldehyde in an Anaerobic Membrane Bioreactor.*Journal of Hazardous, Toxic, and Radioactive Waste*. **17**: 74-79.

Bhorodwaj, S.K. and Dutta, D.K. 2011. Activated clay supported heteropoly acid catalysts for esterification of acetic acid with butanol. *Applied Clay Science*. **53**: 347-352.

Bhutta, M.A.R., Ohama, Y. and Tsuruta, K. 2010. Strength properties of polymer mortar panels using methyl methacrylate solution of waste expanded polystyrene as binder. *Construction and Building Materials.* **25**: 779-784.

Bianchi, C.L., Ragaini, V., Pirole, C. and Carvoli, G. 2003. A new method to clean industrial water from acetic acid via esterification. *Applied Catalysis B: Environmental*. **40**: 93-99.

Blagov, S., Parada, S., Bailer, O., Moritz, P., Lam, D., Weinand, R. and Hasse, H. 2005. Influence of ion-exchange resin catalysts on side reactions of the esterification of Butanol with acetic acid. *Chemical Engineering Science.* **61**: 753-765.

Boreskov, G.V. 2003. *Heterogeneous catalysis*, United States of America: Nova Sciences.

Brahmkhatri, V. and Patel, A. 2011. 12 tungstophosphoric acid anchored to SBA-15: an efficient, environmentally benign reusable catalyst for biodiesel production by esterification fatty acids. *Applied Catalysis A: General.* **403**: 161-172.

Brahmkhatri, V. and Patel, A. 2012. Esterification of lauric acid with butanol-1 over $H_3PW_{12}O_{40}$ supported on MCM-41. *Fuel.* ***102:*** 1-6.

Cabrera-Lafaurie, W. a., Román, F.R. and Hernández-Maldonado, A.J. 2014. Removal of salicylic acid and carbamazepine from aqueous solution with Y-zeolites modified with extraframework transition metal and surfactant cations:

Equilibrium and fixed-bed adsorption. *Journal of Environmental Chemical Engineering*. **2**: 899-906.

Campanati, M., Fornasari, G. and Vaccari, A. 2003. Fundamentals in the preparation of heterogeneous catalysts. *Catalysis Today*. **77**: 299-314.

Chai, K. and Ji, H. 2012. Dual functional adsorption of benzoic acid from wastewater by biological-based chitosan grafted β-cyclodextrin. *Chemical Engineering Journal*. **203:** 309-318.

Chakrabarti, A. and Sharma, M.M. 1993. Cationic ion exchange resins. *Reactive Polymers*. **20**: 41-45.

Chaudhari, R.., Seayad, A., and Jayasree, S. 2001. Kinetic modeling of homogeneous catalytic processes. *Catalysis Today*, **66**: 371-380.

Chen, L., Yin, P., Qu, R., Chen, X., Xu, Q. and Tang, Q. 2011. Production of n-butyl stearate over PA/NaY catalyst. *Chemical Engineering Journal*. **173**: 583-591.

Chen, X., Xu, Z. and Okuhara, T. 1999. Liquid phase esterification cation of acrylic acid with 1-butanol catalyzed by solid acid catalysts. *Applied Catalysis A: General*. **180**: 261-269.

Chen, Y., Cheng, J.J. and Creamer, K.S. 2008. Inhibition of anaerobic digestion process: A review. *Bioresource Technology*. **99**: 4044-4064.

Chorkendorff, I. and Niemantsverdriet, J.W. 2003. *Concepts of Modern Catalysis and Kinetics*. Republic of Germany: Wiley-VCH.

Craig, L.H. and Christina, M.P-M. 1995. Homogeneous catalysis by transition metal oxygen anion clusters. *Coordination Chemistry Reviews*. **143**: 407-455.

Das, J. and Parida, K.M. 2006. Heteropoly acid intercalated Zn/Al HTlc as efficient catalyst for esterification of acetic acid using n-butanol. *Journal of Molecular Catalysis A: Chemical*. **264**: 248-254.

Deborath, M.R., Damiani, D.E. and Tonetto, G.M. 2014. Zinc glycerolate as a novel heterogeneous catalyst for the synthesis of fatty acid methyl esters. *Applied Catalysis B: Environmental*. **144:** 308-316.

Delhomme, C. 2011. *Process Integration of Fermentation and Catalysis for the Production of Succinic Acid Derivatives.* Ph.D. Thesis. Technical University of Munich, Germany.

Demirer, G.N. and Speece, R.E. 1998. Anaerobic biotransformation of four carbon 3-carbon compounds (acrolein, acrylic acid, allyl alcohol and n-propanol) in UASB reactors . *Water Resources*. **32**: 747-759.

Duan, J., Wilson, F., Graham, N. and Hwa Tay, J. 2002. Adsorption of humic acid by powdered activated carbon in saline water conditions. *Desalination.* **151**: 53-66.

Dunnewijk, J., Bosch, H. and de Haan, a. B. 2004. Reverse flow adsorption: integrating the recovery and recycling of homogeneous catalysts. *Separation and Purification Technology*. **40**: 317-320.

Dupont, P., Vedrine, J.C., Paumard, E., Hecquet, G. and Lefebvre, E. 1995. Heteropolyacids supported on activated carbon as catalysts for the esterification of acrylic acid by butanol. *Applied Catalysis A: General*. **129**: 217-227.

Essayem, N., Martin, V., Riondel, A. and Vedrine, J.C. 2007. Esterification of acrylic acid with but-1-ene over sulfated Fe- and Mn-promoted zirconia. *Applied Catalysis A: General*.**326**: 74-81.

Feng, Y., He, W., Zhang, X., Jia, Z. and Zhao, H. 2006. The preparation of nanoparticle zirconium phosphate. *Materials Letters*. **61**: 3258-3261.

Fogler, H.S. 2008. *Elements of Chemical Reaction Engineering.* Fourth Edition, United State of America: Pearson Education.

Fomin, V.A., Etlis, I.V. and Kulemin, V.I. 1991. Some aspects of esterification of acrylic acid with 2-ethylhexyl alcohol on sulfonic cation-exchangers.*Journal Applied Chemistry*. **64**: 1811-1815.

Forni, L. 1999. Mass and heat transfer in catalytic reactions. *Catalysis Today*. **52**: 147-152.

Gan, M., Pan, D. and Ma, L. 2009. The kinetics of the esterification of free fatty acids in waste cooking oil using $Fe_2(SO_4)_3$/C catalyst. *Chinese Journal of Chemical Engineering.* **17**: 83-87.

Gan, S. Ng, H. and Ooi, C. 2010. Ferric sulphate catalysed esterification of free fatty acids in waste cooking oil. *Bioresource Technology.* **101**: 7338-7343.

Geng, L., Wang, Y., Yu, G. and Zhu, Y. 2011. Efficient carbon-based solid acid catalysts for the esterification of oleic acid. *Catalysis Comunications*. **13**: 26-30.

Geng, L., Yu, G. and Wang, Y. 2012. $PhSO_3H$ modified mesoporous carbon as an efficient catalyst for the esterification of oleic acid. *Applied Catalysis A: General.* **427-428**: 137-144.

Grossi, C.V., de Oliveira Jardim, E., de Araujo, M.H., Lago, R.M. and da Silva, M.J. 2010. Sulfonated polystyrene: A catalyst with acid and superabsorbent properties for the esterification of fatty acids. *Fuel*. **89**: 257-259.

Hermida, L., Abdullah, A and Mohamed, A. 2011. Synthesis of monoglyceride through glycerol esterificationwith lauric acid over propyl sulfonic acid post synthesis functionalized SBA-15 mecsoporous catalyst. *Chemical Engineering Journal*. **174**: 668-676.

Hoydonckx, H.E., De Vos, D.E., Chavan, S.A. and Jacobs, P.A. 2004. Esterification and transesterification of renewable chemicals. *Topics in Catalysis*. **27**: 1-4.

Huang, H., Xiao, D., Pang, R., Han, C. and Ding, L. 2014. Simultaneous removal of nutrients from simulated swine wastewater by adsorption of modified zeolite combined with struvite crystallization. *Chemical Engineering Journal*. **256**: 1-33.

Huang, J., Yin, X.-Y., Yang, J-Y. and Guo, M-L. 2014. Solid protonic acids and luminescent carbon dots derived from waste expanded polystyrene. *Materials Letters*. **117**: 112-115.

Ibarbalz, F.M., Figuerrola, E.L.M. and Erijman, L. 2013. Industrial activated sludge exihibit unique bacterial community at high taxonomic ranks.*Water Research*. **47**: 3854-3864.

Idriss, A. 2002. Acrylic acid for developing an ambient air quality guide.Technical report. Alberta: T/659.

Igarashi, T., Yagyu, D., Naito, T., Okumura, Y., Nakajo, T., Mori, Y. and Kobayashi, S. 2012. Dehydrative esterification of carboxylic acids with alcohols catalyzed by diarylammonium p-dodecylbenzenesulfonates in water. *Applied Catalysis B: Environmental*. **119-120**: 304-307.

Inagaki, Y., Kuromiya, M., Noguchi, T and Watanabe, H. 1998. Reclamation of Waste Polystyrene by Pulfonation. *Langmuir Journal*. **15**: 4171-4175.

Izci, A. and Bodur, F. 2007. Liquid-phase esterification of acetic acid with isobutanol catalyzed by ion-exchange resins. *Reactive and Functional Polymers*. **67**: 1458-1464.

Jayswal, A. and Chudasama, U. 2007. Iranian Chemical Society Synthesis and Characterization of a New Phase of Zirconium Phosphate for the Separation of Metal Ions. *Journal of The Iranian Chemical Society*. **4**: 510-515.

Jermy, B.R. and Pandurangan, A. 2005. Catalytic application of Al-MCM-41 in the esterification of acetic acid with various alcohols. *Applied Catalysis A: General*. **288**: 25-33.

Jiang, Yangyang., Xia, H., Mahmood, I., Liu, C. and Liu, H. 2008. Magnetic nanoparticles supported ionic liquids for lipase immobilization: Enzyme activity in catalyzing esterification. *Journal of Molecular Catalysis B: Enzymatic*. **58**: 103-109.

Jiang, Yuwang., Lu, J., Sun, K., Ma, L. and Ding, J. 2013. Esterification of oleic acid with ethanol catalyzed by sulfonated cation exchange resin: Experimental and kinetic studies. *Energy Conversion and Management*. **76**: 980-985.

Johannessen, T., Larsen, J. and Chorkendoff, I. 2000. Catalyst dynamics: consequences for classical kinetic description reactors. *Chemical Engineering Journal*. **82**: 219-230.

Ju, I.B., Lim, H-W., Jeon, W., Suh, D.J., Park, M-J. and Suh, Y-W. 2010. Kinetic study of catalytic esterification of butyric acid and n-butanol over Dowex 50Wx8-400. *Chemical Engineering Journal*. **168**: 293-302.

Kamiya, Y., Sakata, S., Yoshinaga, Y., Ohnishi, R. and Okuhara, T. 2004. Zirconium phosphate with a high surface area as a water-tolerant solid acid. *Catalysis Letters*. **94**: 45-47.

Kara, A., and Erdem, B. 2011. Synthesis, characterization and catalytic properties of sulfonic acid functionalized magnetic-poly(divinylbenzene-4-vinylpyridine) for esterification of propionic acid with methanol. *Journal of Molecular Catalysis A: Chemical*. ***349***: 42-47.

Karakus, S., Sert, E., Buluklu, A.D and Atalay, F.S. 2014. Liquid Phase Esterification of Acrylic Acid with Isobutyl Alcohol Catalyzed by Different Cation Exchange Resins*Industry Engineering Chemistry Research*. **53**: 4192-4198.

Kartal, F., Jannssen, M.H.A., Hollman, F., Sheldon, R.A. and Kilinc, A. 2011. Improved esterification activity of Candida rugosa lipase in organic solvent by immobilization as Cross-linked enzyme aggregates (CLEAs). *Journal of Molecular Catalysis B: Enzymatic*. **71**: 85-89.

Khan, N.A., Jung, B.K., Hassan, Z. and Jhung, S.H. 2014. Adsorption and removal of phthalic acid and diethyl phthalate from water with zeolitic imidazolate and metal-organic frameworks. *Journal of Hazardous Materials*.

Kricheldorf, H.S. 1991. *Handbook of Polymer Synthesis:Part A.*USA: Marcel Dekker, Inc.

Komoń, T., Niewiadomksi, P., Oracz, P. and Jamroz, M.E. 2013. Esterification of acrylic acid with 2-ethylhexan-1-ol: Thermodynamic and kinetic study. *Applied Catalysis A: General*. **451**: 127-136.

Kong, P.S., Aroua, M.K. and Raman, A.A. 2011. Kinetics Study of Esterification Reaction of 2-Methyl-4-Chlorophenoxyacetic Acid (MCPA Acid) Kinetics Study of Esterification Reaction of 2-Methyl-4-Chlorophenoxyacetic Acid (MCPA). *Internatianal Journal of Chemical*. **9**: 1-24.

Kucera, F. and Jancar, J. 1998. Homogeneous and heterogeneous sulfonation of polymers: A review. *Polymer Engineering and Science*. **38**: 783-792.

Kuchta, F.D., van Herk, A. M. and German, A.L. 2000. Propagation kinetics of acrylic acid and methacrylic acid in water and organic solvents studied by pulsed-laser polymerization. *Macromolecules.* **33**: 3641-3649.

Kumar, A., Prasad, B. and Mishra, I.M., 2009. Isotherm and kinetics study for acrylic acid removal using powdered activated carbon. *Journal of Hazardous Materials*. **176**: 774-83.

Kumar, P., Raghavendra, P.V.K. and Chand, S. 2006. Catalytic wet air oxidation of carboxylic acid present in wastewater. *Journal of Scientific and Industrial Research.* **65**: 838-842.

Kumar, V.A., Valenzuela-Calahorro, C., Juarez, J.M., Molina-Sabio, M., Silvestre-Albero, J. and Rodriguez-Reinoso, F. 2010. Hybrid isotherms for adsorption and capillary condensation of N_2 at 77 K on porous and non-porous materials. *Chemical Engineering Journal*. **162**: 424-429.

Landim, A.S., Rodrigues Filho, G. and de Assunção, R.M.N. 2007. Use of polystyrene sulfonate produced from waste plastic cups as an auxiliary agent of coagulation, flocculation and flotation for water and wastewater treatment in Municipal Department of Water and Wastewater in Uberlândia-MG, Brazil. *Polymer Bulletin.* **58**: 457-463.

Lilja, J., Murzin, D.Y., Salmi, T., Aumo, J., Arvela, P.M and Sundell, M. 2002. Esterification of different acids over heterogeneous and homogeneous catalysts and correlation with the Taft equation. *Journal of Molecular Catalysis A: Chemical*. **183**: 555-563.

Lilja, J., Warna, J., Salmi, T., Pettersson, L.J., Ahlkvist, J., Grenman, H., Ronnholm, M. and Murzin, D.Y. 2005. Esterification of propanoic acid with ethanol, 1-propanol and butanol over a heterogeneous fiber catalyst. *Chemical Engineering Journal*. **115**: 1-12.

Liu, Y., Loreto, E. and Goodwinjr, J. 2005. Effect of water on sulfuric acid catalyzed esterification. *Journal of Molecular Catalysis A: Chemical*. **245**: 132-140.

Liu, Y., Lotero, E. and Goodwinjr, J. 2006. Effect of carbon chain length on esterification of carboxylic acids with methanol using acid catalysis. *Journal of Catalysis*. **243**: 221-228.

Mao, Y. and Fung, B. 1997. A Study of the Adsorption of Acrylic Acid and Maleic Acid from Aqueous Solutions onto Alumina. *Journal of Colloid and Interface Science*. **191**: 216-21.

Marchetti, J.M. and Errazu, a. F. 2008. Comparison of different heterogeneous catalysts and different alcohols for the esterification reaction of oleic acid. *Fuel*. **87**: 3477-3480.

Miao, S. and Shanks, B. 2011. Mechanism of acetic acid esterification over sulfonic acid functionalized mesoporous silica. *Journal of Catalysis.* **279** : 136-143.

Miller, W.S., Castagna, C.J. and Pieper, A.W. 1981. Understanding Ion-Exchange Resins For Water Treatment Systems. Technical Report.

Morales, G., Van Grieken, R. and Martin, A. 2010. Sulfonated polystyrene modified mesoporous organosilicas for acid catalyzed process. *Chemical Engineering Journal*. **161**: 388-396

Mulijani, S., Dahlan, K. and Wulanawati, A. 2014. Sulfonated polystyrene copolymer: synthesis, characterization and its application of membrane for direct methanol fuel cell (DMFC). *International Journal of Materials, Mechanics and Manufacturing*. **2**: 36-40.

Niesbach, A., Daniels, J., Schroter, B., Lutze, P. and Gorak, A. 2013. The inhibition of acrylic acid and acrylate ester polymerisation in a heterogeneously catalysed pilot-scale reactive distillation column. *Chemical Engineering Science*. **88**: 95-107.

Oguzhan, I. 2014. Investivation of reaction parameters, kinetics and mechanism of oleic acid esterification with methanol by using amberlyst 46 as catalyst. *Fuel Processing Technology*. **124**: 134-139.

Oliviero, L., Jacques Barbier Jr., Duprez, D. and Guerrero-Ruiz, A. 2000. Catalytic wet air oxidation of phenol and acrylic acid over Ru/C and Ru – CeO_2/C catalysts. *Applied Catalysis B: Environmental*. **25**: 267-275.

Omota, F., Dimian, a. and Bliek, a. 2003. Fatty acid esterification by reactive distillation: Part 2—kinetics-based design for sulphated zirconia catalysts. *Chemical Engineering Science*. **58**: 3175-3185.

Oneto, S.J., Portela, J.R., Nebot, E. and Martinez-de-la-Ossa, E.J. 2004. Wet air oxidation of long-chain carboxylic acids. *Chemical Engineering Journal*. **100**: 43-50.

Osorio-Viana, W., Duque-Bernal, M., Fontalvo, J., Dobrosz-Gomez, I. and Gomez-Garcia, M.A. 2013. Kinetic study on the catalytic esterification of acetic acid with isoamyl alcohol over Amberlite IR-120. *Chemical Engineering Science.* **101**: 755-763.

Ostaniewicz-Cydzik, A.M., Pereira, C.S.M., Molga, E. and Rodrigues, A.E. 2014. Reaction Kinetics and Thermodynamic Equilibrium for Butyl Acrylate Synthesis from n - Butanol and Acrylic Acid. *Industry, engineering chemistry resources.* **53**: 6647-6654.

Ostrowski, S., Jamróz, M.E. and Dobrowolski, J.C. 2011. Formation of heavy adducts in esterification of acrylic acid: A DFT study. *Computational and Theoretical Chemistry*. **974**: 100-108.

Pappu, V.K.S., Kanyi, V., Santhanakrishnan, A., Lira, C.T and Miller, D.J. 2012. Butyric acid esterification kinetics over Amberlyst solid acid catalysts: the effect of alcohol carbon chain length. *Bioresource Technology*. **130**: 793-797.

Park, D.-W., Haam, S., Ahn, I-S., Lee T.G., Kim, H-S. and Kim, W-S. 2004. Enzymatic esterification of β-methylglucoside with acrylic/methacrylic acid in organic solvents. *Journal of Biotechnology*. **107**: 151-160.

Park, J.-Y., Wang, Z-M., Kim, D-K. and Lee, J-S. 2009. Effects of water on the esterification of free fatty acids by acid catalysts. *Renewable Energy*. **35**: 14-618.

Patel, H.K., Joshi, R.S. and Chudasama, U.V. 2008. Use of zirconium (IV) phosphate as a solid acid catalyst in some esterification reactions. *Indian Journal of Chemistry*. **47**: 348-352.

Patricia, D., Sanz, M.T. and Beltran, S. 2007. Kinetic study for esterification of lactic acid with ethanol and hydrolysis of ethyl lactate using an ion-exchange resin catalyst. *Chemical Engineering Journal*. **126**: 111-118.

Peters, T.A., Benes, N.E., Holmen, A. and Keurentjes, J.T.F. 2006. Comparison of commercial solid acid catalysts for the esterification of acetic acid with butanol. *Applied Catalysis A: General*. **297**: 182-188.

Poletto, M. Dettenborn, J., Zeni, M. and Zattera, A.J. 2010. Characterization of composites based on expanded polystyrene wastes and wood flour. *Waste Management (New York, N.Y.)*. **31**: 779-84.

Ragaini, V., Bianchi, C.L., Pirola, C. and Carvoli, G. 2005. Increasing the value of dilute acetic acid streams through esterification. *Applied Catalysis B: Environmental*. **64**: 66-71.

Ragaini, V., Bianchi, C.L. and Pirola, C. 2007. Kinetic of esterification of diluted acetic acid with pure 2-ethyl-1-hexanol. *Chemical Engineering Journal*. **131**: 257-262.

Rahman, A.E. and Khder, S. 2008. Preparation, characterization and catalytic activity of tin oxide-supported 12-tungstophosphoric acid as a solid catalyst. *Applied Catalysis A: General*. ***343*** (1-2): 109-116.

Rahman, M.B.A., Jumbri, K., Mohd Ali Hanafiah, N.A., Abdul Malek, E., Tejo, B.A., Basri, M. and Salleh, A.B. 2012. Enzymatic esterification of fatty acid esters by tetraethylammonium amino acid ionic liquid-coated *Candida rugosa* lipase. *Journal of Molecular Catalysis B: Enzymatic*. **79**: 61-65.

Raita, M., Laothanachareon, T., Champreda, V. and Laosiripojana, N. 2011. Biocatalytic esterification of palm oil fatty acids for biodiesel production using glycine-based cross-linked protein coated microcrystalline lipase. *Journal of Molecular Catalysis B: Enzymatic*. **73**: 74-79.

Rattanaphra, D., Harvey, A.P., Thanapimmetha, A. and Srinophakun, P. 2011. Kinetic of myristic acid esterification with methanol in the presence of triglycerides over sulfated zirconia. *Renewable Energy*. **36**: 2679-2686.

Raweewan, K., Matthias, A., and Wolfgang, F.H. 2011. *Mass transfer- advanced aspects*. Crotia: Intech.

Safe handling and storage of acrylic acid. 2012. 18 September: 9-14.

Saha, B. and Sharma, M. 1995. Esterification of formic acid, acrylic acid and methacrylic acid with cyclohexene in batch and distillation column reactors: ion-exchange resins as catalysts. *Reactive and Functional Polymers*. **28**: 263-278.

Saha, B, Chopade, S.P. and Mahajani, S.M. 2000. Recovery of dilute acetic acid through esterification in a reactive distillation column. *Catalysis Today*. **60**: 147-157.

Sani, Y., Wan Daud, W.M.A. and Abdul Aziz, A.R. 2013. Activity of solid acid catalyst for biodiesel production: A critical review. *Applied Catalysis: A general*. **470**: 140-161.

Sarkar, A., Ghosh, Pramanik, S.K. and Panchanan. 2010. Investigation of the catalytic efficiency of a new mesoporous catalyst SnO_2/WO_3 towards oleic acid esterification.*Journal of Molecular Catalyst A: Chemical*. **327**: 73-79.

Sayyed Hussain, S., Mazhar Farooqui, N. and Gaikwad Digambar, D. 2010. Kinetic and mechanism study of oxidation of ester by $KMnO_4$. *International Journal of Chemical Technology*. **2:** 242-249.

Schimdt-Traub, H. and Gorak, A. 2006. *Integrated Reaction and Separation Operations: Modelling and Experimental*. New York: Springer.

Schmitt, M., Hasse, H., Althaus, K., Shoenmakers, H., Gotze, L. and Morits, P. 2004. Synthesis of n-hexyl acetate by reactive distillation. *Chemical Engineering and Processing: Process Intensification*. **43**: 397-409.

Schildhauer, T.J., Hoek, I., Kapteijn, F. and Moulijn, J.A. 2009. Zeolite BEA catalysed esterification of hexanoic acid with 1-octanol: kinetics, side reaction and the role of water. *Applied Catalysis A: General*. **358**: 141-145.

Schonberg, J.C., Bhattacharya, S.K., Madura, R.L., Mason, S.H. and Conway, R.A. 1997. Evaluation of anaerobic treatment of selected petrochemical wastes. *Journal of Hazardous Materials*. **54**: 47-63.

Sekharan, R.V., Abraham, B.T. and Thachil, E.T. 2012. Utilization of waste expanded polystyrene: Blends with silica-filled natural rubber. *Materials and Design*. **40**: 221-228.

Sert, E. and Atalay, F.S., 2009. Kinetic study of the esterification of acetic acid with butanol catalyzed by sulfated zirconia. *Reaction, Kinetic, Mechanism and Catalysis*. **99**: 125-134.

Sert, E. and Atalay, F.S. 2014. n-Butyl acrylate production by esterification of acrylic acid with n-butanol combined with pervaporation. *Chemical Engineering and Processing: Process Intensification*. **81**: 41-47.

Sert, E., Buluklu, A.D., Karakus, S. and Atalay, F.S. 2013. Kinetic study of catalytic esterification of acrylic acid with butanol catalyzed by different ion exchange resins. *Chemical Engineering and Processing: Process Intensification*. **73**: 23-28.

Sharma, M., Toor, A.P. and Wanchoo, R.K. 2014. Kinetics of the esterification reaction between pentanoic acid and methanol catalyzed by noncorrosive cation exchange resin. *Chemical and Biochemical Engineering Quartery*. **28**: 79-85.

Shin, H.-D., Kim, J-H., Kim, T-K., Kim, S-H. and Lee, Y-H. 2002. Esterification of hydrophobic substrates by lipase in the cyclodextrin induced emulsion reaction system. *Enzyme and Microbial Technology*. **30**: 835-842.

Shi, W., He, B. and Li, J. 2011. Esterification of acidified oil with methanol by SPES/PES catalytic membrane. *Bioresource Technology*. **102**: 5389-93.

Shu, Q., Gao, Y., Liao, Y. and Wang, J. 2011. Reaction kinetics of biodiesel synthesis from waste oil using carbon based solid acid catalyst. *Chinese Journal of Chemical Engineering*. **19**: 163-168.

Silva, A.M., Marques, R.R.. and Quinta-Ferreira, R.M. 2003. Catalysts based in cerium oxide for wet oxidation of acrylic acid in the prevention of environmental risks. *Applied Catalysis B: Environmental*. **47**: 269-279.

Silva, V.M.T.M. and Rodrigues, A.E. 2005. Kinetic studies in a batch reactor using ion exchange resin catalysts for oxygenates production: Role of mass transfer mechanisms. *Chemical Engineering Science*. **61**: 316-331.

Sinhamahapatra, A., Sutradhar, N., Roy, B., Tasafdar, A., Bajaj, H.C. and Panda, A.B. 2010. Mesoporous zirconium phosphate catalyzed reactions: Synthesis of industrially important chemicals in solvent-free conditions. *Applied Catalysis A: General*. **385**: 22-30.

Song, C., Qi, Y., Deng, T., Hou, X. and Qin, Z. 2009. Kinetic model for the esterification of oleic acid catalyzed by zinc acetate in subcritical methanol. *Renewable Energy*. **35**: 625-628.

Srilatha, K., Sree, R., Prabhavathi Devi, B.L., Sai Prasad, P.S., Prasad, R.B.N. and Lingaiah, N. 2012. Preparation of biodiesel from rice bran fatty acids catalysed bu heterogeneous cesium exchangd 12 tungstophosphoric acids. *Bioresource Technology*. **116**: 53-57.

Staples, C.A., Murphy, S.R., McLaughlin, J.E., Leung, H-W., Cascieri, T.C. and Farr, C.H. 2000. Determination of selected fate and aquatic toxicity characteristics of acrylic acid and a series of acrylic esters. *Chemosphere*. **40**: 29-38.

Stewart, M.S., Bhattacharya, S.K., Madura. R.L., Mason, S.H. and Schonberg, J.S. 1995. Anaerobic treatability of selected organic toxicants in petrochemical wastes. *Water Resources.* **29**: 2730-2738.

Strohlein, G., Assuncaou, Y., Dube, N., Bardow, A., Mazzotti, M. and Morbidelli, M. 2006. Esterification of acrylic acid with methanol by reactive chromatography: Experiments and simulations. *Chemical Engineering Science*. **61**: 5296-5306.

Teo, H. and Saha, B, 2004. Heterogeneous catalysed esterification of acetic acid with isoamyl alcohol: kinetic studies. *Journal of Catalysis*. **228**: 174-182.

Tesser, R., Casale, L., Verde., D., Di Serio, M. and Santacesaria, E. 2010. Kinetics and modeling of fatty acids esterification on acid exchange resins. *Chemical Engineering Journal*. **157**: 539-550.

Thakkar, R. and Chudasama, U. 2009. Synthesis and characterization of zirconium titanium phosphate and its application in separation of metal ions. *Journal of Hazardous Materials*.**172**:129-37.

Toor, A.P., Sharma, M. and Wanchoo, R.K. 2011. Kinetic Study of Esterification of Acetic Acid with n- butanol and isobutanol Catalyzed by Ion Exchange Resin. *Chemical Reaction Engineering and Catalysis*. **6**: 23-30.

Tsukamoto, J. and Franco, T. 2009. Enzymatic Esterification of D-Fructose with Acrylic Acid in Organic Media. *New Biotechnology*. **25**: 108-109.

Tuchlenski, A., Beckmann, A., Reush, D., Dussel, R., Weidlich, U. and Janowsky, R. 2001. Reactive distillation-industrial applications, process design & scale-up. *Chemical Engineering Science.* **56**: 387-394.

Vahteristo, K., Laari, A., Haario, H. and Solonen, A. 2007. Estimation of kinetic parameters in neopentyl glycol esterification with propionic acid. *Chemical Engineering Science*. **63**: 587-598.

Vincolli, J.W. 1996. *Risk Management for Hazardous Chemicals.* Volume 1. USA: CRC Press, Inc.

Wang, L., Wang., D., Zhang, S. and Tian, H. 2012. Synthesis and characterization of sulfonated graphene as a highly active solid acid catalyst for ester-exchange reaction. *The Royal Society of Chemistry*. **5**: 1-7.

Widegren, J.A. and Finke, R.G. 2002. A review of the problem of distinguishing true homogeneous catalysis from soluble or other metal-particle heterogeneous catalysis under reducing conditions. *Journal of Molecular Catalysis A: Chemical*. **198**: 317-341.

Xiaobo, X.U., Jianping, L.I.N. and Peilin, C.E.N. 2006. Advances in the Research and Development of Acrylic Acid Production from Biomass. *Chinese Journal of Chemical Engineering*. **14**: 419-427.

Xu, H., Zhou, Q. and Wang, J. 2013. Treatment of Sebacic Acid Industrial Wastewater by Extraction Process Using Castor Oil Acid as Extractant. *Chinese Journal of Chemical Engineering*. **21**: 967-973.

Yadaw, V.P. 2010. *Study on esterification of ethylene glycol with acetic acid in the present of seralite SRC-120 and molecular sieve 13X catalyst*. Master. Thesis. National Institute of Technology Rourkela, India.

Yadav, G.D. and Thathagar, M.B. 2002. Esterification of maleic acid with ethanol over cation-exchange resin catalysts. *Reative and Functional Polymers*. **52**: 99-110.

Yagyu, D., Ohishi, T., Igarashi, T., Okumura, Y, Nakajo, T., Mori, Y. and Kobayashi, S. 2013. Recovery of acetic acid from dilute aqueous solutions using catalytic dehydrative esterification with ethanol. *Chemosphere*. **91**: 61-7.

Yang, Z. Zhou, C. and Zhang, W. 2008. B-MnO_2 nanorods: a new and efficient catalyst for isomyl acetate synthesis. *Colloids and Surface A: Physicochemical and Engineering Aspects*. **356**: 134-139.

Yixin, Q., Shaojun, P., Shui, W. and Zhiqiang, Z. 2009. Kinetic Study of Esterification of Lactic Acid with Isobutanol and n-Butanol Catalyzed by Ion-exchange Resins. *Chinese Journal of Chemical Engineering*. **17**: 773-780.

Zaidi, A., Gainer, J.L., Carta, G., Mrani, A., Kadiri, T., Belarbi, Y. and Mir, A. 2002. Esterification of fatty acids using nylon-immobilized lipase in n-hexane: kinetic parameters and chain-length effects. *Journal of Biotechnology*. **93**: 209-16.

Zatta, L., Gardolinski, J.E.F.D.C. and Wypych, F. 2011. Raw halloysite as reusable heterogeneous catalyst for esterification of lauric acid. *Applied Clay Science*. **51**: 165-169.

APPENDIX A

STANDARD CALIBRATION CURVE OF ACRYLIC ACID

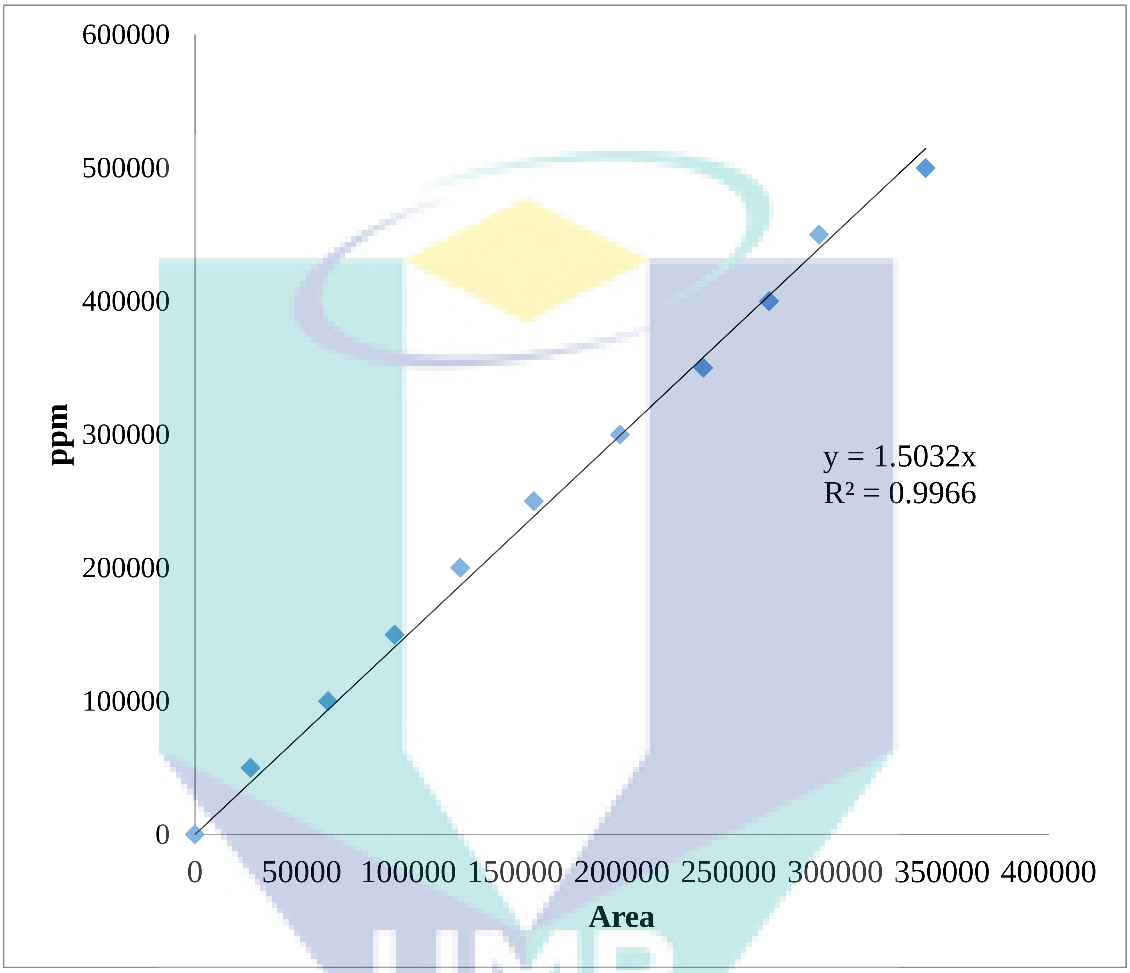

APPENDIX B

STANDARD CALIBRATION CURVE OF BUTYL ACRYLATE

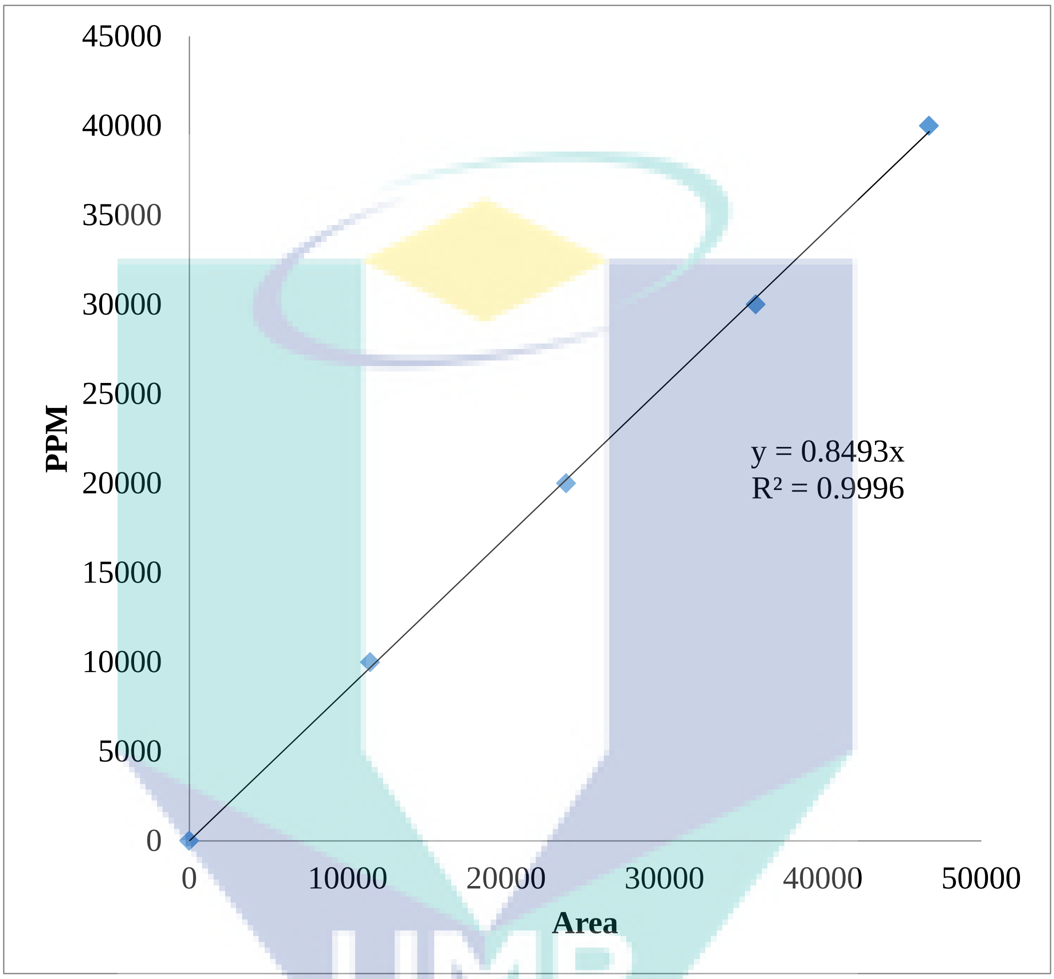

APPENDIX C

UNIFAC (VLE) FOR ESTERIFICATION SYSTEM

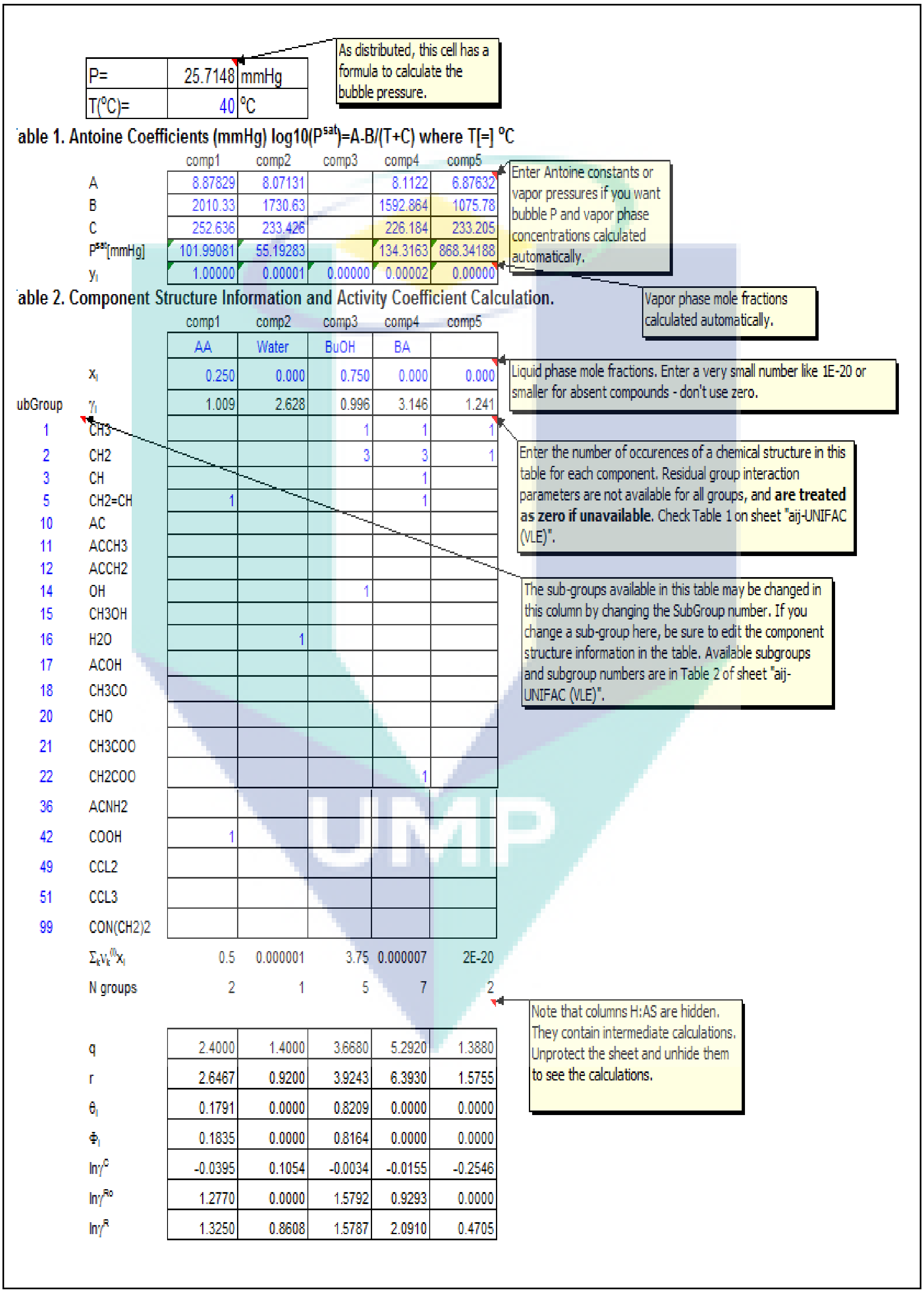

P=	25.7148	mmHg
T(°C)=	40	°C

As distributed, this cell has a formula to calculate the bubble pressure.

able 1. Antoine Coefficients (mmHg) $\log10(P^{sat})=A-B/(T+C)$ where T[=] °C

	comp1	comp2	comp3	comp4	comp5
A	8.87829	8.07131		8.1122	6.87632
B	2010.33	1730.63		1592.864	1075.78
C	252.636	233.426		226.184	233.205
P^{sat}[mmHg]	101.99081	55.19283		134.3163	868.34188
y_i	1.00000	0.00001	0.00000	0.00002	0.00000

Enter Antoine constants or vapor pressures if you want bubble P and vapor phase concentrations calculated automatically.

Vapor phase mole fractions calculated automatically.

able 2. Component Structure Information and Activity Coefficient Calculation.

ubGroup		comp1	comp2	comp3	comp4	comp5
		AA	Water	BuOH	BA	
	x_i	0.250	0.000	0.750	0.000	0.000
	γ_i	1.009	2.628	0.996	3.146	1.241
1	CH3			1	1	1
2	CH2			3	3	1
3	CH				1	
5	CH2=CH	1			1	
10	AC					
11	ACCH3					
12	ACCH2					
14	OH			1		
15	CH3OH					
16	H2O		1			
17	ACOH					
18	CH3CO					
20	CHO					
21	CH3COO					
22	CH2COO				1	
36	ACNH2					
42	COOH	1				
49	CCL2					
51	CCL3					
99	CON(CH2)2					
	$\Sigma_k v_k^{(i)} x_i$	0.5	0.000001	3.75	0.000007	2E-20
	N groups	2	1	5	7	2

Liquid phase mole fractions. Enter a very small number like 1E-20 or smaller for absent compounds - don't use zero.

Enter the number of occurences of a chemical structure in this table for each component. Residual group interaction parameters are not available for all groups, and **are treated as zero if unavailable.** Check Table 1 on sheet "aij-UNIFAC (VLE)".

The sub-groups available in this table may be changed in this column by changing the SubGroup number. If you change a sub-group here, be sure to edit the component structure information in the table. Available subgroups and subgroup numbers are in Table 2 of sheet "aij-UNIFAC (VLE)".

q	2.4000	1.4000	3.6680	5.2920	1.3880
r	2.6467	0.9200	3.9243	6.3930	1.5755
θ_i	0.1791	0.0000	0.8209	0.0000	0.0000
Φ_i	0.1835	0.0000	0.8164	0.0000	0.0000
$\ln\gamma^C$	-0.0395	0.1054	-0.0034	-0.0155	-0.2546
$\ln\gamma^{Ro}$	1.2770	0.0000	1.5792	0.9293	0.0000
$\ln\gamma^R$	1.3250	0.8608	1.5787	2.0910	0.4705

Note that columns H:AS are hidden. They contain intermediate calculations. Unprotect the sheet and unhide them to see the calculations.

APPENDIX D

CALCULATION OF MEARS CRITERION (C_{M})

$$C_M = \frac{r_{A,obs} \times \rho_b R_c \times n}{K_c \times C_{Ab}} < 0.15$$

Where:

$r_{A,obs}$: Reaction rate

ρ_b : Bulk density of catalyst

R_c : Catalyst radius

n : Reaction order

C_{ab} : Bulk concentration of limiting reactant

Reaction rate, $r_{A,obs}$

$$r_{A,obs} = \frac{moles\ of\ limiting\ reactant\ in\ reaction\ time, t\ (mol)}{catalyst\ loading\ (gcat) x\ reaction\ time, t\ (s)}$$

Mol AA at time,t	Time (s)	Catalyst loading (g)	$r_{A,obs}$(kmol/kg.s
0.161602	900	1.3663	0.00013142
0.150145	900	1.3663	0.0001221
0.142996	900	1.3663	0.00011629
0.141241	900	1.3663	0.00011486

Mass transfer coefficient, K_c

$$K_c = \frac{2D_{AB}}{d_p} + 0.31\ N_{Sc}^{-2/3} (\frac{\Delta\rho\mu_c g}{\rho_c^2})^{1/3}$$

Diffusivity, D_{AB}

Obtain from multi component diffusivity correlation from Perkin and Geankoplis method as shown below:

$$D_{Am}\mu_m^{0.8} = \sum_{\substack{j=1 \\ j\neq A}}^{n} x_j D_{Aj}\mu_j^{0.8}$$

Where

D_{Am} : Dilute diffusion coefficient of *A* through mixture

μ_m : Mixture viscosity

D_{Aj} : Dilute binary diffusion of *A* in *j*

X_j : Mole fraction

D_{Aj} is obtain from Wilke-Chang correlation from Perry Handbook

$$D_{AB}^{o} = 1.173 \times 10^{-8}(\Phi_B M_B)^{1/2}\frac{T}{\mu_B V_A^{0.6}}$$

where,

Φ : Association parameter of solvent
M_B : Molecular weight of solvent B, kg/mol
T : Temperature, K
μ_B : Viscosity of B, kg/m.s
V_A : Specific molar volume of limiting reactant, m^3/kg mol

Atomic volume (m^3/kg mol) values are shown in Table below (from Geankoplis):

Material	Atomic volume (m^3/kg mol)
C	14800
H	3700
O	7400

The atomic volume for butanol ($C_4H_{10}O$) is 103600 m^3/kg mol
The viscosity of mixture:

$$\ln\mu_m = \sum_{i=1}^{n} x_i \ln\mu_i$$

where:

μ_m : Viscosity mixture
x_i : Mole fraction
μ_i : Viscosity of fraction

From Yaw's Handbook, the viscosities of *i*th component

Comp	A	B	C	D	T	log10 (μ liq)	μ liq(cp)	μ (kg/m.s)
AA	-15.418	2354.1	0.0336	-2.7354×10^{-5}	353.15	-0.2976	0.5040	0.0005040
BuOH	-5.397	1325.6	0.0062	-5.5062×10^{-6}	353.15	-0.1405	0.7236	0.0007236

The viscosity of mixture is 0.000604 kg/ms.

The $D_{Aj}=D_{AB}^{o}$

Φ	1
M (kg/kmol)	72.06
x_j	**0**.5
T (K)	353.15
Mm(kg/m.s)	0.000603854
DAj (m^2/s)	4.75793E-05

So, the diffusivity of *A* through mixture is 2.7493×10^{-5} m^2/s

Density calculation:

From Albright Handbook and assume the liquid mixture is ideal

$$v^{id} = \sum_i x_i v_i$$

Where V is molar volume (m^3/mol). The density of component are calculated based on Yaw's Handbook

ρ (g/cm^3) =A(B^-(1-T/Tc)^n)

	A	B	n	Tc	T	ρ (g/cm3)	V (m3/mol)
AA	0.3322	0.2515	0.2946	498	353.15	0.37391	0.000192731
BuOH	0.2689	0.2667	0.2457	562.93	353.15	0.303491	0.000244235

Molar volume is 0.0002184

Molar mass of mixture:

$$M = \sum_i x_i MW_i$$

M= 0.07309kg/mol

So, the density of liquid mixture is 334.55 kg/m^3

Schmidt number, Nsc:

$$N_{Sc} = \frac{\mu_c}{\rho_c D_{AB}}$$

Where

μ_c : Viscosity of mixture (kg/m.s)

ρ_c : Density of mixture (g/ml)

D_{AB} : Diffusivity (m^2/s)

So, the Schmidt number is 0.01717

Mears Criterion for different stirring rate:

rpm	CM
0	0.004404
200	0.004092
400	0.003897
600	0.003849

APPENDIX E

CALCULATION OF WEISZ-PRATER CRITERION (C_{WP})

$$C_{WP} = \frac{-r_{A,obs}\rho_c R_c^2}{D_{eff}C_{li}} < 1$$

where:

$-r_{A,obs}$	: Reaction rate at given time, t
P_c	: Catalyst density
R_c	: Effective radius of catalyst
D_{eff}	: Effective diffusivity
C_{li}	: Concentration of limiting reactant in mixture

Effective diffusivity:

$$\mathrm{D_{eff}} = \mathrm{D_{AA}}\left(\frac{\varepsilon}{\tau}\right) = \mathrm{D_{AA}} \times \varepsilon^2$$

$$\varepsilon_p = \frac{V_{pore}}{V_p} = \frac{\rho_s - \rho_p}{\rho_s}$$

The porosity is 0.279 and effective diffusivity is 0.03704 cm^2/s.

True radius:

The ‘true radius’ calculated based on equation below and assumed that SEP is sphere.

$$R = \sqrt[3]{\frac{swelling\ in\ mixture\ (\%)}{swelling\ in\ BuOH\ (\%)}} \times mean\ radius$$

The SEP swell in reaction mixture is 515% and in BuOH is 740%. The radius is 0.4mm and the ‘true’ radius s 0.4640 mm. The densiy of catalyst is 1.279 g/cm^3. The C_{WP} is calculated and values shows below:

Stirring rate (rpm)	C_{WP}
0	0.003351733
200	0.003114103
400	0.002965825
600	0.002929424

APPENDIX F

SULFONATION REACTION PATHWAY

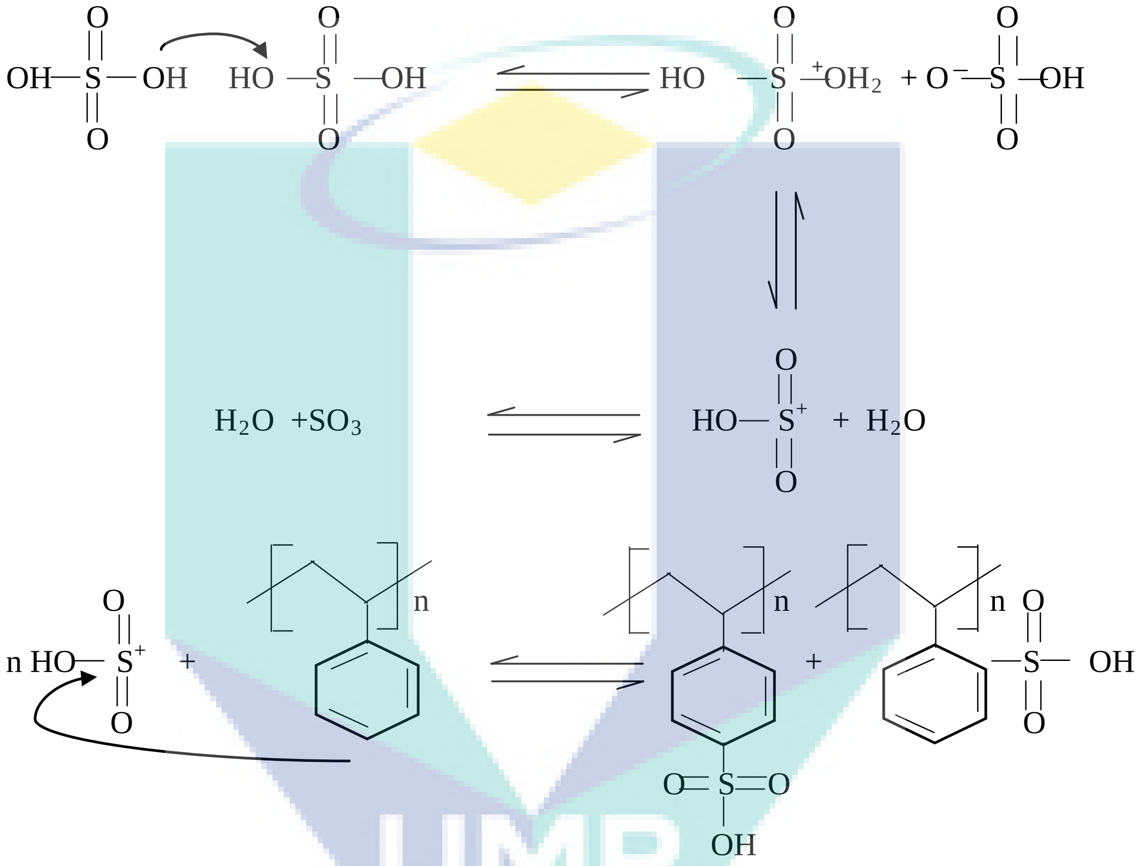

APPENDIX G

CALCULATION OF YIELD AND CONVERSION

Yield

From GC chromatogram, gives the area under the graph is 2000 pA*s. So, yield of BA are calculated as follow:

$$yield(\%)=\frac{mol_{BA}}{mol_{AA^0}}\times 100\%$$

1. Standard curve
    a. Y=1.503 x X
    where Y is the concentration of BA in mg/l and X is the area of BA under the graph of GC chromatogram.
2. Molecular weight of BA is 72.06
3. Initial mol of AA is 0.08751

Concentration of BA = Area x 1.503 x dilution factor x
= 2000 x 0.8493 x 10
= 16986 mg/l
Mol of BA = Concentration of BA x Volume total ÷ molecular weight of BA
= 16986 mg/l x 30 ml ÷ (128.17 g/mol/1000/1000)
= 0.0040 mol
Yield of = (0.0040/0.08757) x100
= 4.5%

Conversion

From GC chromatogram, gives the area under the graph of AA is 2000 pA*s. So, conversion of AA are calculated as follow:

$$conversion\ (\%) = \frac{mol_{AA^0} - mol_{AA}}{mol_{AA^0}} \times 100\%$$

1. Standard curve
    a. Y= 1.503x X

       where Y is the concentration of mol of BA in mg/l and X is the area of AA under the graph of GC chromatogram.
2. Molecular weight of AA is 72.06 g/mol
3. Initial mol of AA is 0.08751 g

Concentration of AA = Area x 1.503 x dilution factor x
= 2000 x 1.503 x 10
= 30060 mg/l

Mol of AA = Concentration of AA x Volume total ÷ molecular weight of AA
= 30060 mg/l x 30 ml ÷ (72.06 g/mol/1000/1000)
= 0.0125 mol

Conversion = (0.08751-0.0125)/0.08751) x 100
= 85.7%

APPENDIX H

ACRYLIC ACID SELF POLYMERISATION MECHANISM

$$\mathrm{AA} + \mathrm{AA}^{*} \rightarrow \mathrm{AA} - \mathrm{AA}^{*}$$

$$\mathrm{AA} - \mathrm{AA}^{*} + \mathrm{O_2} \rightarrow \mathrm{AA} - \mathrm{AA} - \mathrm{O_2^{*}}$$

$$\mathrm{AA} - \mathrm{AA} - \mathrm{O_2^{*}} + \mathrm{MEHQ} \rightarrow \mathrm{AA} - \mathrm{AA} - \mathrm{O_2} - \mathrm{MEHQ}^{*}$$

$$\mathrm{AA} - \mathrm{AA} - \mathrm{O_2^{*}} + \mathrm{AA} - \mathrm{AA} - \mathrm{O_2} - \mathrm{MEHQ}^{*} \rightarrow \text{Saturated Quinone}$$